



**KLIMA- OG  
FORURENSNINGS-  
DIREKTORATET**

Statlig program for forurensningsovervåking  
Rapportnr. 1145/2013

Monitoring of greenhouse gases and aerosols at Svalbard and  
Birkenes: Annual report 2011

TA  
3035  
2013



Utført av NILU – Norsk institutt for luftforskning







KLIMA- OG  
FORURENSNINGS-  
DIREKTORATET

**Statlig program for forurensningsovervåking:**

Monitoring of greenhouse gases and aerosols at the Zeppelin Observatory, Svalbard, and Birkenes Observatory, Aust-Agder, Norway

SPFO-rapport: 1145/2013

TA-3035/2013

ISBN 978-82-425-2580-2 (print)

ISBN 978-82-425-2581-9 (electronic)

Oppdragsgiver: Klima- og forurensningsdirektoratet (Klif)

Utførende institusjon: NILU – Norsk institutt for luftforskning

**Monitoring of greenhouse gases  
and aerosols at Svalbard and  
Birkenes**

Rapport  
3035/2013

Annual report 2011



Authors: C.L. Myhre, O. Hermansen, A.M. Fjæraa, C. Lunder, M. Fiebig, N. Schmidbauer, T. Krognes, K. Stebel

NILU project no.: O-99093/105020

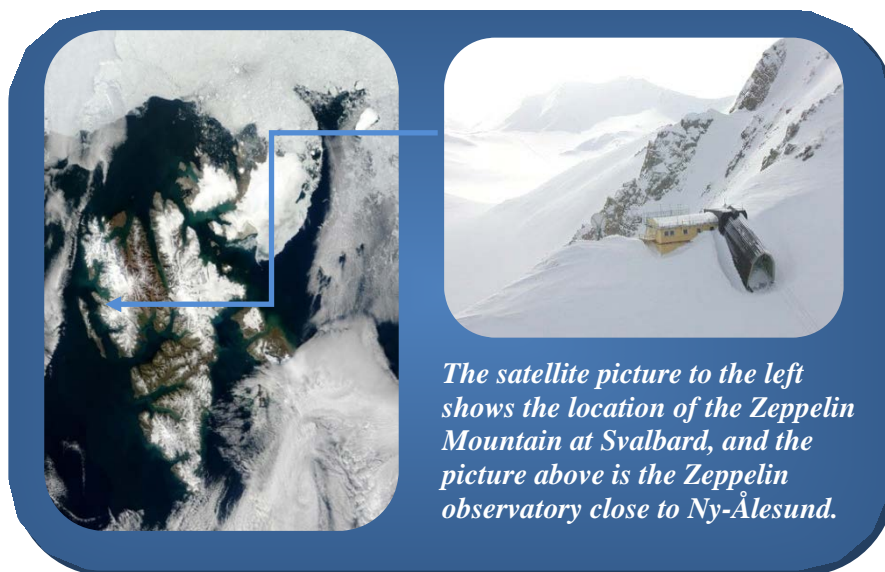
NILU report no.: OR 18/2013



## Preface

In 1999 The Climate and Pollution Agency (Klif, the former SFT) and NILU – Norwegian Institute for Air Research signed a contract commissioning NILU to run a programme for monitoring greenhouse gases at the Zeppelin station, close to Ny-Ålesund at Svalbard. This collaborative Klif/NILU programme includes monitoring of 23 greenhouse gases at the Zeppelin observatory in the Arctic. In 2009 NILU upgraded and extended the observational activity at the Birkenes Observatory in Aust-Agder. From 2010 the Klif/NILU monitoring programme was extended to also include the new observations from Birkenes of the greenhouse gases CO<sub>2</sub> and CH<sub>4</sub> and selected aerosol observations particularly relevant for the understanding of climate change.

The unique location of the Zeppelin observatory at Svalbard together with the infrastructure of the scientific research community at Ny-Ålesund makes it ideal for monitoring the global changes of the atmosphere. There are few local sources of emissions, and the Arctic location is also important as the Arctic is a particularly vulnerable region. The observations at the Birkenes Observatory complement the Arctic site. Birkenes Observatory is located in a forest area with few local sources. However, the observatory often receives long range transported pollution from Europe and the site is ideal to analyse the contribution of long range transported greenhouse gases and aerosol properties.



In 1987 the Montreal Protocol was signed and entered into force in 1989 in order to reduce the production, use and eventually emission of the ozone-depleting substances (ODS). The amount of most ODS in the troposphere is now declining slowly and one expects to be back to pre-1980 levels around year 2050. It is crucial to follow the development of the concentration of these ozone depleting gases in order to verify that the Montreal Protocol and its amendments work as expected. Further these gases and their replacement gases are strong greenhouse gases making it even more important to follow the development of their concentrations. In December 1997 the Kyoto protocol was adopted. The target set by the Kyoto protocol is to reduce the total emissions of greenhouse gases from the industrialized countries during the period 2008 to 2012. The six most important groups of greenhouse gases included are: CO<sub>2</sub>, CH<sub>4</sub>, N<sub>2</sub>O, fluorinated hydrocarbons (HFCs and PFCs) and sulphurhexafluoride (SF<sub>6</sub>).

The following greenhouse gases are regulated through the Montreal protocol and measured at the Zeppelin Observatory: chlorofluorocarbons (CFC), hydrochlorofluorocarbons (HCFC), and halones as well as other halogenated organic gases. Further the following gases included in the Kyoto protocol are monitored; methane (CH<sub>4</sub>), nitrous oxide (N<sub>2</sub>O) from 2010, hydrofluorocarbons (HFC), sulphurhexafluoride (SF<sub>6</sub>). Additionally carbon monoxide (CO) and tropospheric ozone (O<sub>3</sub>) are a part of the programme. The amount of particles in the air above the stations is also measured. The station is hosting measurements of carbon dioxide (CO<sub>2</sub>) performed by ITM, University of Stockholm as well, but the availability of data is limited. This activity is funded by the Swedish Environmental Protection Agency.

NILU – Norwegian Institute for Air Research is responsible for the operation and maintenance of the monitoring programme. The purpose of the programme is to:

- Provide continuous measurements of greenhouse gases in the Arctic region resulting in high quality data that can be used in trend analysis
- Provide continuous measurements of the greenhouse gases CO<sub>2</sub> and CH<sub>4</sub> at the Birkenes Observatory resulting in high quality data that can be used in trend analysis
- Provide trend analysis and interpretations of the observations from Zeppelin assess the influence regional anthropogenic emissions of greenhouse gases has on the radiative balance
- Provide information on the status and the development of the greenhouse gases with a particular focus on the gases included in the international conventions the Montreal and Kyoto protocol.
- Provide results of aerosol observations of relevance to the understanding of climate change
- Indicate sources regions with high influence on the measurements.

Observations and results from the monitoring programme are processed and used to assess the progress towards compliance with international agreements like the Kyoto and the Montreal Protocols. This report summarises the activities and results of the greenhouse gas and aerosol monitoring programme for the year 2011, and comprises a trend analysis for the period 2001-2011 including interpretation of the results.

Kjeller, February 2013

Cathrine Lund Myhre  
Senior scientist and project manager

## Table of Contents

<b>1.</b>	<b>Executive summary .....</b>	<b>7</b>
<b>2.</b>	<b>Introduction .....</b>	<b>13</b>
<b>3.</b>	<b>The Zeppelin and Birkenes Observatories; Norwegian atmospheric supersites .....</b>	<b>16</b>
3.1	Norwegian atmospheric supersites as part of European atmospheric research infrastructures .....	17
3.2	The Zeppelin Observatory .....	17
3.3	The Birkenes Observatory .....	19
<b>4.</b>	<b>Observations and trends of greenhouse gases at the Zeppelin Observatory in the Norwegian Arctic .....</b>	<b>21</b>
4.1	Greenhouse gases with natural and anthropogenic sources .....	22
4.1.1	Observations of Methane in the period 2001-2011 .....	22
4.1.2	Observations of Nitrous Oxide at the Zeppelin Observatory .....	26
4.1.3	Observations of Carbon Dioxide in the period 1988-2011 .....	27
4.1.4	Observations of Methyl Chloride in the period 2001-2011 .....	29
4.1.5	Observations of Methyl Bromide in the period 2001-2011 .....	30
4.1.6	Observations of tropospheric ozone in the period 1990-2011 .....	31
4.1.7	Observations of CO in the period 2001-2011 .....	33
4.2	Greenhouse gases with solely anthropogenic sources .....	34
4.2.1	Observations of Chlorofluorocarbons (CFCs) in the period 2001-2011 .....	35
4.2.2	Observations of Hydrochlorofluorocarbons (HCFCs) in the period 2001-2011 .....	37
4.2.3	Observations of Hydrofluorocarbons (HFCs) in the period 2001-2011 .....	39
4.2.4	Observations of halons in the period 2001-2011 .....	41
4.2.5	Observations of other chlorinated hydrocarbons in the period 2001-2011 .....	43
4.2.6	Perfluorinated compounds .....	44
<b>5.</b>	<b>Observations of CO<sub>2</sub> and CH<sub>4</sub> at the Birkenes Observatory in Aust-Agder .....</b>	<b>46</b>
<b>6.</b>	<b>Analysis of CO from satellite observations to support ground based measurements at Birkenes .....</b>	<b>49</b>
<b>7.</b>	<b>Aerosols and climate: Observations from Zeppelin and Birkenes Observatories .....</b>	<b>52</b>
7.1	Observations of climate relevant aerosol properties: recent developments in Norway and internationally .....	53
7.2	Optical aerosol properties measured at Birkenes: estimating the local, instantaneous direct aerosol radiative forcing .....	55
7.3	Physical aerosol properties measured at Birkenes in 2011 .....	59
7.4	Observations of the total aerosol load above Zeppelin and Birkenes Observatories .....	62
7.4.1	Measurements of the total aerosol load above Ny-Ålesund .....	63
7.4.2	Measurements of the total aerosol load above the Birkenes observatory .....	67
7.5	Utilization of satellite data as a complement to aerosol observations above Scandinavia and the European Arctic .....	69
<b>8.</b>	<b>Transport of air to the Zeppelin Observatory .....</b>	<b>75</b>
<b>9.</b>	<b>References .....</b>	<b>78</b>
	<b>Appendix I: Description of instruments, methods and trend analysis .....</b>	<b>83</b>

**Appendix II: Acknowledgments ..... 94**

## 1. Executive summary

This annual report describes the activities and main results of the programme “*Monitoring of greenhouse gases and aerosols at the Zeppelin Observatory, Svalbard, and Birkenes Observatory, Aust-Agder, Norway*”. This is a part of the Governmental programme for monitoring pollution in Norway. The report comprises all natural well mixed greenhouse gases, the most important anthropogenic greenhouse gases and various particle’s properties with high relevance to climate. Many of the gases also have strong ozone depleting effect.

The concentration in the atmosphere of the main greenhouse gases with high anthropogenic emissions has been increasing over the period of investigation, except for the few of the CFCs and halogenated gases. These gases have strong ozone depleting effect and are regulated through the successful Montreal protocol. The positive effect of this is without any doubt and also a benefit for the climate. The uneven growth of the concentration of methane makes it special difficult to identify the sources for the growth. This will demand an extension of monitoring of methane both in Norway as well as in international networks.

The trends of all gases included in the programme are shown in Table 1, and commented briefly in the summary. Further details and interpretations of the results are presented in section 3 of the report. Our observations are also compared to global mean development of the concentrations of the main gases.

### **Greenhouse gases regulated through the Kyoto protocol - Key findings from the Zeppelin and Birkenes observatories**

---

The report includes the 6 greenhouse gases or groups of gases regulated through the Kyoto protocol. The key findings are:

**Methane – CH<sub>4</sub>** : In 2011 the mixing ratios of methane increased to **new record level globally**. At Zeppelin the annual mean value of 1879 ppb was a little lower than in both 2010 and 2009. Still, the methane increase at the Zeppelin observatory from 2005 to 2011 (37 ppb or around 2%) was larger than the global increase in the same period (approx. 1.4 %). Both values constitute a relatively large change compared to the evolution of the methane levels in the period from 1998-2005, when the change was close to zero both at Zeppelin and globally, after a strong increase during the 20<sup>th</sup> Century (Forster et al., 2007). The first full year of measurements of CH<sub>4</sub> at Birkenes showed an annual mean value for 2011 of 1895.5 ppb, higher than the annual values both for Zeppelin and the global mean – 1812 ppb.

There is yet no clear explanation for the global increase in methane that started in 2005, but a probable explanation is increased methane emissions from wetlands, both in the tropics as well as in the Arctic region. Melting permafrost, both in terrestrial regions and at the sea floor, might introduce new possible methane emission sources initiated by the temperature increase the last years. Observations indicate however that these potential sources are not the cause of the recent increase observed at Zeppelin (Fisher et al. 2011) If this should be the case, it would be an alarming development, given the extensive stocks of methane that can be released from in the permafrost.

To improve our understanding of the ongoing processes an extension of the monitoring of methane is needed, to better identify the various source strengths in the Arctic. Methane from

various sources has different isotopic ratios of  $^{13}\text{C}/^{12}\text{C}$ . Isotopic measurements of methane at Zeppelin combined with transport modeling as well as climate modeling would be a very powerful tool to distinguish between methane from various sources as wetlands, oceans and exploitation of gas fields included gas transportation. Measurements are currently included in research projects at NILU financed by The Research Council of Norway.

*Table 1: Key findings; Greenhouse gases measured at Ny-Ålesund; lifetimes in years<sup>1</sup>, global warming potential (GWP), absolute change in concentrations since 2010, concentrations in 2011, their trends per year over the period 2001-2011, and relevance to the Montreal and Kyoto Protocols. All concentrations are mixing ratios in ppt<sub>v</sub>, except for methane and carbon monoxide (ppb<sub>v</sub>) and carbon dioxide (ppm<sub>v</sub>).*

Compound	Formula	Life-time	GWP <sup>2</sup>	Change last year	2011	Trend / Year	Montreal or Kyoto Prot.	Comments on sources for the halocarbons
<b>Methane</b>	CH <sub>4</sub>	12 <sup>3</sup>	25	-1	1879	<b>+4.3</b>	<b>K</b>	
<b>Carbon monoxide</b>	CO	Months		-10.5	166	<b>-1.2</b>		
<b>Carbondioxide<sup>4</sup></b>	CO <sub>2</sub>		1	2.2	392.5	<b>+2.1</b>	<b>K</b>	
<b>Chlorofluorocarbons</b>								
CFC-11*	CCl <sub>3</sub> F	45	4750	-2.5	238	<b>-2.08</b>	<b>M</b> phased out	foam blowing, aerosol propellant
CFC-12*	CF <sub>2</sub> Cl <sub>2</sub>	100	10900	-2.9	531	<b>-1.59</b>	<b>M</b> phased out	temperature control
CFC-113*	CF <sub>2</sub> ClCFCl <sub>2</sub>	640	6130	-0.9	74.6	<b>-0.66</b>	<b>M</b> phased out	solvent, electronics industry
CFC-115*	CF <sub>3</sub> CF <sub>2</sub> Cl	1020	7370	0.0	8.42	<b>+0.03</b>	<b>M</b> phased out	temperature control, aerosol propellant
<b>Hydrochlorofluorocarbons</b>								
HCFC-22	CHClF <sub>2</sub>	11.9	1810	6.1	226	<b>+6.85</b>	<b>M</b> freeze	temperature control, foam
HCFC-141b	C <sub>2</sub> H <sub>3</sub> FCI <sub>2</sub>	9.2	725	1.0	23.0	<b>+0.55</b>	<b>M</b> freeze	foam blowing, solvent
HCFC-142b*	CH <sub>3</sub> CF <sub>2</sub> Cl	17.2	2310	0.6	22.7	<b>+0.87</b>	<b>M</b> freeze	foam blowing
<b>Hydrofluorocarbons</b>								
HFC-125	CHF <sub>2</sub> CF <sub>3</sub>	28.2	3500	1.6	10.9	<b>+0.84</b>	<b>K</b>	temperature control
HFC-134a	CH <sub>2</sub> FCF <sub>3</sub>	13.4	1430	5.1	68.5	<b>+4.65</b>	<b>K</b>	temperature control, foam, solvent, aerosol propellant
HFC-152a	CH <sub>3</sub> CHF <sub>2</sub>	1.5	124	0.4	10.1	<b>+0.77</b>	<b>K</b>	foam blowing
<b>Halons</b>								
H-1211*	CBrClF <sub>2</sub>	16	1890	-0.1	4.2	<b>-0.02</b>	<b>M</b> phased out	fire extinguishing
H-1301	CBrF <sub>3</sub>	65	7140	0.0	3.3	<b>+0.03</b>	<b>M</b> phased out	fire extinguishing
<b>Halogenated compounds</b>								
Methylchloride	CH <sub>3</sub> Cl	1.0	13	-10.3	508	<b>-0.05</b>		natural emissions (algae)
Methylbromide	CH <sub>3</sub> Br	0.8	5	-0.2	7.1	<b>-0.18</b>	<b>M</b> freeze	agriculture, natural emissions (algae)
Dichloromethane	CH <sub>2</sub> Cl <sub>2</sub>	0.38	8.7	-0.1	41.2	<b>+1.11</b>		solvent
Chloroform	CHCl <sub>3</sub>	0.5	30	0.6	12.0	<b>+0.06</b>		solvent, natural emissions
Methylchloroform	CH <sub>3</sub> CCl <sub>3</sub>	5	146	-1.3	6.5	<b>-3.08</b>	<b>M</b> phased out	solvent
Trichloroethylene	CHClCCl <sub>2</sub>			0.0	0.6	<b>-0.00</b>		solvent
Perchloroethylene	CCl <sub>2</sub> CCl <sub>2</sub>			-0.2	2.8	<b>-0.18</b>		solvent
Sulphurhexafluoride*	SF <sub>6</sub>	3200	22800	0.3	7.5	<b>+0.26</b>	<b>K</b>	Mg-production, electronics

\* The measurements of these components have higher uncertainty. See Appendix I for more details.

<sup>1</sup> From Scientific Assessment of Ozone Depletion: 2010 (WMO, 2011b) and the 4<sup>th</sup> Assessment Report of the IPCC

<sup>2</sup> GWP (Global warming potential) 100 years time period, CO<sub>2</sub> = 1

<sup>3</sup> The lifetime for CH<sub>4</sub> includes feedbacks of indirect effects on the lifetime. The lifetime is close to 9 year without adjustments.

<sup>4</sup> Measurements of CO<sub>2</sub> is performed by Stockholm University. This is preliminary data and there is no trend calculation.

- **CO<sub>2</sub> reached new record levels in 2011 both globally and at the Zeppelin Observatory.** The global value was 390.9 according to WMO (2012) and the preliminary analysis of the Zeppelin measurements indicates a mixing ratio of 392.4 ppm. The annual growth rates were slightly higher than the last years, above 2 ppm per year both globally and at Zeppelin. The first full year of measurements of CO<sub>2</sub> at Birkenes showed an annual mean value of 396.5 ppm.
- **Nitrous Oxide –N<sub>2</sub>O:** The global mean level of N<sub>2</sub>O has increased from around 270 ppb prior to industrialization and up to an average global mean of 324.2 ppb in 2011 (WMO, 2012) which is new record level. In 2009 NILU installed a new instrument at Zeppelin measuring N<sub>2</sub>O to follow the evolution of this compound in the future in the Arctic. The instrument has been in full operation since April 2010 and the observations are presented in this report. The annual mean for 2011 was 324.2 ppb at Zeppelin, coincidentally the same as the global mean. The recent Assessment of the ozone depletion (WMO, 2011) suggests that current emissions of N<sub>2</sub>O are presently the most significant substance that depletes ozone with consequences for the ozone layer.
- **Hydrofluorocarbons - HFCs:** These gases replace the strongly ozone depleting substances CFC's, and are relatively new gases emitted to the atmosphere. They are all of solely anthropogenic origin. The mixing ratios of HFC-125, HFC-134a, HFC-152a have **increased by as much as 446%, 230% and 255% respectively since 2001** at the Zeppelin observatory. However, their concentrations are still very low, thus the total radiative forcing of these gases since the start of their emissions around 1970 and up to 2011 is only about 0.014 W m<sup>-2</sup>. For comparison: The forcing of a typical 2 ppm annual increase in CO<sub>2</sub> is around 0.03 W m<sup>-2</sup> and the forcing of these HFCs is less than 1 % of the radiative forcing from the change in CO<sub>2</sub> since pre-industrial time. Thus the contribution from these manmade gases to the global warming is small today, but given the observed extremely rapid increase in the use and atmospheric concentrations, it is crucial to follow the development of these gases in the future.
- **The perfluorinated compound – SF<sub>6</sub>:** The only perfluorinated compound measured at Zeppelin is Sulphurhexafluoride, SF<sub>6</sub>. This is an **extremely potent greenhouse gas**, but the concentration is still low. However, measurements show that the concentration has increased more than 50% since 2001.

## Greenhouse gases regulated through the Montreal protocol – Key findings

---

All gases regulated through the Montreal protocol are substances depleting the ozone layer. In addition they are all greenhouse gases. The amount of most of the ozone-depleting substances (ODS) in the troposphere is now declining slowly globally and is expected to be back to pre-1980 levels around the year 2050. The gases included in the monitoring programme at Zeppelin are the man-made greenhouse gases called chlorofluorocarbons (CFCs), the hydrogen chlorofluorocarbons (HCFCs), which are CFC substitutes, and halons.

- **CFCs:** In total the development of the CFC gases measured at the global background site Zeppelin give reason for optimism. The mixing ratio of the observed CFCs, **CFC-11**,

**CFC-12 and CFC-113 are declining.** The mixing ratios of these gases are now at a lower level than in 2001 when measurements started at Zeppelin, and are reduced with approx. 8%, 2.8% and 8.4% respectively since the start. **CFC-115 seems to have stabilised and was in 2011 at the same level as in 2009**

- **HCFCs:** The CFC substitutes **HCFC-22, HCFC-141b and HCFC-142b all had a relatively strong increase in the levels measured at Zeppelin from 2001-2011.** HCFC-22 used for temperature control and foam blowing had the largest growth rate. This is the most abundant substance of the HCFCs and its mixing ratio at Zeppelin increased by a rate of 6.9 ppt/year which is almost 4% per year, and the increase is as much as a 42% since 2001. HCFC-142b had the strongest relative increase with more than 56% since 2001.

- **Halons:** Halons are the Bromine containing halocarbons. The levels of the two gases monitored have been relatively stable over the observation period at Zeppelin. The recent results indicate that there was a maximum in 2004 for halon-1211 at Zeppelin, and a small decline after that. Since 2001 this compound is reduced with approx. 5%. According to the last Ozone Assessment (WMO, 2011) the total stratospheric Bromine concentration is no longer increasing, and Bromine from halons stopped increasing during the period 2005-2008.

### **Greenhouse gases not regulated through the protocols – Key findings**

---

The monitoring programme also includes five greenhouse gases not regulated through any of the two protocols.

- **Chlorinated greenhouse gases:** The following five chlorinated gases are measured at the Zeppelin Observatory: methylchloride ( $\text{CH}_3\text{Cl}$ ), dichloromethane ( $\text{CH}_2\text{Cl}_2$ ), chloroform ( $\text{CHCl}_3$ ), trichloromethane ( $\text{CHClCCl}_3$ ), perchloroethylene ( $\text{CCl}_2\text{CCl}_2$ ). Four of these gases have increased the last years and a considerable increase in chloroform is evident at Zeppelin from 2006-2011, and since 2008 the component has increased with approx. 14%. The reason for this is not yet clear. **Dichloromethane shows an increase of almost 32% since 2001.** The main use of this compound is as an active ingredient in paint removers.

### **Long range transport of pollutions; aerosols and reactive gases – Key findings**

---

Aerosols are small particles in the atmosphere. Major sources of anthropogenic aerosols are burning of fossil fuel, coal and biomass including waste from agriculture and forest fires. Aerosols can have a cooling or warming effect depending on the chemical composition. Globally the cooling effect dominates and has offset the warming of the greenhouse gases since the year 1750 by around 1/3. However, this is connected with considerable uncertainty and the uncertainty with respect to the effects of aerosols on the radiative balance and climate is one of the main reasons for the large uncertainty in IPCC's projected range of the increase in global temperature. Measuring a wide range of aerosol variables is therefore crucial for improved understanding of global warming and its mitigation.

- **Zeppelin Observatory:** Observations of the total amount of aerosol particles above Ny-Ålesund show increased concentration levels during spring time compared to the rest of the year. This phenomena, called Arctic haze, is due to transport of pollution from lower

latitudes (mainly Europe and Russia) during winter/spring. In 2011 this aerosol pollution was at approximately the same level as previous years. There were also shorter episodes with elevated levels of particles later than springtime. An extension of the aerosol observations at Zeppelin with measurements of the aerosol absorption properties will be very useful to improve the knowledge about the different types of aerosols and their effects in the Arctic atmosphere. Unfortunately we lack access to a comprehensive measurement program of aerosols at Zeppelin, as is available at Birkenes.

- **Birkenes Observatory:** Aerosol observations from the Birkenes observatory are included in the program since 2010 with focus on physical and optical properties important for the understanding of aerosol and climate. Prior to this the aerosol chemical properties were included in the EMEP programs since ca. the year 2000, and measurement from mid 1990s is available. The program is now comprehensive, and provides the necessary information to understand the influence of aerosols on the radiative balance at this site. The aerosols observed at Birkenes are characterized by long-range transport from Great Britain, Central Europe, and the Arctic, with occasional long-range transport episodes also from North America including forest fire aerosols. In addition to the long range transported aerosols, also aerosols from local or regional emissions, either natural or anthropogenic are observed. With respect to local or regional influence on the forming of aerosol particles, it seems like natural emissions from vegetation dominate in summer, whereas anthropogenic emissions dominate in winter at Birkenes. The climate effect of aerosols observed at Birkenes seems in average for the whole year to be cooling, but there is a seasonal variation indicating the influence of a strong source of combustion aerosol in winter. With all caution due to the limited statistical significance of a one-year data series, it can be stated that the annual cycle of aerosols observed at Birkenes is very likely due to local and regional emissions of domestic biomass burning.

**Reactive gases:** Tropospheric ozone and CO have elevated levels in polluted regions like central Europe. They are suitable indicators for long range transport of pollution from the continents to Svalbard, and CO is also a proper tracer for transport of emissions from biomass burning and other fire events. There were fewer episodes with elevated levels of CO at Zeppelin in 2011 than normal. In general there has been **a reduction in the CO concentration at Zeppelin in the period 2003-2011 of approx. 18%**. The reason for this is not yet understood. The annual mean value for 2011 was 116 ppb compared to 126 ppb in 2010. The important greenhouse gas ozone is included in the KLIF program "Monitoring of long-range transboundary air pollution" and analysis of this is presented in Aas, et al., (2012), only a brief overview is presented in this report

### **The crucial link to European atmospheric research infrastructures and legalisation based network**

---

A key point in the analysis and understanding of atmospheric variables are quality assured and harmonised measurements within Europe, as well as on larger geographical scale. NILU acts as the Chemical Coordinating Centre for EMEP<sup>5</sup> and coordinates the atmospheric monitoring work under the Convention on Long-Range Transboundary Air Pollution (under United Nations Economic Commission for Europe). There are mutual benefits and close links between selected infrastructure programs in EU and EMEP. In particular NILU is involved in

---

<sup>5</sup> EMEP: European Monitoring and Evaluation Programme: <http://www.emep.int/>

ACTRIS (Aerosols, Clouds, and Trace gases Research InfraStructure Network, [www.actris.net](http://www.actris.net)) and InGOS (Integrated non-CO<sub>2</sub> greenhouse gases observing system). NILU is also involved in ICOS (Integrated Carbon Observation System), but without any funding. Birkenes and Zeppelin will become ICOS sites if national funding is established. The infrastructure projects are improving the national monitoring program significantly with respect to quality, giving access to more data, and processed products combining data across Europe. The projects are focusing on both long-lived and short-lived climate forcers. International collaboration and harmonisation of these types of observations are required for processes understanding and satisfactory quality of measurement to assess trends. It is important to underline that these projects are crucial for the national monitoring programmes.

## 2. Introduction

The greenhouse effect is a naturally occurring process in the atmosphere caused by trace gases, especially water vapour (H<sub>2</sub>O), carbon dioxide (CO<sub>2</sub>), methane (CH<sub>4</sub>) and nitrous oxide (N<sub>2</sub>O) that naturally occur in the atmosphere. The content of the last three gases in the atmosphere are closely related to emissions from main sources, whilst the water content varies mainly with temperature. Without these gases the global mean temperature would have been much lower. These gases absorb infrared radiation and thereby trap energy emitted by the Earth. Due to this energy trapping the global mean temperature is approximately 13.7°C, more than 30 degrees higher than it would have been without these gases present (IPCC, 2007). This is the natural greenhouse effect. The enhanced greenhouse effect refers to the additional effect of the greenhouse gases from human activities. In the industrial era, after 1750, the concentration of greenhouse gases in the atmosphere has increased significantly. The global atmospheric mean mixing ratios of CO<sub>2</sub> has increased by 39% (from 280 ppm as a pre-industrial concentration to 390 ppm in 2011) and methane has increased by as much as 170% from 700 ppb to 1813 ppb in 2011) according to WMO (WMO, 2012). 2011 showed new record levels of both these gases. The overall changes in the concentrations of the greenhouse gases are the main cause of the global mean temperature rise of 0.74°C over the last century reported by IPCC (2007). Depending on the various emission scenarios used and natural feedback mechanisms the temperature is predicted to increase with 1.1-6.4°C approaching the year 2100, according to IPCC (2007).

Radiative forcing<sup>6</sup> is a useful tool to estimate the relative climate impacts of various components inducing atmospheric radiative changes. The influence of external factors on the climate can be broadly compared using this concept. Revised global-average radiative forcing estimates from the 4<sup>th</sup> IPCC assessment report are shown in Figure 1 (IPCC, 2007). The estimates represent radiative forcing caused by changes in anthropogenic factors since pre-industrial time and up to the year 2005.

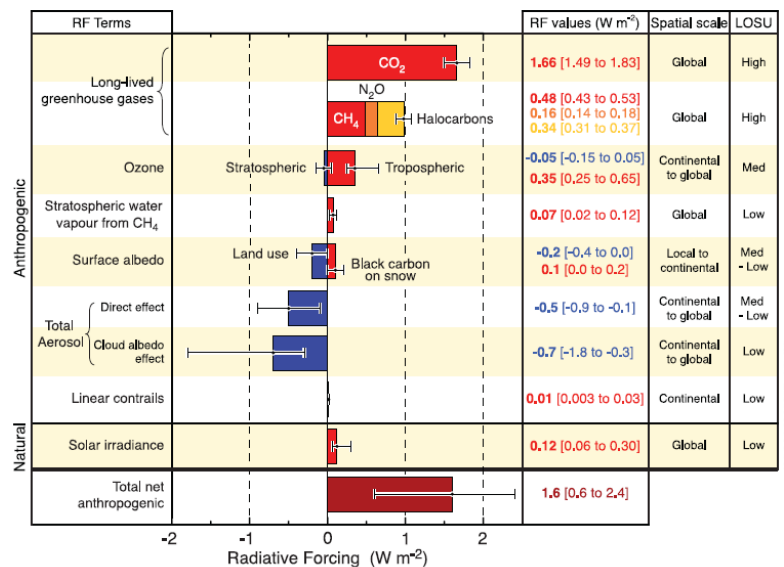


Figure 1: Global-average radiative forcing (RF) estimates for important anthropogenic agents and mechanisms together with the typical spatial scale of the forcing and the assessed level of scientific understanding (LOSU).

<sup>6</sup> Radiative forcing is a measure of the influence a factor has in altering the balance of incoming and outgoing energy in the Earth-atmosphere. It is an index of the importance of the factor as a potential climate change mechanism. It is expressed in Wm<sup>-2</sup> and positive radiative forcing tends to warm the surface. A negative forcing tends to cool the surface.

The most important greenhouse gas emitted from anthropogenic activities is CO<sub>2</sub> with a radiative forcing of 1.66 W m<sup>-2</sup> given in the 4<sup>th</sup> IPCC report (IPCC, 2007). This is an increase of 0.2 W m<sup>-2</sup> since the IPCC report from 2001. CH<sub>4</sub> and N<sub>2</sub>O are other components with strong forcings of 0.48 W m<sup>-2</sup> and 0.16 W m<sup>-2</sup> respectively. It is worth noting that even the change in CO<sub>2</sub> radiative forcing since 2001 is stronger than the total forcing of e.g. N<sub>2</sub>O since 1750, emphasising the importance of CO<sub>2</sub>.

The joint group of halocarbons is also a significant contributor to the radiative forcing. Halocarbons include a wide range of components. The most important ones are the ozone depleting gases regulated through the Montreal protocol. This includes the CFCs, the HCFCs, chlorocarbons, bromocarbons and halons. Other gases are the HFC (fluorinated halocarbons), PFCs (per fluorinated halocarbons), and SF<sub>6</sub>. These fluorinated gases are regulated through the Kyoto protocol. The total forcing of the halocarbons is 0.337 Wm<sup>-2</sup>, and the single component CFC-12 is presently stronger than N<sub>2</sub>O, but the concentration of CFC-12 seems to have reached its peak value. The trend for CFC-12, to lower concentrations, gives reason for optimism for this substance. Observations of the halocarbons and methane are central activities at the Zeppelin observatory. Most of the halocarbons have now a negative trend in the development of the atmospheric mixing ratios.

The diagram below shows the relative contribution (in percent) of the long-lived greenhouse gases and ozone to the anthropogenic greenhouse warming since pre-industrial times (1750). The numbers are based on the radiative forcing estimates in the last IPCC report. The diagram shows that CO<sub>2</sub> has contributed to 55% of the changes in the radiative balance while methane has contributed 16% since pre-industrial times. The halocarbons have contributed 11% to the direct radiative forcing of all long-lived greenhouse gases.

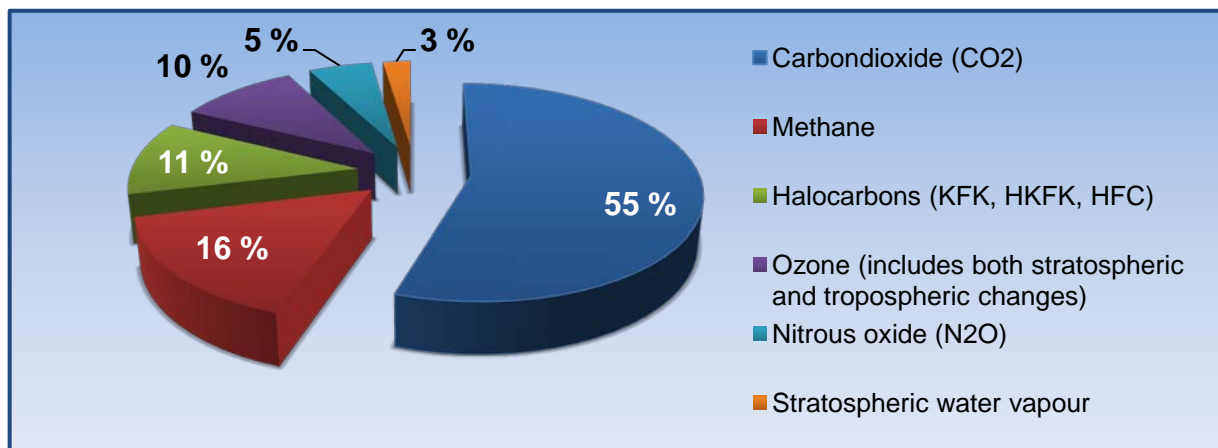


Figure 2: The relative contribution in percent of the long-lived greenhouse gases and ozone to the anthropogenic warming since pre-industrial times (1750). The numbers are based on the radiative forcing estimates in the last IPCC report.

According to the last IPCC report (IPCC, 2007), a large source of uncertainty in climate predictions is caused by insufficient understanding of the atmospheric aerosol processes and historic evolution.

There are two dominant pathways for atmospheric aerosols to influence climate, both exerting a cooling effect in most cases. On one hand, aerosol scatter incoming solar radiation back into

space, preventing it from reaching the ground and warm the surface. This is the so-called direct aerosol climate effect. Additionally, aerosols are activated to cloud particles. Increasing the number of aerosols will in turn increase the cloud particles and also the reflectivity and lifetime of the cloud, again with a cooling effect. This is called indirect aerosol climate effect. Both effects are quantified by negative aerosol radiative forcing in Figure 1 leading to cooling of the surface. The negative aerosol radiative forcing partially offsets the positive, warming radiative forcing by greenhouse gases. In this way the aerosols mask the warming of the greenhouse gases, the magnitude is still uncertain.

***The main objective of NILU's monitoring programme*** is to observe, analyse and interpret the changes in the atmospheric concentrations of the gases included in the Montreal protocol and the Kyoto protocol. An overview of all gases observed together with their trends, lifetime and GWP is given in Table 1 in the Summary. Furthermore the programme shall provide relevant information about aerosols observations important for increased understanding of climate change.

The international collaboration regarding the protection of the ozone layer leading to the Montreal protocol started with the Vienna convention in 1985. Two years later the Montreal protocol was signed and for the first time there was an international agreement forcing the participating countries to reduce and phase out anthropogenic substances. Halocarbons and their relation to the Montreal protocol are indicated in Table 1. Today more than 190 countries have ratified the protocol and many countries have also ratified the later additions to the protocol. The Montreal protocol has goals and strategies for all of the ozone reducing substances and the protocol is a part of the UN environmental program UNEP. According to the last ozone assessment report from WMO (WMO, 2011) the total combined abundance of anthropogenic ozone-depleting gases in the troposphere has continued to decrease from the peak value observed in the 1992-1994 time period. However, the decrease is slower than previous projected due to slower decrease in CFC-11 and CFC12, and also larger increase in HCFC than anticipated. The reduction is around 28% relative to the peak value. In the stratosphere the peak is later, around 200-2002, and the reduction since then is close to 10% (WMO, 2011).

The target set by the Kyoto protocol is to reduce the total emissions of greenhouse gases from the industrialized countries during the period 2008 to 2012. The four most important greenhouse gases and two groups of gases are included: CO<sub>2</sub>, CH<sub>4</sub>, N<sub>2</sub>O, SF<sub>6</sub> (sulphur-hexafluoride), hydrofluorocarbons (HFCs) and perfluorocarbons (PFCs). The emissions are calculated as annual mean values during the period 2008-2012. The gases are considered jointly and weighted in accordance with their global warming potentials as given by IPCC (2007) and shown in Table 1.

A Norwegian introduction to the Montreal and Kyoto protocol can be found at "Miljøstatus Norge" (<http://www.miljostatus.no>). The English link to the Montreal protocol is [http://ozone.unep.org/Ratification\\_status/montreal\\_protocol.shtml](http://ozone.unep.org/Ratification_status/montreal_protocol.shtml) whereas the Kyoto protocol can be found at [http://unfccc.int/essential\\_background/kyoto\\_protocol/items/1678.php](http://unfccc.int/essential_background/kyoto_protocol/items/1678.php).

### 3. The Zeppelin and Birkenes Observatories; Norwegian atmospheric supersites



*Figure 3: Location of NILU's atmospheric supersites measuring greenhouse gases and aerosol properties.*

There are considerable future challenges connected with the understanding of atmospheric change, and the effects of this. This includes the evolution and assessments of long-lived greenhouse gases (LLGHG) as well as the understanding of short-lived climate forces (SLCF) with near time forcing. SLCF includes aerosols and tropospheric ozone in particular, and related gases as CO, NO<sub>x</sub>, methane and volatile organic compounds (VOC). Furthermore also the interaction between aerosols and clouds is largely unknown. Norway has a national interest and particular responsibility to develop harmonized and high quality observation infrastructures in the northern region including the Sub-arctic and Arctic areas. Long range transport of air pollution from the central-European continent is occurring, and of high relevance. There is also transport from the North-American continent, China and other Asian regions (Stohl, 2006) detected at Zeppelin. Furthermore, the industrial development in the Arctic regions, increasing the in oil, gas, and ship activities, will influence the levels of both GHGs and aerosols in this vulnerable region. Moreover, possible emission from the huge reservoirs of methane in the Arctic region is crucial to follow over long time. These are typical emissions from

regions with thawing of permafrost, changes in wetlands and thaw lakes, and methane hydrates at the sea floor. All are sensitive to global warming, with strong positive feedbacks.

The measurement activities at the Zeppelin and Birkenes Observatories contribute to a number of global, regional and national monitoring networks and are atmospheric supersites observatories included in atmospheric research infrastructures as described in 3.1

- EMEP (European Monitoring and Evaluation Programme under "UN Economic Commission for Europe")
- AGAGE (Advanced Global Atmospheric Gases Experiment)
- Global Atmospheric Watch (GAW under WMO)
- Network for detection of atmospheric change (NDAC under UNEP and WMO)
- Arctic Monitoring and Assessment Programme (AMAP)

Most data are public available through the international data base hosted at NILU: <http://ebas.nilu.no>.

### 3.1 Norwegian atmospheric supersites as part of European atmospheric research infrastructures

A key point in the analysis and understanding of atmospheric variables are quality assured and harmonised measurements within Europe, as well as on larger geographical scale. NILU acts as the Chemical Coordinating Centre for EMEP<sup>7</sup> and coordinates the atmospheric monitoring work under the Convention on Long-Range Transboundary Air Pollution (under United Nations Economic Commission for Europe). This is a scientifically based and policy driven programme with high relevance for the institute's involvement in, and relation to, international research infrastructure projects and ESFRI (European Strategy Forum on Research Infrastructures) research infrastructures. There are mutual benefits and close links between selected infrastructure programs in EU and EMEP. In particular NILU is involved in ACTRIS (Aerosols, Clouds, and Trace gases Research InfraStructure Network, [www.actris.net](http://www.actris.net)) and InGOS (Integrated non-CO<sub>2</sub> greenhouse gases observing system). NILU is also involved in ICOS (Integrated Carbon Observation System) and Birkenes and Zeppelin will become ICOS sites if national funding is established. An application to the Norwegian Research Council is currently under review.

The importance of these projects is high for the development of optimised observational infrastructures (both with respect to equipments, analysis and cost) to meet the future needs for studying atmospheric compositional change. The projects are focusing on both long-lived and short-lived climate forcers. International collaboration and harmonisation of these types of observations are crucial for processes understating and satisfactory quality to assess trends. As a part of our work and involvement in InGOS in 2012 our methane analysis is re-evaluated and harmonised with the protocols, guidelines and methods recommended. This is further

described in Appendix I.

The map in Figure 4 shows the sites include in the research infrastructure project ACTRIS ([www.actris.net](http://www.actris.net)). This project started 1. April 2011 and NILU is involved in many parts of the project.

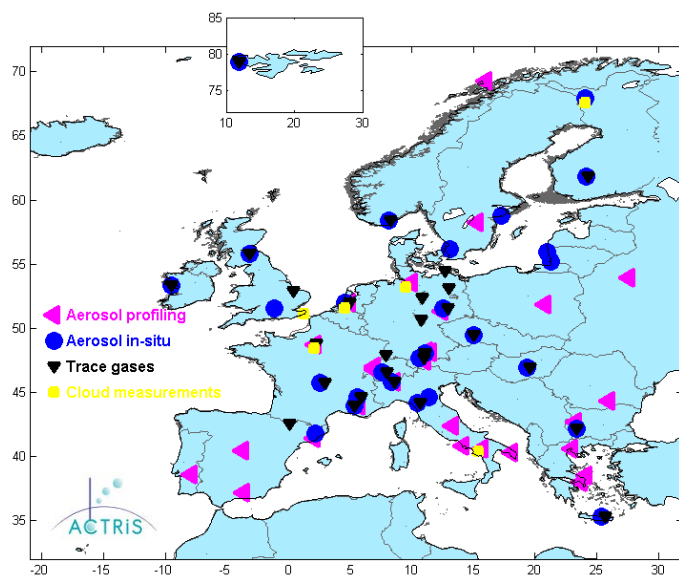


Figure 4: The map shows sites in ACTRIS and the distribution of various types atmospheric measurements.

### 3.2 The Zeppelin Observatory

The monitoring observatory is located in the Arctic on the Zeppelin Mountain, close to Ny-Ålesund at Svalbard. At 79° north the station is placed in an undisturbed arctic environment, away from major pollution sources. Situated 474 meters a.s.l and most of the time above the inversion

layer, there is minimal influence from local pollution sources in the nearby small community of Ny-Ålesund.

<sup>7</sup> EMEP: European Monitoring and Evaluation Programme: <http://www.emep.int/>

The unique location of the station makes it an ideal platform for the monitoring of global atmospheric change and long-range transport of pollution. The main goals of NILU's research activities at the Zeppelin station are:

- Studies of climate related matters and stratospheric ozone
- Exploration of atmospheric long-range transport of pollutants. This includes greenhouse gases, ozone, persistent organic pollutants, aerosols and others.
- Characterization of the arctic atmosphere and studies of atmospheric processes and changes

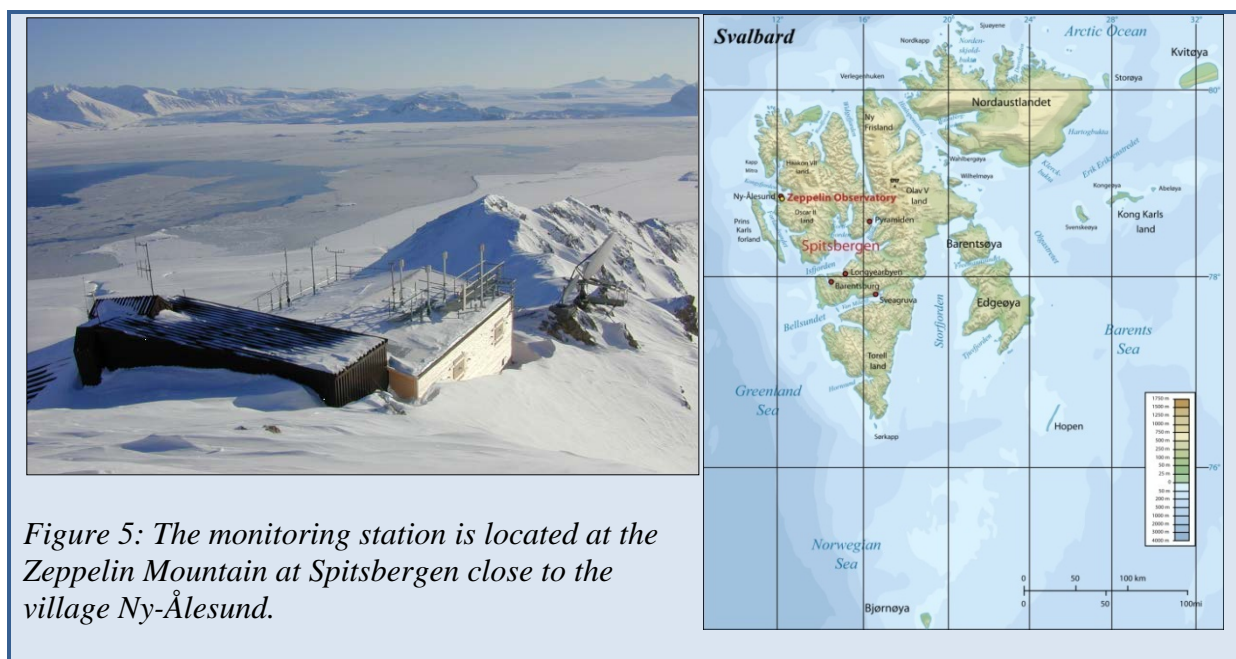


Figure 5: The monitoring station is located at the Zeppelin Mountain at Spitsbergen close to the village Ny-Ålesund.

The Zeppelin station is owned and maintained by the Norwegian Polar Institute. NILU is co-ordinating the scientific activities at the station. The station was built in 1989-1990. After 10 years of use, the old building was removed to give place to a new modern station that was opened in May 2000. The building contains several separate laboratories, some for permanent use by NILU and Stockholm University, others intended for short-term use like measurement campaigns and visiting scientists. A permanent data communication line permits on-line contact with the station for data reading and instrument control.

NILU performs measurements of more than 20 greenhouse gases including halogenated greenhouse gases, methane and carbon monoxide. In Appendix I there are more details about sampling techniques and frequency of observations. CH<sub>4</sub> and CO are sampled 3 times per hour. This high sampling frequency gives valuable data for the examination of episodes caused by long-range transport of pollutants as well as a good basis for the study of trends and global atmospheric change. Close cooperation with AGAGE-partners on the halocarbon instrument and audits on the methane and CO-instruments performed by EMPA (see <http://www.empa.ch>) on the behalf of GAW/WMO results in show data of high quality.

The amount of particles in the air is monitored by a Precision-Filter-Radiometer (PFR) sun photometer. This instrument gives the aerosol optical depth (AOD). AOD is a measure of the aerosols attenuation of solar radiation in the total atmospheric column.

The instrumentation measuring aerosol microphysical and optical properties, which is operated by Stockholm University and has been the same since the opening of the station in 1991, has been modernized with the aim of meeting operation guidelines and quality standards set out by the European Supersites for Atmospheric Aerosol Research<sup>8</sup> (EUSAAR) network.

The station at Zeppelin Mountain is also used for a wide range of other measurements, which are not reported here, including daily measurements of sulphur and nitrogen compounds ( $\text{SO}_2$ ,  $\text{SO}_4^{2-}$ ,  $(\text{NO}_3^- + \text{HNO}_3)$  and  $(\text{NH}_4^+ + \text{NH}_3)$ ), main compounds in precipitation (performed in Ny-Ålesund), total gaseous mercury, particulate heavy metals, persistent organic pollutants (HCB, HCH, PCB, DDT, PAH etc.) in air, as well as tropospheric ozone. Zeppelin observatory is also widely used in campaigns as during the International Polar Year.

At the Zeppelin station carbon dioxide ( $\text{CO}_2$ ) is measured by Stockholm University (SU) (Institute of Applied Environmental Research, ITM). SU maintain an infrared  $\text{CO}_2$  instrument measuring  $\text{CO}_2$  continuously. The instrument has been in operations since 1989. The continuous data are enhanced by the weekly flask sampling programme in co-operation with NOAA CMDL. Analysis of the flask samples provide  $\text{CH}_4$ ,  $\text{CO}$ ,  $\text{H}_2$ ,  $\text{N}_2\text{O}$  and  $\text{SF}_6$  data for the Zeppelin station in addition to  $\text{CO}_2$ .

### 3.3 The Birkenes Observatory

Birkenes is located in Southern-Norway at 58° 23'N, 8° 15'E, 190 m a.s.l. Birkenes atmospheric observatory in Aust-Agder fills a central position in the Norwegian climate monitoring programme since it represents Norway's South also downwind from Europe receiving long range transported air pollution. The observatory has been in operation since 1971 and is one of the longest-running sites in Europe, and it is one of the core EMEP sites. In 2009, the aerosol observation programme at Birkenes Atmospheric Observatory received a major upgrade along with the upgrade of the general station infrastructure. The observatory was moved a few hundred meters and considerably upgraded in 2009 now measuring  $\text{CO}_2$  and  $\text{CH}_4$  with a Picarro instrument and a comprehensive aerosol program. The old station was situated in a hollow with limited line of sight to the oncoming flow. Since summer 2009, the observations are housed in a container assembly on the top of a hill a, with free line of sight to the oncoming flow in all directions (see Figure 6). The land use in the close vicinity of the site is characterized by 65% forest, 10% meadow, 15% freshwater lakes, and 10% agricultural areas (low intensity). This relocation improved the regional representativeness of the station significantly. The observation programme concerning atmospheric aerosol parameters was augmented by measurements of coarse mode particle size distribution, spectral particle scattering coefficient, and aerosol optical depth. It meets now EUSAAR and GAW standards, and comprises now almost all observations considered by the GAW aerosol scientific advisory group as relevant for aerosol climate effect assessments. This upgrade is also an important improvement of the Norwegian observation programme of climate forcing agents, which so far was more focussed on the polar regions. Accurate observations of climate relevant aerosol properties are a prerequisite for better climate predictions for this region.

In 2012, a cloud condensation nucleus counter (CCNC) has been taken into operation at Birkenes. A CCNC measures the number of aerosol particles able to act as nucleus for liquid-phase cloud drops as a function of water vapour supersaturation. This is a key parameter in

---

<sup>8</sup> EUSAAR: European Supersites for Atmospheric Aerosol Research <http://www.eusaar.net>

constraining the indirect aerosol climate effect, i.e. the aerosol effect on cloud lifetime and reflectivity (“colour”). Birkenes is so far the first and only site in continental Norway including this observation. In addition, the instrumentation for measuring the aerosol absorption coefficient has been upgraded from single wavelength to three wavelength operation. Old and new instrument will be operated in parallel for at least a year to ensure a continuous time series.

All electrical and data infrastructure is new and upgrade with Near-Real-Time measurements controlled at NILU. Data from Birkenes (e.g. daily measurements  $\text{SO}_2$ ,  $\text{SO}_4^{2-}$ ,  $\text{NO}_3^- + \text{HNO}_3$  and  $\text{NH}_4^+ + \text{NH}_3$ , main compounds in precipitation, mercury and other heavy metals, persistent organic pollutants, tropospheric ozone) have been essential for the study of long-range transport and deposition of air pollution to Scandinavia. The monitoring at this site, together with other central European regional sites, has provided the necessary background for establishing international binding agreements for targeting emission reductions, c.f. the convention for long-range transboundary air pollutions (CLTRAP) and the protocols hereunder. Personnel is visiting the observatory on a daily basis, and engineers from NILU are present at the station regularly (approximately once per month).

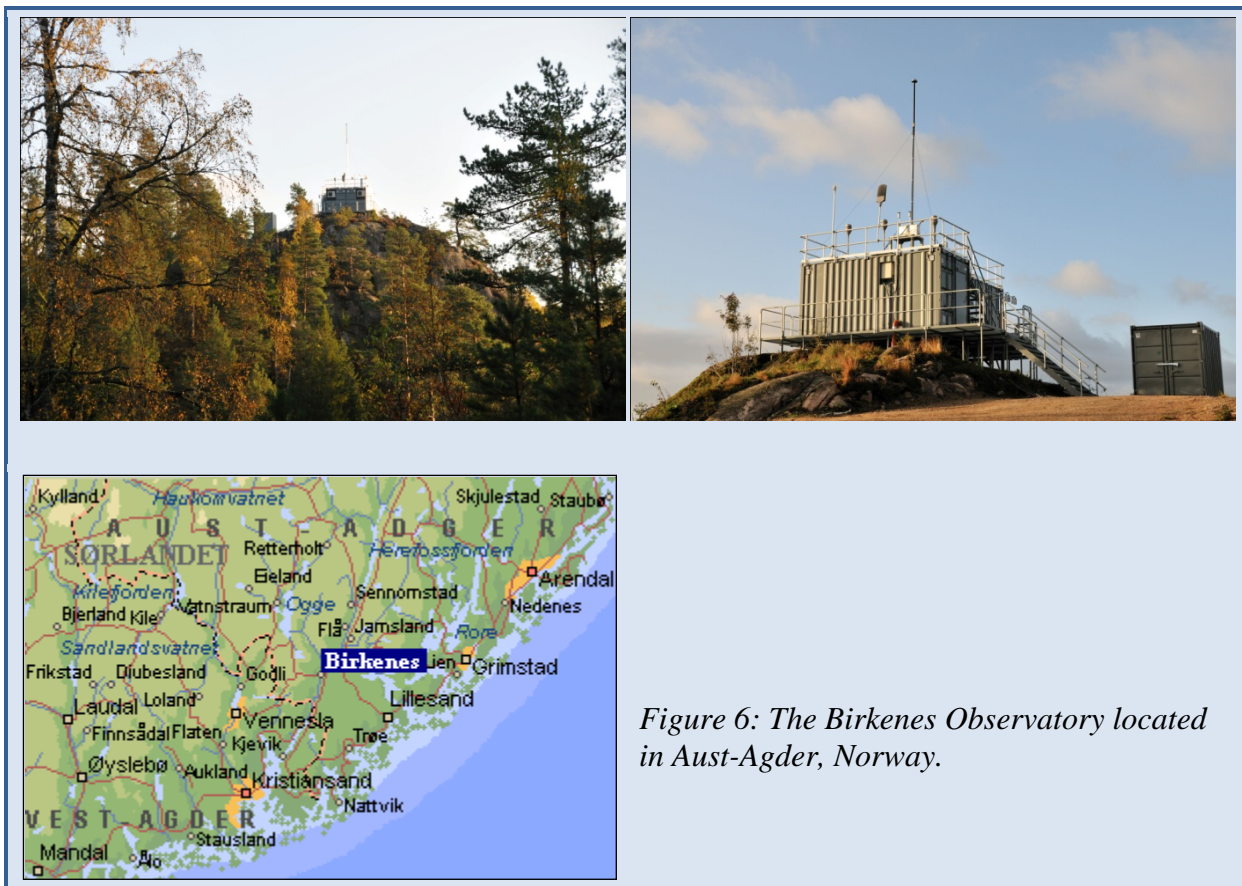


Figure 6: The Birkenes Observatory located in Aust-Agder, Norway.

## 4. Observations and trends of greenhouse gases at the Zeppelin Observatory in the Norwegian Arctic

NILU measures 23 greenhouse gases at the Zeppelin observatory at Svalbard. The results from the measurements, analysis and interpretations are presented in this chapter. Also observations of CO<sub>2</sub>, which are performed by the Stockholm University - Department of Applied Environmental Science (ITM), are included in the report.

Table 2 presents the main results with annual mean values since the beginning of the observation period in 2001. Also trend per year and change (acceleration) in the trend for each component is given. The change in trend (acceleration in the trend) show how the growth rate has changed the last few years<sup>9</sup>.

*Table 2: Yearly average concentration levels of greenhouse gases measured at the Zeppelin station for the years 2001-2011. All concentrations are in ppt<sub>v</sub>, except for methane and carbon monoxide (ppb<sub>v</sub>) and CO<sub>2</sub> (ppm<sub>v</sub>). The trends are calculated from observations for the period 2001-2011.*

Compound	Formula	2001	2011	Trend / year (1 $\sigma$ ) <sup>c</sup>	Change in trend (1 $\sigma$ ) <sup>c</sup>
<b>Methane</b>	CH <sub>4</sub>	1851	1879	+4.3 (0.10)	+0.74 (0.08)
<b>Carbon monoxide</b>	CO		116	-1.2 (0.09)	-0.58 (0.07)
<b>Carbon dioxide<sup>b</sup></b>	CO <sub>2</sub>	370.9	392.5	2.1 <sup>b</sup> (0.02)	-0.07** (0.01)
<b>Chlorofluorocarbons</b>					
CFC-11 <sup>a</sup>	CFCl <sub>3</sub>	259	238	-2.08 (0.008)	-0.04 (0.005)
CFC-12 <sup>a</sup>	CF <sub>2</sub> Cl <sub>2</sub>	547	532	-1.59 (0.02)	-0.51 (0.01)
CFC-113 <sup>a</sup>	CF <sub>2</sub> ClCFCl <sub>2</sub>	81.5	74.6	-0.66 (0.003)	0.01 (0.002)
CFC-115 <sup>a</sup>	CF <sub>3</sub> CF <sub>2</sub> Cl	8.23	8.42	+0.03 (0.001)	-0.005 (0.0006)
<b>Hydrochlorofluorocarbons</b>					
HCFC-22	CHF <sub>2</sub> Cl	159	226	+ 6.9 (0.01)	0.33 (0.01)
HCFC-141b	CH <sub>3</sub> CFCl <sub>2</sub>	16.5	23.0	+ 0.55 (0.002)	-0.02 (0.001)
HCFC-142b <sup>a</sup>	CH <sub>3</sub> CF <sub>2</sub> Cl	14.5	22.7	+ 0.87 (0.002)	+0.03 (0.001)
<b>Hydrofluorocarbons</b>					
HFC-125	CHF <sub>2</sub> CF <sub>3</sub>	2.0	10.9	+0.84 (0.001)	+0.10 (0.0009)
HFC-134a	CH <sub>2</sub> FCF <sub>3</sub>	20.7	68.5	+4.65 (0.003)	+0.03 (0.002)
HFC-152a	CH <sub>3</sub> CHF <sub>2</sub>	2.8	10.1	+0.77 (0.002)	-0.03 (0.002)
<b>Halons</b>					
H-1211 <sup>a</sup>	CF <sub>2</sub> ClBr	4.4	4.2	- 0.02 (0.0002)	-0.02 (0.0001)
H-1301	CF <sub>3</sub> Br	3.0	3.3	+ 0.03 (0.0006)	-0.01 (0.0004)
<b>Halogenated compounds</b>					
Methyl Chloride	CH <sub>3</sub> Cl	505	508	-0.05 (0.10)	-1.28 (0.07)
Methyl Bromide	CH <sub>3</sub> Br	8.9	7.1	-0.181 (0.003)	-0.063 (0.002)
Dichloromethane	CH <sub>2</sub> Cl <sub>2</sub>	31.1	41.2	+1.1 (0.01)	+ 0.20 (0.0009)
Chloroform	CHCl <sub>3</sub>	10.8	12.0	+0.06 (0.004)	+0.07 (0.002)
Methylchloroform	CH <sub>3</sub> CCl <sub>3</sub>	38.3	6.5	-3.08 (0.003)	+0.51 (0.002)
Trichloroethylene	CHClCCl <sub>2</sub>	0.7	0.6	-0.008 (0.003)	+0.02 (0.002)
Perchloroethylene	CCl <sub>2</sub> CCl <sub>2</sub>	4.6	2.8	-0.18 (0.008)	+0.08 (0.006)
Sulphurhexafluoride <sup>a</sup>	SF <sub>6</sub>	4.96	7.50	+0.26 (0.0005)	+0.01 (0.0004)

<sup>a</sup>The measurements of these components are not within the required precision of AGAGE. See Appendix I for more details.

<sup>b</sup>Measurements of Carbon dioxide are performed by Stockholm University, Department of Applied Environmental Science (ITM).

<sup>c</sup>Standard errors from model fit to the data (see appendix A)

<sup>9</sup> As the time series still are short and the seasonal and annual variations are large for many of the components, there are considerable uncertainties connected with the results.

Greenhouse gases have numerous sources both anthropogenic and natural. Trends and future changes in concentrations are determined by their sources and the sinks, and in section 4.1 are observations and trends of the monitored greenhouse gases with both natural and anthropogenic sources presented in more detail. In section 4.2 are the detailed results of the gases with purely anthropogenic sources presented. These gases are not only greenhouse gases but also a considerable source of chlorine and bromine in the stratosphere, and are thus responsible for the ozone depletion and the ozone hole discovered in 1984. The ozone depleting gases are controlled and regulated through the successful Montreal protocol. Section 3 describes the Zeppelin observatory at Svalbard where the measurements take place and the importance of the unique location. Zeppelin observatory is a unique site for observations of changes in the background level of atmospheric components. All peak concentrations of the measured gases are significantly lower at Ny-Ålesund than at other sites, due to the stations remote location. A description of the instrumental and theoretical methods applied is included in Appendix I.

## **4.1 Greenhouse gases with natural and anthropogenic sources**

All gases presented in this section (methane, carbon dioxide, methyl chloride, methyl bromide, carbon monoxide and tropospheric ozone) have both natural and anthropogenic sources. This makes it complex to interpret the observed changes as the sources and sinks are numerous. Moreover, several of these gases are produced in the atmosphere from chemical precursor gases and often also dependant on the solar intensity.

### **4.1.1 Observations of Methane in the period 2001-2011**

Methane (CH<sub>4</sub>) is the second most important greenhouse gas from human activity after CO<sub>2</sub> with a radiative forcing of 0.48 W m<sup>-2</sup> since 1750 and up to 2005 (Forster et al., 2007). In addition to be a dominating greenhouse gas, methane also plays a significant role for the atmospheric chemistry. The atmospheric lifetime of methane is approx. 9 years and about 12 years when indirect effects are included (Forster et al., 2007).

The average CH<sub>4</sub> concentration in the atmosphere is determined by a balance between emission from the various sources at the earth's surface and reaction and removal by free hydroxyl radicals (OH) in the troposphere. In the atmosphere methane is destroyed by reaction with OH giving water vapour and CO<sub>2</sub>. A small fraction is also removed by surface deposition.. Since the reaction with OH also represents a significant loss path for the oxidant OH, additional CH<sub>4</sub> emission will suppress OH and thereby increase the CH<sub>4</sub> lifetime, implying further increases in atmospheric CH<sub>4</sub> concentrations (Isaksen and Hov, 1987; Prather et al., 2001). This positive chemical feedback is estimated to be significant in the current atmosphere with a feedback factor of about 1.4<sup>10</sup> (Prather et al., 2001). The OH radical has a crucial role in the tropospheric chemistry by reactions with many emitted components and is responsible for the cleaning of the atmosphere (like removal of CO, hydrocarbons, HFCs, and others). A stratospheric impact of CH<sub>4</sub> is due to the fact that CH<sub>4</sub> contributes to water vapor buildup in this part of the atmosphere, influencing the ozone layer

The atmospheric mixing ratio of methane has, after a strong increase during the 20<sup>th</sup> century, been relatively stable over the period 1998-2005. The global average change was close to zero for this period according to IPCC (Forster et al, 2007), and also at Zeppelin site for the short period 2001-2004. 2003 was an exception globally and at Zeppelin; a maximum annual mean of 1856 ppb at Zeppelin was obtained, considerable higher than the other years. This was

---

<sup>10</sup> This means that with current atmospheric chemical distribution a 10 % increase in emission of methane, the atmospheric composition increases will reach 14 %.

probably caused by increased precipitation in the tropical regions leading to increased methane emissions from wetland areas and a global rise in the concentration. Recently an increase in the methane levels is evident from both our observations, and observations at other sites (Rigby et al., 2008; WMO, 2011).

Figure 7 depict the observations of methane at Zeppelin since the start in 2001. During 2012 the methane data series from Zeppelin has been revised as part of the EU project InGOS (see section 3.1 and Appendix I). All original measurement signals have been processed with new improved software to recalculate every single measurement over the last 12 years.

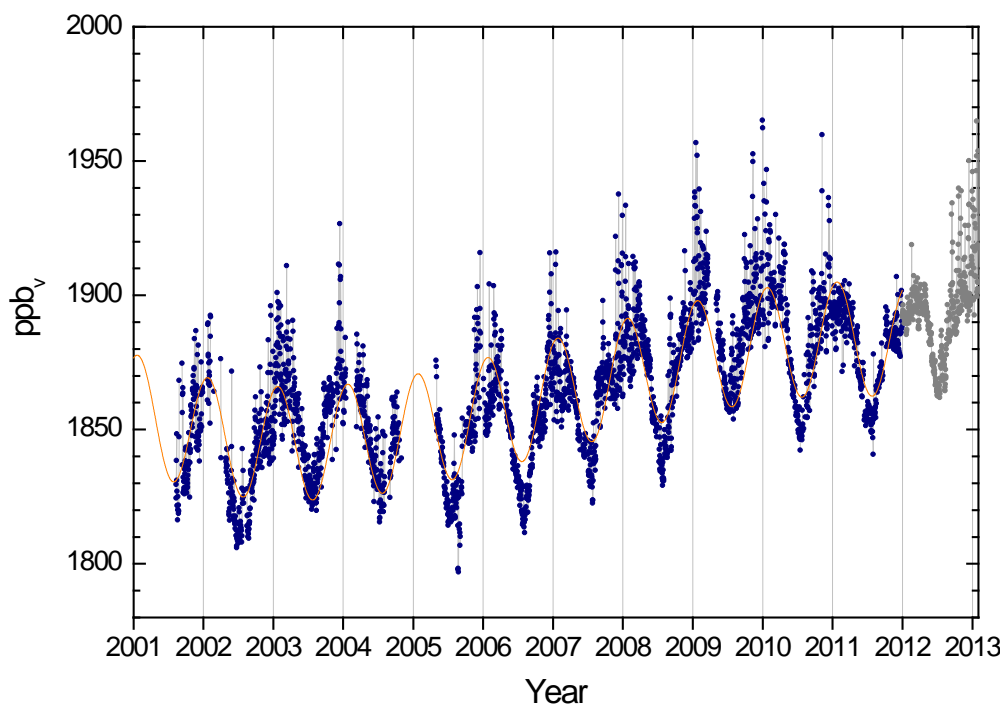


*Figure 7: Observations of daily averaged methane mixing ratio for the period 2001-2011 at the Zeppelin observatory. Blue dots: daily mean observations, orange solid line: modelled background methane mixing ratio, grey dots; preliminary daily mean for the period 01.01.2012- 01.02.2013.*

As can be seen there has been an increase in the concentrations of methane observed at Zeppelin the last years. The pronounced increase started in November/December 2005 and continued throughout the years 2007 - 2009, and is particularly evident in the late summer-winter 2007, and summer-autumn 2009. A maximum methane mixing ratio as high as 1965 ppb was observed 31<sup>st</sup> December 2009. This is the highest value ever recorded at Zeppelin. There were no values nearly as high as this in 2011. The year 2011 showed new record globally, but slightly lower level at Zeppelin, compared to 2009 and 2010. However there were other special characteristics in 2011 at Zeppelin. As can be seen there is remarkable lower variability in the daily mean in 2011 with fewer episodes than the typical situation previous years. This characteristic is also partly evident for CO, displayed in Figure 18 at page 33. The reason for this is still uncertain and under analysis. A simplified analysis of the general transport pattern of air to Zeppelin for 2011 year does not seem to differ from normal situation (see “*Figure 51: The percentage of polluted and clean air arriving at Zeppelin in the period 2001-2011 from the various sectors.*” at page 76). We operated two different instruments in parallel parts of 2012 with satisfactory results (see page 90). There have also

been other changes and improvements at the station during this period (see the Appendix I, particularly section *Methane and nitrous oxide* at page 88). There will be more work on the understanding of this development in relation to the analysis of 2012 data. Note that although there seem to be a small levelling off last year, the *preliminary* results for 2012 indicate a significant continued increase (the grey symbols in Figure 7).

To retrieve the annual trend in the methane for the entire period the observations have been fitted by an empirical equation. The modelled methane values are shown as the orange solid line in Figure 7. Only the observations during periods with clean air arriving at Zeppelin are used in the model, thus the model represents the background level of methane at the site (this is described in Appendix I, page 93). Chapter 8 and Figure 52 visualise the daily mean methane observations when clean air is arriving, compared to daily mean when air from the polluted sections is arriving. At Zeppelin the average annual growth rate is +4.3 ppb<sub>v</sub> per year for the period 2001-2011. This corresponds to an increase of 0.15% per year. For comparison, during 1980s when the methane mixing ratio showed a large increase, the annual global mean change was around 15 ppb<sub>v</sub> per year.

The increase in the methane levels the last years is visualized in Figure 8 showing the CH<sub>4</sub> annual mean mixing ratio for the period 2001-2011. The annual means are based on a combination of the observed methane values and the modelled background values; during periods with lacking observations we have used the modelled background mixing ratios in the calculation of the annual mean.

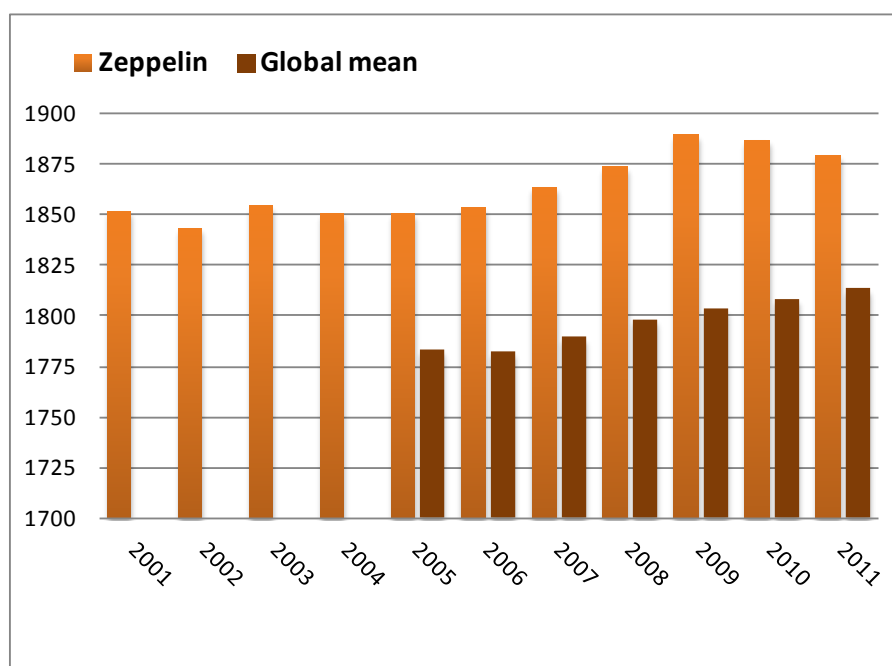


Figure 8: Development of the annual mean mixing ratio of methane in ppb measured at the Zeppelin Observatory (orange bars) for the period 2001-2011 compared to global mean (WMO, 2012).

This diagram clearly illustrates the increase in the concentrations of methane during 2004-2008, with 2009 as the maximum year, and small decrease in both 2010 and 2011. The reduction from 2010-2011 is probably mainly due to reduced variability and fewer episodes

as described above, but might also be due to larger uncertainty connected to the observation in 2010. In 2010 unfortunately more data had to be rejected than previous years due to contamination and a problem with ventilation at the station. A final assessment and correction of this is still in progress.

The annual mean mixing ratio for 2011 was 1879 ppb while the level was 1890 ppb<sub>v</sub> in 2009. The increase since 2005 at Zeppelin is 37.5 ppb (approx. 2 %) which is considered as relatively large compared to the development of the methane mixing ratio in the period from 1999-2005 both at Svalbard and globally. It is also larger than the global mean increase since 2005 which is 30 ppb (WMO, 2009; 2011a). The global mean shows a steady increase the last 3 years of 5 ppb, while larger fluctuations are evident at Zeppelin.

The main sources of methane include boreal and tropical wetlands, rice paddies, emission from ruminant animals, biomass burning, and fossil fuels combustion. Further, methane is the principal component of natural gas and e.g. leakage from pipelines, off-shore and on-shore installations are a known source of atmospheric methane. The distribution between natural and anthropogenic sources is approximately 40% natural sources, and 60% of the sources are direct a result of anthropogenic emissions. Of natural sources there is a large unknown potential methane source at the ocean floor, so called methane hydrates. Other sources include mud volcanoes which are connected with deep geological faults. Further a large unknown amount of methane is bounded in the permafrost layer in Siberia and North America and this might be released if the permafrost layer melts as a feedback to climate change. According to a paper in Nature (Schuur and Abbot, 2011), there is a high risk of permafrost thaw and substantial release of both CO<sub>2</sub> and CH<sub>4</sub>. They estimated a release of 30-63 billion tonnes carbon from Arctic soil before the year 2040 as response to a predicted Arctic temperature increase and scenario with 7.5°C by the year 2100. This is 1.7-5.2 times larger than previous estimates. They assume that most of the carbon release will be as CO<sub>2</sub>, and less than 3% will be emitted as CH<sub>4</sub>. However, because CH<sub>4</sub> has much higher global warming potential (25 compared to CO<sub>2</sub>), almost half of the climate effect will be caused by CH<sub>4</sub>. According to the last IPCC report (Alley et al., 2007) the temperature of the top of the permafrost layer has generally increased by up to 3°C since 1980s.

The recent observed increase in the atmospheric methane concentrations has led to enhanced focus and intensified research to improve the understanding of the methane sources and changes particularly in responses to global and regional temperature increase. Currently the observed increase the last years is not explained or understood. The high level observed in 2003 was a global feature, and is still not fully understood. It is essential to find out if the increase since 2005 is due to large point emissions or if it is caused by newly initiated processes releasing methane to the atmosphere like e.g. the thawing of the permafrost layer. Recent and ongoing scientific discussions point in the direction of increased emissions from wetlands located both in the tropical region and in the Arctic region.

One valuable method to study various methane sources is to exploit isotopic measurements. Many arctic methane sources have different isotopic ratios of  $\delta^{13}\text{C}$  in CH<sub>4</sub>. Combined with model studies of air transport to Zeppelin it is possible to improve the quantification of emission from wetlands, gas from fossil fuel, and emission from methane hydrates at the sea floor. This has been done in selected periods during 2008 and 2009 at Zeppelin and the results are described in Fischer et al. (2011). The study shows that the dominant Arctic summer CH<sub>4</sub> source in 2008 and 2009 was from wetlands. During winter time fossil gas emissions dominated the CH<sub>4</sub> input. Submarine emissions along the West Spitsbergen slope was found

to have negligible CH<sub>4</sub> input to the atmosphere in summer, despite the fact that it was possible to identify methane bubbles in the sea from the sea floor. Gas hydrates at the sea floor are widespread in thick sediments in this area between Spitsbergen and Greenland. If the sea bottom warms, this might initiate further emissions from this source. Our results presented in Fisher et al. (2011) are in agreement with the findings of Bousquet et al. (2011). They have used models to study global source attribution to the changes in atmospheric methane for 2006-2008. Their conclusions were that in 2007 tropical wetland contributed 2/3 to the global increase, but with a significant contribution also from wetlands at high latitudes boreal regions.

Wetland CH<sub>4</sub> emissions respond rapidly to warming. In particular, Arctic and boreal wetlands are likely to respond immediately to sustained heat waves and increases in precipitation. Fire CH<sub>4</sub> is also more likely with elevated temperatures. There is a strong need for more regular CH<sub>4</sub> isotopic measurements in the high Arctic. High effort should be put on the issue to understand the increase in the CH<sub>4</sub> concentrations as the consequence might be severe. Currently NILU has two research projects<sup>11</sup> financed by Norwegian Research Council where the objectives are to understand greenhouse gas budgets and establish isotopic methane measurements at Zeppelin and the infrastructure for improved understanding of the carbon cycle is the main goal of ICOS (see section 3.1)

#### 4.1.2 Observations of Nitrous Oxide at the Zeppelin Observatory

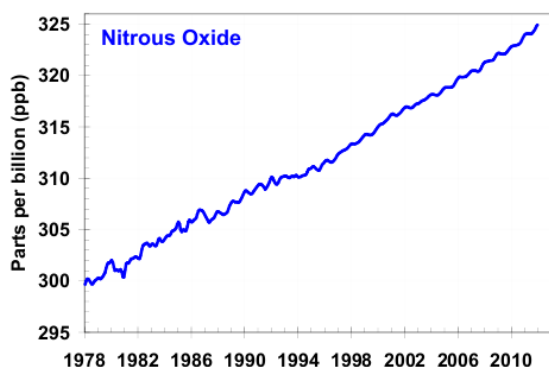


Figure 9: Global average abundances of, nitrous oxide from the NOAA global air sampling network are plotted since the beginning of 1979-2011. <http://www.esrl.noaa.gov/gmd/aggi/>

Nitrous Oxide (N<sub>2</sub>O) is a greenhouse gas with both natural and anthropogenic sources. The sources include oceans, tropical forests, soil, biomass burning, cultivated soil and use of fertilizer, and various industrial processes. There are large uncertainties in the major soil, agricultural, combustion and oceanic sources of N<sub>2</sub>O and also frozen peat soils in Arctic tundra is reports as a potential significant source (Repo et al., 2009). N<sub>2</sub>O has a lifetime of approx. 114 years and the GWP is 310 (Forster et al., 2007). Thus N<sub>2</sub>O is an important greenhouse gas with a radiative forcing of 0.16 W m<sup>-2</sup> since 1750 contributing around 5-6 % to the overall long lived

greenhouse gas forcing over the industrial era. The gas is regulated through the Kyoto protocol. Additionally, N<sub>2</sub>O is also the major source of the ozone-depleting nitric oxide (NO) and nitrogen dioxide (NO<sub>2</sub>) in the stratosphere thus the component is also influencing the stratospheric ozone layer. The recent Assessment of the ozone depletion (WMO, 2011) suggests that current emissions of N<sub>2</sub>O are presently the most significant substance that depletes ozone.

N<sub>2</sub>O has increased from around 270 ppb prior to industrialization and up to an average global mean of 324.2 ppb in 2011 (WMO, 2012a). The, mean annual absolute increase during last

<sup>11</sup> GAME: Causes and effects of Global and Arctic changes in the Methane budget: <http://game.nilu.no>  
GHG-Nor: Greenhouse gases in the North: from local to regional scale

10 years was 0.78 ppb/year (WMO, 2012a). Figure 9 is taken from NOAA and shows the average global development of N<sub>2</sub>O since 1978. The NOAA observations are based on flask samples with mostly weekly or lower time resolution. There are few continuous observations of N<sub>2</sub>O, and particularly in the Arctic region. In 2009 NILU installed a new instrument at Zeppelin to measure N<sub>2</sub>O with high time resolution; 15 minutes. The instrument was in full operation in April 2010 and the results for 2010 and 2011 are presented in Figure 10. The Figure also shows short periods lacking observations sin 2011.

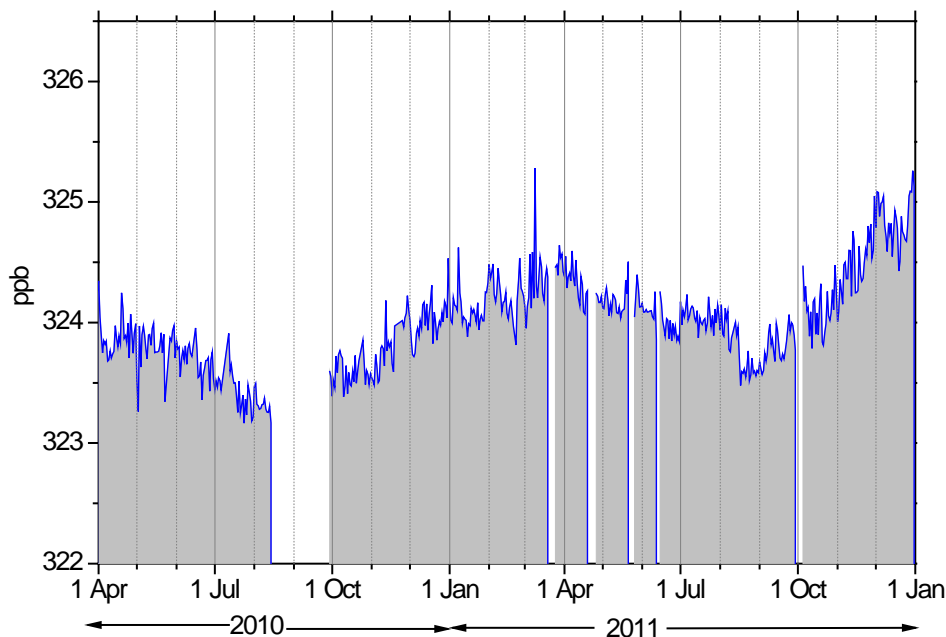


Figure 10: Measurements of N<sub>2</sub>O at the Zeppelin Observatory for 2010-2011.

According to WMO 2012 the global mean value for 2011 was 324.2 with an increase of 1 ppb since 2010. Annual mean for Zeppelin in 2011 was 324.2 with a standard deviation of 0.4 ppb, exactly the same level as global mean values.

#### 4.1.3 Observations of Carbon Dioxide in the period 1988-2011

CO<sub>2</sub> is the most important greenhouse gases with a radiative forcing of 1.66 W m<sup>-2</sup> since 1750 and an increase in the forcing of as much as 0.2 W m<sup>-2</sup> since the IPCC report from 2001 (Forster et al., 2007). CO<sub>2</sub> is the end product in the atmosphere of the oxidation of all main organic compounds and has shown an increase of as much as 45 % since the pre industrial time (WMO, 2012). This is mainly due to emissions from combustion of fossil fuels (fossil fuel CO<sub>2</sub> emissions were 9.1±0.5 PgC in 2010 according to Global Carbon Project (<http://www.globalcarbonproject.org>) and land-use change.

Norway does not perform own measurements of CO<sub>2</sub> at the Zeppelin Observatory but the atmospheric CO<sub>2</sub> concentration measured at Zeppelin Observatory for the period 2001-2011 is presented in Figure 11. These data are provided by ITM University of Stockholm and we acknowledge the effort they are doing in monitoring CO<sub>2</sub> at the site. Note that the data are preliminary and have not undergone full quality assurance.

The results show a continued increase since the start of the observations and in Figure 12 is the development of the annual mean concentrations measured at Zeppelin observatory for the period 1988-2011 shown.

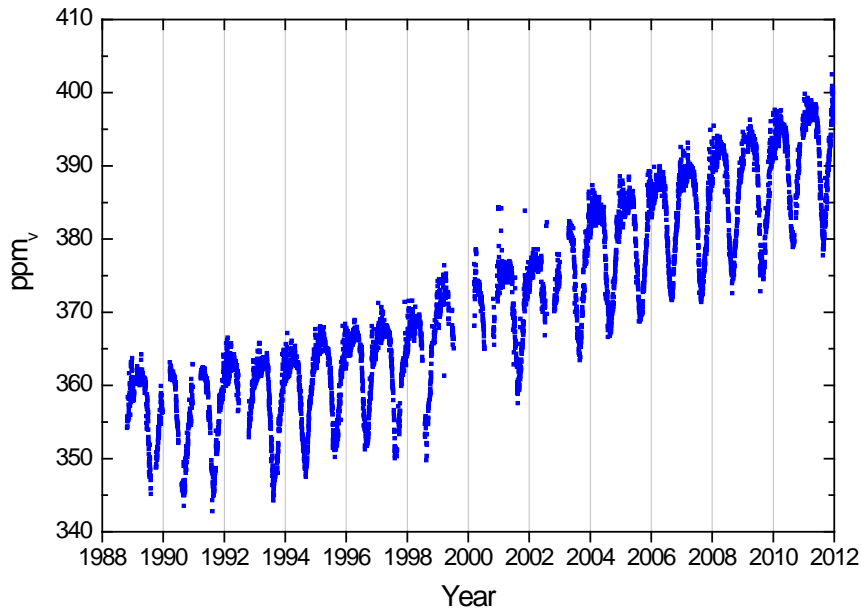


Figure 11: The CO<sub>2</sub> concentration measured at Zeppelin Observatory for the period 2001-2011.

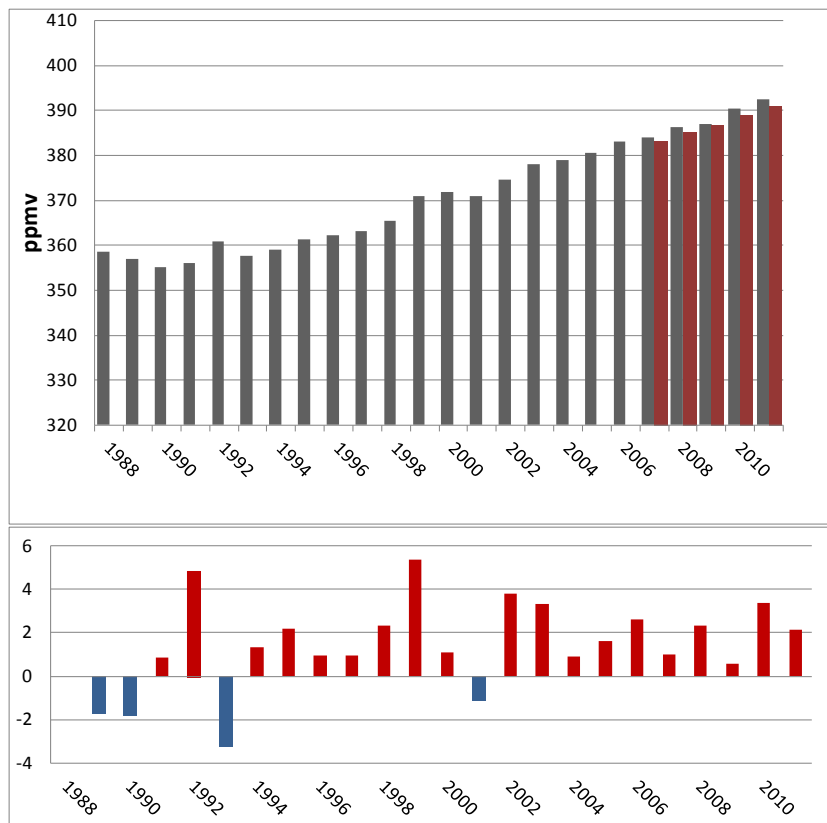


Figure 12: Upper panel: Development of the annual mean mixing ratio of CO<sub>2</sub> measured at Zeppelin observatory for the period 1988-2011. The grey bars are the results from Zeppelin,

and the red bars show the global annual mean for 2007-2011 (WMO, 2012). Lower panel: Yearly change in ppb at Zeppelin.

The preliminary results show that 2011 is a new record year for the annual mixing ratio of CO<sub>2</sub> at Zeppelin, and the increase is larger than the global mean increase with an increase at Zeppelin of 2.2 ppb and a global mean increase of 1.9 ppb (WMO, 2012). This is a lower increase at Zeppelin than last year. ITM University of Stockholm have not completed their analysis of the observations, thus the mean values for the last years are preliminary. The global mean value for 2011 is 390.9 ppb (WMO, 2012). The main reason why the CO<sub>2</sub> level is higher at Zeppelin than globally is that in general the CO<sub>2</sub> emissions is lower in the Southern hemisphere, and the global mixing takes a certain time.

#### 4.1.4 Observations of Methyl Chloride in the period 2001-2011

Methyl chloride (CH<sub>3</sub>Cl) is the most abundant chlorine containing organic gas in the atmosphere, and it contributes approx. 16% to the total Chlorine from the long lived gases in the troposphere (WMO, 2011). The main sources of Methyl Chloride in the atmosphere are natural, and dominating source is thought to be emissions from warm coastal land, particularly from tropical islands are shown to be a significant source but also algae in the ocean, and biomass burning. Several of these sources are expected to vary with global temperature change. Due to the dominating natural sources, this compound is not regulated through any of the Montreal or Kyoto protocols, but is an important natural source of Chlorine to the stratosphere. The degradation of the compound is dependent on solar intensity. To reach the stratosphere, the lifetime in general needs to be in the order of 2-4 years to have significant chlorine contribution, but this is also dependant on the source strength and their regional distribution. Methyl Chloride has relatively high mixing ratios, and contributes to the stratospheric Chlorine burden. With respect to the warming potential this substance is 16 times stronger than CO<sub>2</sub> per kg gas emitted.

The results of the observation of this substance for the period 2001-2011 are shown in Figure 13.

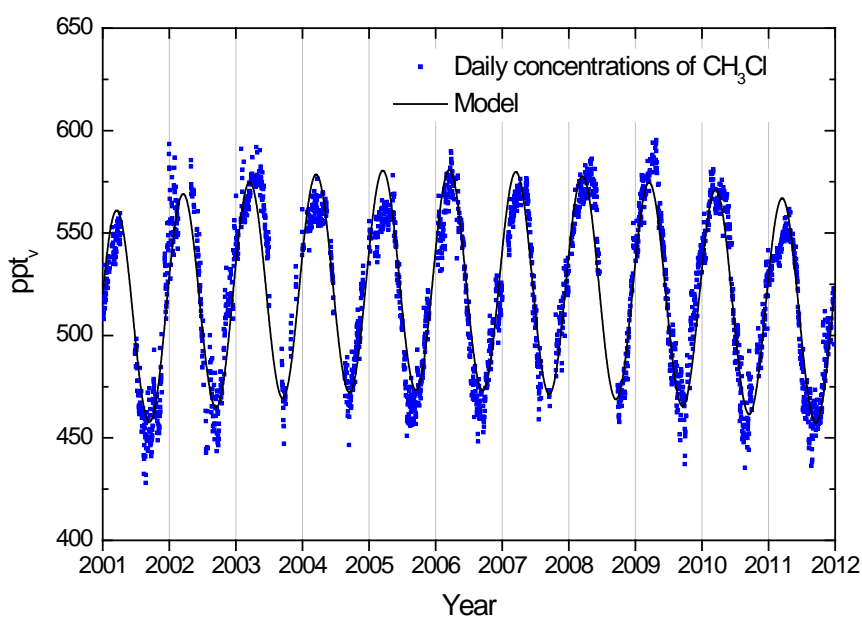
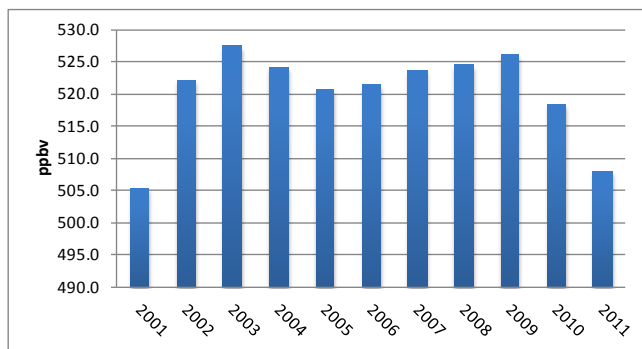


Figure 13: Observations of methyl chloride, CH<sub>3</sub>Cl, for the period 2001-2011 at the

*Zeppelin observatory. Dots: daily averaged concentrations from the observations, solid line: modelled background mixing ratio.*

There is a remarkable decrease the last years. The lifetime of the compound is only 1 year resulting in large seasonal fluctuations as shown in the Figure and rapid response to changes in sources.



*Figure 14: Development of the annual means methyl chloride measured at the Zeppelin Observatory for the period 2001-2011.*

(approx. 3.5%). The reason for this is not understood, and a closer study of sources variation for this compound is recommended, also by WMO (WMO, 2011) as sources are also related to atmospheric temperature change.

By use of the model described in Appendix I we have calculated the annual trend, and the change in the trend is also given in Table 2. The trend for the period 2001-2011 is -0.05 ppt per year, and the change in the trend is -1.28, last 2 years show an apparent change in the development.

The annual means of methyl chloride for the period 2001-2011 is presented in Figure 14. The period 2002-2009 was relatively stable, but since 2009 there is a decrease of as much as 18 ppt

#### **4.1.5 Observations of Methyl Bromide in the period 2001-2011**

The sources of Methyl Bromide ( $\text{CH}_3\text{Br}$ ) are both from natural and anthropogenic activities. The natural sources such as the ocean, plants, and soil, can also be a sink for this substance. Additionally there are also significant anthropogenic sources; it is used in a broad spectrum of pesticides in the control of pest insects, nematodes, weeds, pathogens, and rodents. Biomass burning is also a source and it is also used in agriculture primarily for soil fumigation, as well as for commodity and quarantine treatment, and structural fumigation. While methyl bromide is a natural substance, the additional methyl bromide added to the atmosphere by humans contributes to the man made thinning of the ozone layer. Total organic bromine from halons and methyl bromide peaked in 1998 and has declined since. The tropospheric abundance of bromine is decreasing, and the stratospheric abundance is no longer increasing (WMO, 2011). The observed decrease in stratospheric Bromine was solely a result of declines observed for methyl bromide. Bromine (Br) from halons continues to increase, but at slower rates in recent years, see section 4.2.4 on page 41.

The results of the daily averaged observations of this compound for the period 2001-2011 are shown in Figure 15.

A relatively large change is evident after the year 2007, a reduction of approx. 20% since the start of our measurements at Zeppelin. Methyl bromide is a greenhouse gas with a lifetime of 0.8 years and it is 5 times stronger than  $\text{CO}_2$ , if the amount emitted of both gases were equal. The short life time explains the large annual and seasonal variations of this compound.

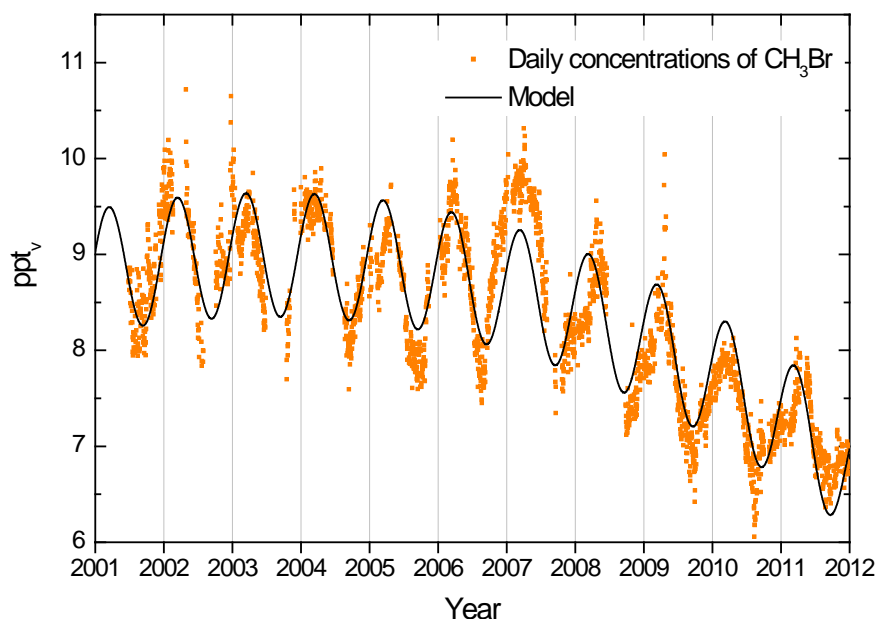


Figure 15: Observations of methyl bromide,  $\text{CH}_3\text{Br}$ , for the period 2001-2011 at the Zeppelin observatory. Dots: daily averages mixing ratios from the observations, solid line: modelled background mixing ratio.

We have calculated the annual trend by use of the model described in Appendix I. The trend and change in the trend is given in Table 2. For the period 2001-2011 there is a reduction in the mixing ratio of  $-0.18$  ppt per year, with relaxation in the trend of  $-0.06$ . However, note that the observed changes are small (approx. 1.6 ppt since 2007) and the time period relatively short thus the seasonal and annual variations of the trends are uncertain.

The development of the annual means for the period 2001-2011 is presented in Figure 16, clearly illustrating the decrease the last years. In general atmospheric amounts of methyl bromide have declined since the beginning in 1999 when industrial production was reduced as a result of the Montreal protocol. The global mean mixing ratio was 7.3-7.5 ppt in 2008, slightly lower than at Zeppelin and also the annual mean reduction is slower than at Zeppelin,  $0.14$  ppt/year (WMO, 2011). The differences are explained by slower inter hemispheric mixing. The recent reduction is explained by considerable reduction in the use of this compound; in 2008 the use was 73% lower than the peak year in late 1990s (WMO, 2011).

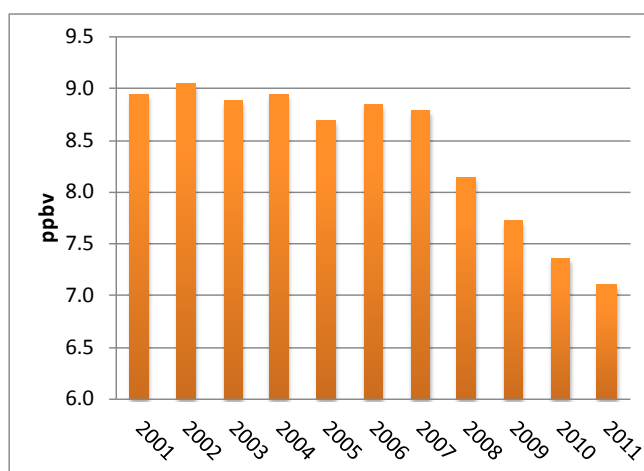


Figure 16: Development of the annual means of Methyl Bromide measured at the Zeppelin Observatory for the period 2001-2011.

#### 4.1.6 Observations of tropospheric ozone in the period 1990-2011

Tropospheric ozone, which is the ozone in the lower part of the atmosphere, is a natural constituent of the atmosphere and plays a vital role in many atmospheric processes. It is also a

short-lived greenhouse gas with a radiative forcing of  $+0.35 \text{ W m}^{-2}$  (IPCC, 2007) due to man made changes in the concentrations since 1750. This is 10% of the overall global radiative forcing since 1750 making this component as the third most influencing greenhouse gas (see Figure 1 on page 13). Tropospheric ozone is a central short-lived climate forcer (SLCF) receiving enhanced focus the last years in both research and monitoring internationally. In a recent report UNEP<sup>12</sup> advocates for SLCF mitigation strategies to complement  $\text{CO}_2$  reductions. In addition to ozone, SLCF includes aerosols, black carbon (in aerosols) and sometime also direct or indirect effects of methane. Ozone is not emitted directly to the atmosphere, but it is rather produced from precursor gases; the formation of ozone is due to a large number of photochemical reactions taking place in the atmosphere and depends on the temperature, humidity and solar radiation as well as the primary emissions of nitrogen oxides, CO and volatile organic compounds. Anthropogenic emissions of VOC and nitrogen oxides have increased the photochemical formation of ozone in the troposphere. Until the end of the 1960s the problem was basically believed to be one of the big cities and their immediate surroundings. In the 1970s, however, it was found that the problem of photochemical oxidant formation is much more widespread. The ongoing monitoring of ozone at rural sites throughout Europe shows that episodes of high concentrations of ground-level ozone occur over most parts of the continent every summer. Future observations and understanding of precursors gases is targeted both by EMEP and the EU infrastructure project ACTRIS (see section 3.1). As there are no direct anthropogenic sources for ozone; the component is not regulated by the Kyoto protocol.

The 1999 Gothenburg Protocol is designed for a joint abatement of acidification, eutrophication and ground-level ozone. The critical levels defined by ECE for protection of vegetation are  $150 \mu\text{g}/\text{m}^3$  for hourly mean,  $60 \mu\text{g}/\text{m}^3$  for eight-hour mean and  $50 \mu\text{g}/\text{m}^3$  for seven-hour mean (9 a.m. - 4 p.m.) averaged over the growing season (April-September).

The important greenhouse gas ozone is included in the KLIF program “Monitoring of long-range transboundary air pollution” and analysis of this is presented in Aas, et al., (2012), only brief overview is presented here. The observed ozone mixing ratios at the Zeppelin Observatory for the period 1990-2011 are shown in Figure 17.

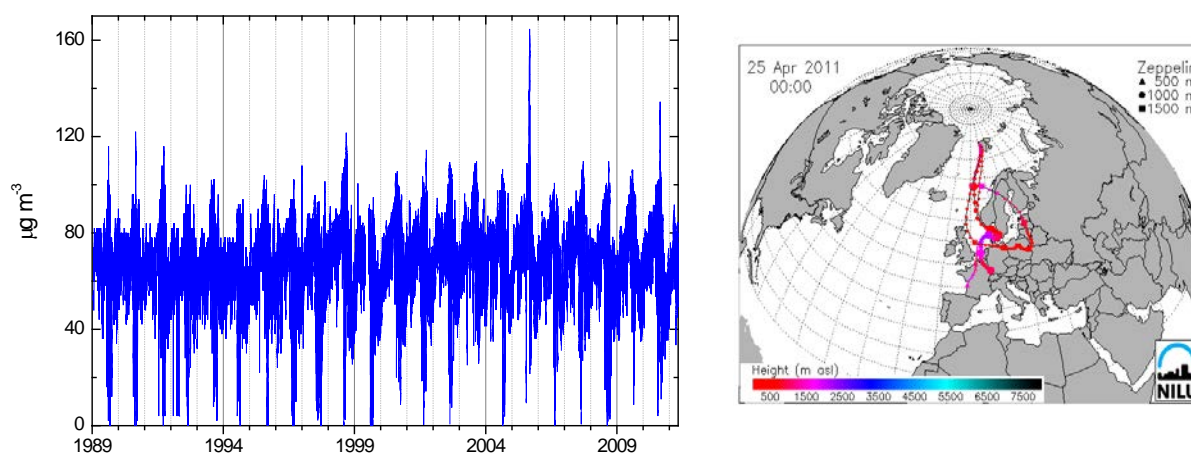


Figure 17: Observations of ozone in the troposphere for the period 1990-2011 at the Zeppelin observatory. Blue line: hourly average concentrations. The panel to the right shows the transport pathway of the air to Zeppelin at the day with maximum value, 25 April 2011.

<sup>12</sup> [http://www.unep.org/dewa/Portals/67/pdf/Black\\_Carbon.pdf](http://www.unep.org/dewa/Portals/67/pdf/Black_Carbon.pdf)

There are large seasonal variations due to relatively short lifetime and the dependency on solar radiation and interactions with precursors gases. In 2006 there was an extreme episode with transport of pollution into the Arctic region and ozone levels as high as  $\sim 160 \mu\text{g m}^{-3}$ . This was above all critical levels. In 2011 there have been few strong episodes, and the maximum ozone level observed was  $134 \mu\text{g m}^{-3}$  at 25<sup>h</sup> of April 2011 during night time. Analysis of the air transport to the Zeppelin Observatory this day shows that the air arrived from Poland and Eastern-Europe.

#### 4.1.7 Observations of CO in the period 2001-2011

Carbon monoxide (CO) is not considered as a direct greenhouse gas, mostly because it does not absorb terrestrial thermal IR energy strongly enough. However, CO is able to modulate the level of methane and production tropospheric ozone which are both very important climate components. CO is closely linked to the cycles of methane and ozone and, like methane; CO plays a key role in the control of the OH radical. CO is also emitted from biomass burning.

The observed CO mixing ratio for the period September 2001-2011 is shown in Figure 18.

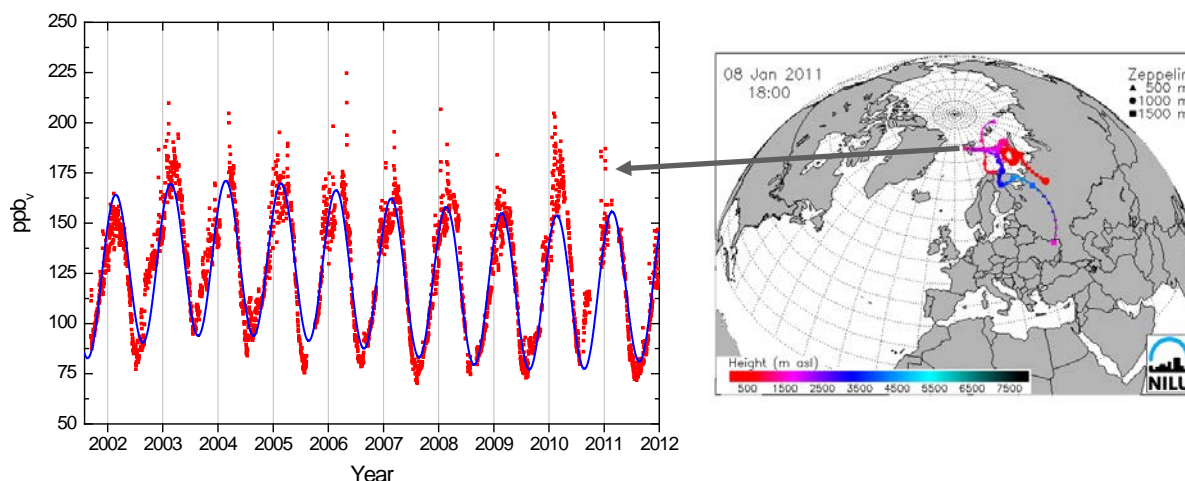


*Figure 18: Observations of carbon monoxide (CO) from the September 2001 to 31.12.2010 at the Zeppelin observatory. Red dots: daily averaged observed mixing ratios. The solid line is the modelled background mixing ratio. The maximum value in 2011 is caused by transport of pollution from North west Russia.*

The concentrations of CO show characteristic seasonal variations with large amplitudes in the Northern Hemisphere and small ones in the Southern Hemisphere. This seasonal cycle is driven by variations in OH concentration as a sink, emission by industries and biomass burning, and transportation on a large scale.

As for methane, the CO measurements for 2011 had lower variability and fewer episodes than most other years. The reasons for this are not clear.

We calculated a trend at Zeppelin of  $-1.21$  ppb per year for the period 2002-2011. The maximum daily average value in 2011 was observed on the 9<sup>th</sup> of January and was 187 ppb. The maximum value is caused by transport of pollution from North West Russia as illustrated to the right in the figure.

The global levels of CO were increasing until the mid-1980s. Thereafter the levels have declined with an averaged global growth rate  $-0.9$  ppb/year for the period from 1992 to 2001. The variability of the growth rates is large. High positive growth rates and subsequent high negative growth rates were observed in northern latitudes and southern low latitudes from 1997 to 1999.

The development of the annual means for the period 2001-2011 is presented in Figure 19, clearly illustrating a maximum in the year of 2003, and a decrease from 2003-2011.

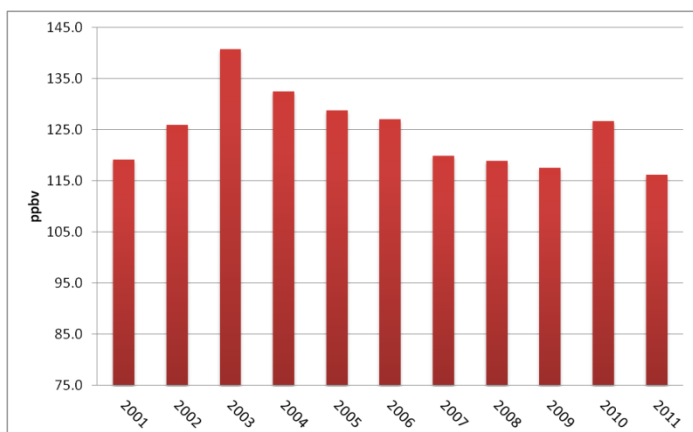


Figure 19: Development of the annual means of CO measured at the Zeppelin Observatory for the period 2001-2011.

In general the CO concentrations measured at Zeppelin show a decrease during the period 2003 to 2011, and 2011 has the lowest annual mean over the period investigated, 116 ppb. For 2010 a small increase is evident as shown in Figure 19. CO is central to monitor as the sources of CO are numerous and complex and the level of this compound is important for the ozone and methane levels.

The highest mixing ratio of CO ever observed at Zeppelin; is 217.2 ppb on the 2<sup>nd</sup> of May 2006. This peak values were due to transport of

polluted air from lower latitudes; urban pollution (e.g. combustion of fossil fuel). CO is an excellent tracer for transport of smoke from fires (biomass burning, agricultural- or forest fires). The compound is very valuable in the interpretation of other variables at Zeppelin. Atmospheric CO sources are oxidation of various organic gases (volatile organic compounds, VOC) from sources as fossil fuel, biomass burning, and also oxidation of methane is important. Additionally emissions from plants and ocean are important sources.

At NILU we wanted to study the influence of biomass burning on our measurement, both aerosols and greenhouse gases at Birkenes and Zeppelin more. This work is performed in a project funded by Norwegian Space Centre and the results so far are described in section 6.

## 4.2 Greenhouse gases with solely anthropogenic sources

All the gases presented in this chapter have solely anthropogenic sources. These are purely man-made greenhouse gases and are called CFCs, HCFCs, HFCs PFCs, SF<sub>6</sub> and halons and most of the gases did not exist in the atmosphere before the 20<sup>th</sup> century. All these gases except for SF<sub>6</sub> are halogenated hydrocarbons. Although the gases have much lower concentration levels than most of the natural gases mentioned in the previous section, they are strong infrared absorbers, many of them with extremely long atmospheric lifetimes resulting in high global warming potentials; see Table 1 on page 8. Together as a group the gases contribute to around 11% to the overall global radiative forcing since 1750.

Some of these gases are ozone depleting, and consequently regulated through the Montreal protocol. Additional chlorine and bromine from CFCs, HCFCs and halons added to the atmosphere contributes to the thinning of the ozone layer, allowing increased UV radiation to reach the earth's surface, with potential impact not only to human health and the environment, but to agricultural crops as well. In 1987 the Montreal Protocol was signed in order to reduce the production and use of these ozone-depleting substances (ODS) and the amount of ODS in the troposphere reached a maximum around 1995. The amount of most of the ODS in the troposphere is now declining slowly and one expects to be back to pre-1980 levels around year 2050. In the stratosphere the peak is reached somewhat later, around the year 2000, and observations until 2004 confirm that the level of stratospheric chlorine has not continued to increase (WMO, 2011).

The CFCs, consisting primarily of CFC-11, -12, and -113, accounted for ~62% of total tropospheric Chlorine in 2004 and accounted for a decline of 9 ppt Chlorine from 2003-2004 (or nearly half of the total Chlorine decline in the troposphere over this period) (WMO, 2007).

There are two generations of substitutes for the CFCs, the main group of the ozone depleting substances. The first generation substitutes is now included in the Montreal protocol as they also influence the ozone layer. This comprises the components called HCFCs listed in Table 1 and Table 2. The second-generation substitutes, the HFCs, are included in the Kyoto protocol. The situation now is that the CFCs have started to decline, while their substitutes are increasing, and many of them have a steep increase.

#### **4.2.1 Observations of Chlorofluorocarbons (CFCs) in the period 2001-2011**

This section includes the results of the observations of the CFCs: CFC-11, CFC-12, CFC-113, CFC-115. These are the main ozone depleting gases, and the anthropogenic emissions started around 1930s and were restricted in the first Montreal protocol. Figure 20 shows the daily averaged observed mixing ratios of these four CFCs. The current instrumentation is not in accordance with recommendations and criteria of AGAGE for measurements of CFCs and there are larger uncertainties in the observations of these compounds, see also Appendix I. As a result also the trends are connected with larger uncertainties. From September 2009 we have new and improved instrumentation installed at Zeppelin providing more accurate observations of these compounds. The higher precisions are clearly visualised in Figure 20.

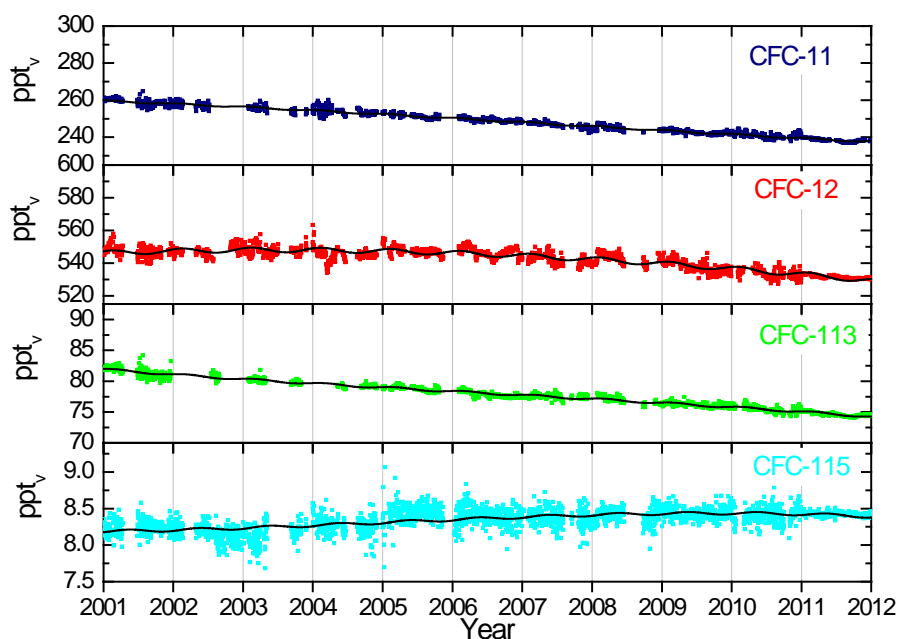


Figure 20: Daily averaged mixing ratios of the monitored CFCs: CFC-11 (dark blue), CFC-12 (red), CFC-113 (green) and CFC-115 (light blue) for the period 2001-2011 at the Zeppelin observatory. The solid lines are modelled background mixing ratio.

The main sources of these compounds were foam blowing, aerosol propellant, temperature control (refrigerators), solvent, and electronics industry. The highest production of the observed CFCs was around 1985 and maximum emissions were around 1987. The life times of the compounds is long as given in Table 1, and also the GWP due to the life time and strong infrared absorption properties is very high.

We have used the model described in Appendix I in the calculation of the annual trends, and changes in the trends. The trends per year for the substances CFC-11, CFC12 and CFC-113 are now all negative given in Table 2, and the changes in the trends are also negative indicating acceleration in the decline<sup>13</sup>. For the compound CFC-115 the trend is still slightly positive, +0.03 ppt/year, but the change in trend is negative and thus we expect the trend for to be negative in few years. In total the development of the CFC levels at the global background site Zeppelin is now very promising.

According to WMO (WMO, 2011) the global mean mixing ratios of CFC-11 are decreasing with approximately 2.0 ppt +/-0.01 ppt and CFC-113 are decreasing by approximately 0.7 ppt from 2007-2008. This is relatively close to our results at Zeppelin for CFC-113 for the period 2001-2011 (-0.7 ppt/yr for 2001-2011), and also for CFC-11 (2.1 ppt/year). The global mean reduction for CFC-12 was -2.2 ppt/year for 2007-2008. For Zeppelin there was a downward trend of 1.6 ppt/year over the period 2001-2011.

<sup>13</sup> The current instrumentation is not in accordance with recommendations and criteria of AGAGE for measurements of the CFCs and there are larger uncertainties in the observations of this compound, see also Appendix I.

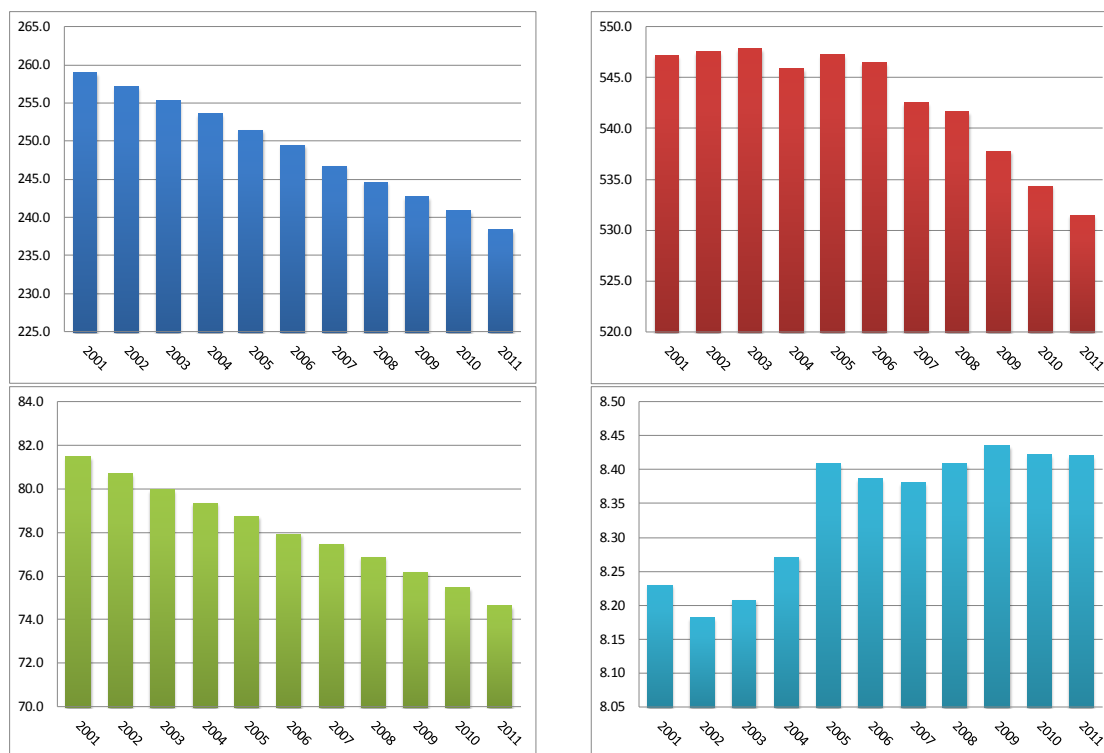


Figure 21: Development of the annual means all the observed CFCs at the Zeppelin Observatory for the period 2001-2011. Upper left panel: CFC-11, upper right panel: CFC-12, lower left panel: CFC-113, lower right panel: CFC-115. See Appendix I for data quality and uncertainty.

The development of the annual means for all the observed CFCs is shown in Figure 21. As described in Appendix I there is now a new instrument at Zeppelin giving improved and more accurate observations of CFCs. The old and new observations are harmonised as described in the appendix. CFC-12 (the red diagram) is the gas with the highest GWP of the CFCs, 10600, and the second highest of all gases observed at Zeppelin. This means that the warming potential of 1 kg emitted CFC-12 gas has 10600 times stronger warming effect than 1 kg emitted CO<sub>2</sub> gas. The global averaged atmospheric mixing ratio of CFC-12 has been decreasing at a rate of 0.5% over the year 2004-2008 (WMO, 2011). This fits well with our observations as illustrated in Figure 21 as CFC-12 has the maximum in 2003-2004, but the variations since 2001 is larger than the global average variation, and there seem to be a clear reduction the last years.

#### 4.2.2 Observations of Hydrochlorofluorocarbons (HCFCs) in the period 2001-2011

This section includes the observations of the following components: HCFC-22, HCFC-141b and HCFC-142b. These are all first generation replacement gases for the CFCs and their lifetimes are rather long. This means that they have potentially strong warming effects, depending on their concentrations and absorption properties; their GWPs are high (see Table 1). The compound HCFC-142b has the highest GWP, and the warming potential is 2400 times stronger than CO<sub>2</sub>, per kg gas emitted. These gases do also contain chlorine, and thus are contributing to the depletion of the ozone layer. The HCFCs accounted for 7.5% of the total tropospheric chlorine in 2004 versus 6% of the total in 2004 (WMO, 2011).

The daily averaged observations of these gases are shown in Figure 22 for the period 2001-2011<sup>13</sup>. As a result also the trends are connected with larger uncertainties. From September 2009 we have new and improved instrumentation installed at Zeppelin providing better observations of these compounds.

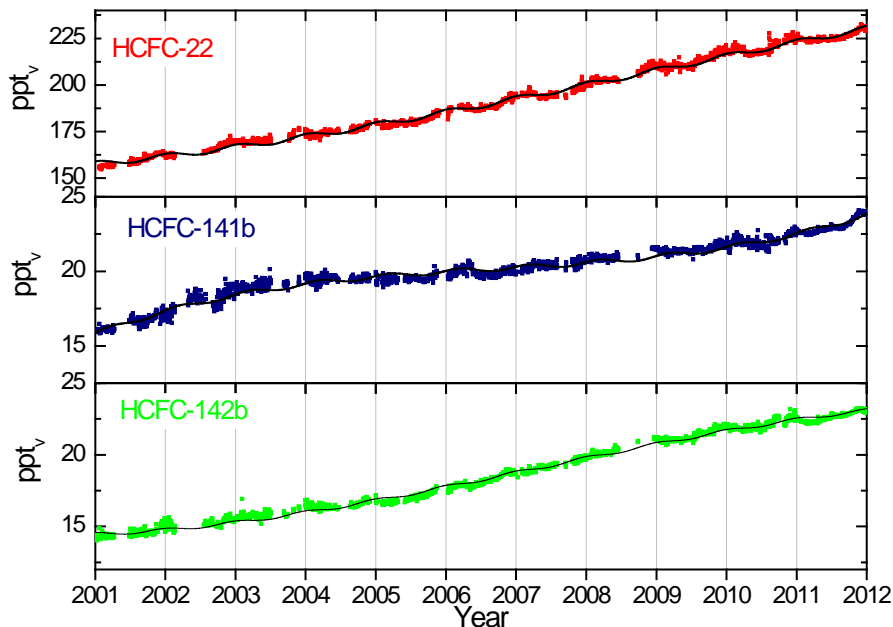


Figure 22: Daily average mixing ratios of the monitored HCFCs: HCFC-22 (red), HCFC-141b (dark blue) HCFC-142b<sup>13</sup> (green) for the period 2001-2011 at the Zeppelin observatory. The solid lines are modelled background mixing ratio.

The trends per year for the compounds HCFC-22, HCFC-141b and HCFC-142b are all positive, and HCFC-22 has the largest change as given in Table 2. HCFC-22 is the most abundant of the HCFCs and is currently increasing at a rate of 6.9 ppt/year over the period 2001-2011. In comparison, the global mean increase for 2007-2008 was approx. 8 ppt according to WMO, (WMO, 2011). Our result for Zeppelin showed an increase of 8.4 ppt for 2007-2008, in close agreement with the annual mean. The mixing ratios of HCFC-141b and HCFC-142b have increased by 0.5 ppt/yr and 0.9 ppt/year, respectively over the same period.

It is worth mentioning that the changes in trends close to zero for HCFC-22 and HCFC-141b, indicating that the yearly increases in the concentrations is stable. The rates of increase for three of these HCFC substances are stronger than or comparable to the scenarios projected in the Ozone Assessment 2006 (WMO, 2011).

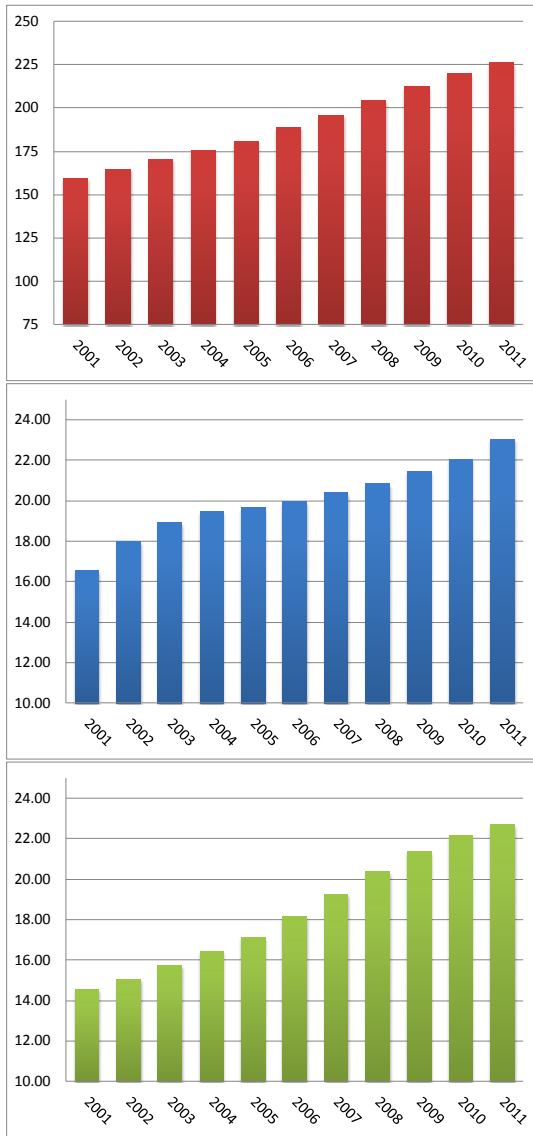


Figure 23: Development of the annual means the observed HCFCs at the Zeppelin Observatory for the period 2001-2011. Red: HCFC-22, Blue: HCFC-141b, and green: HCFC-142b.

Figure 23 shows the annual means for the full period for the three compounds, clearly illustrating the development; an considerable increase. The main sources of these gases are temperature control (refrigerants), foam blowing and solvents, as for the CFCs, which they suppose to replace. All these gases are regulated through the Montreal protocol as they all contain Chlorine. The use of the gases is now frozen, but they are not completely phased out. With lifetimes in the order of 10-20 years it is central to monitor the levels in the future as they have an influence both on the ozone layer, and are strong climate gases.

#### 4.2.3 Observations of Hydrofluorocarbons (HFCs) in the period 2001-2011

The substances called HFCs are the so called second generation replacements of CFCs, which means that they are considered as better alternatives to the CFCs with respect to the ozone layer than HCFCs. This sub-section includes the following components: HFC-125, HFC-134a, HFC-152a with lifetimes in the order of 1.5-29 years. These substances do not contain chlorine thus they do not have a direct influence on the ozone layer, but they are infrared absorbers and contribute to the global warming.

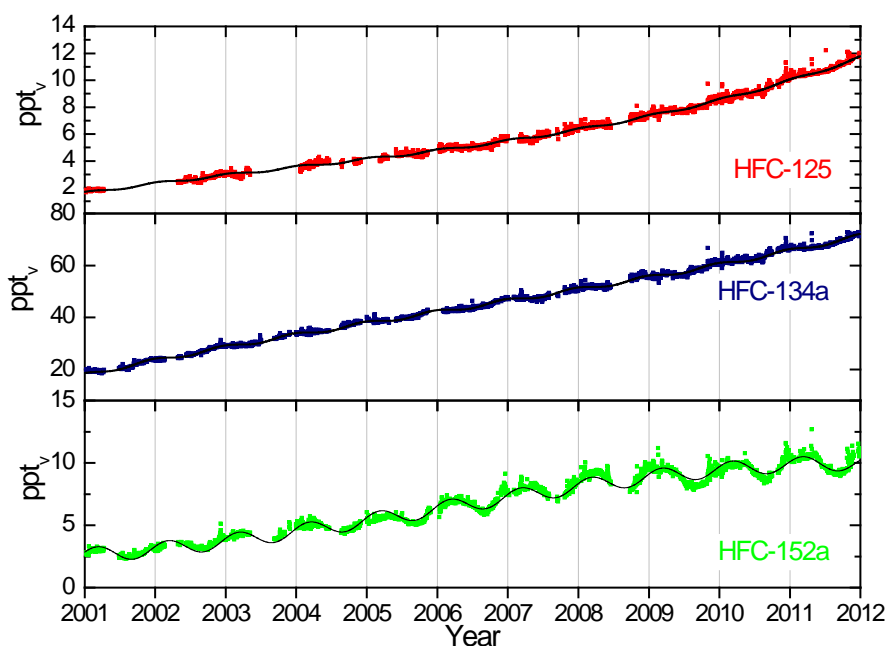


Figure 24: Daily average concentrations of the monitored HFCs: HFC-125 (red), HFC-134a (dark blue), HFC-152a (green) for the period 2001-2011 at the Zeppelin observatory. The solid lines are modelled background mixing ratio.

HFC-152a has the shortest life time and is mainly destroyed in the lowest part of the atmosphere by photolysis and reactions with OH. The seasonal cycle in the observed mixing ratios of these substances is caused by the variation in the incoming solar radiation and is clearly visible in the time series shown in Figure 24 for HFC-152a.

Even if these compounds are better alternatives for the protection of the ozone layer as they do not contain chlorine or bromine, they are still problematic as they are highly potent greenhouse gases. 1 kg of the gas HFC-125 is as much as 3400 times more powerful greenhouse gas than CO<sub>2</sub>. However, still their mixing ratios are rather low, but the background mixing ratios are increasing steeply as our results show. This is also clearly illustrated in Figure 25 showing the development of the annual means. The gases are continuously increasing at a constant rate per year as earlier.

The three main HFCs are HFC-23 (measured at Zeppelin from 2010, not a part of the national monitoring program), HFC-134a and HFC152a. HFC-134a is the most widely used refrigerant (temperature control), and also in air conditioners in cars. Since 1990, when it was almost undetectable in the atmosphere, concentrations of HFC-134a have risen massively. For the period 2001-2011 we find an annual increase per year of 4.6 ppt, which leaves this compound as the one with the second highest change per year of the all the halocarbons measured at Zeppelin. The mixing ratios of HFC-125, HFC-134a and HFC-152a have increased by as much as 360%, 206% and 2037% respectively since 2001. This is a rapid average increase in the interval from ~20-36 % per year. The last ozone Assessment report (WMO, 2011) does not include these compounds as they are not affecting the ozone layer directly.

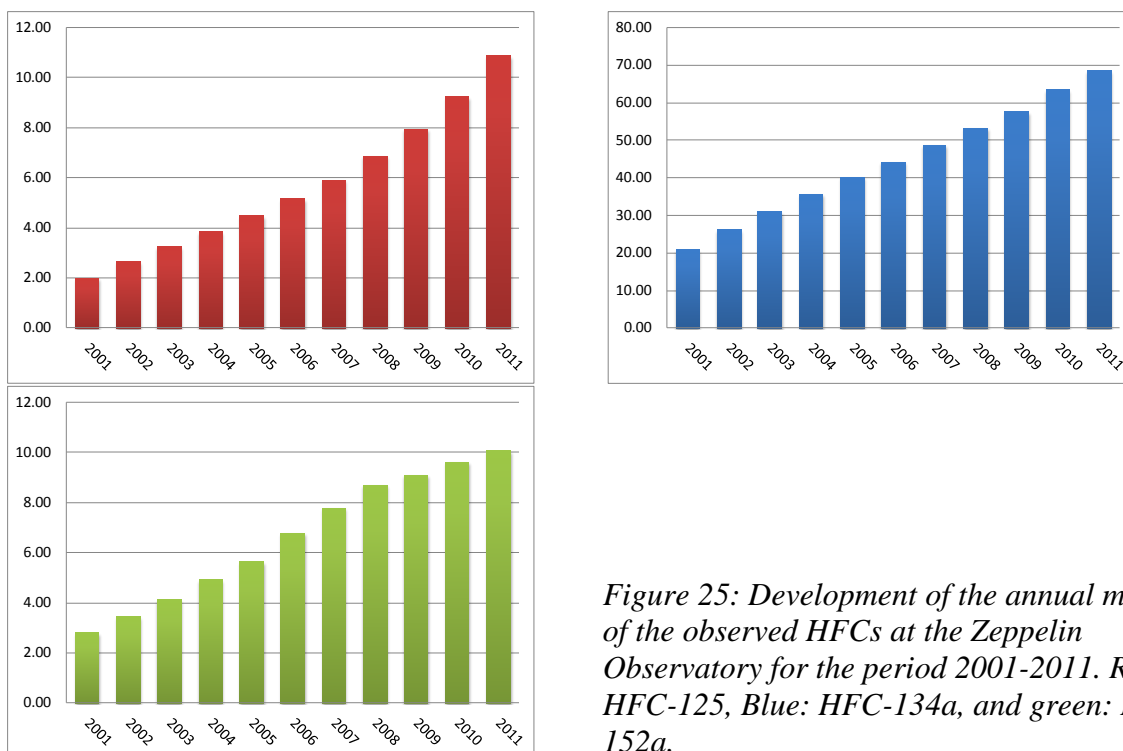


Figure 25: Development of the annual means of the observed HFCs at the Zeppelin Observatory for the period 2001-2011. Red: HFC-125, Blue: HFC-134a, and green: HFC-152a.

Due to the large increase in these compounds it is relevant to calculate the radiative forcing of these observed changes. Based on the assumption that these changes are homogeneous distributed and the same at all locations (constant geographical distribution) we find that the total radiative forcing for these three gases since the start of the emissions is  $0.014 \text{ W m}^{-2}$  (using the forcing efficiency from Forster et al., 2007). Thus the contribution from the recent man made emissions of these gases is still considered as small. This is explained by the (still) low mixing ratios of the compounds. It is important to follow the development of these gases in the future due to the rapid annual growth.

#### 4.2.4 Observations of halons in the period 2001-2011

Halons include the following components: H-1301, H-1211. These climate gases contain bromine, also contributing to the depletion of the ozone layer. Actually, bromine is even more effective in destroying ozone than chlorine. The halons are regulated through the Montreal protocol, and are now phased out. The main source of these substances was fire extinguishers. Figure 26 presents the daily average concentrations of the monitored halons at Zeppelin<sup>13</sup>.

By use of the model described in Appendix I we have calculated the annual trends, and changes in trends, given in Table 2. The trends for the period 2001-2010 shows a small increase for both substances in total, with a very small reduction in the rates indicating that the trend is expected to be lower the next years (if there are no abrupt changes in sources and sinks).

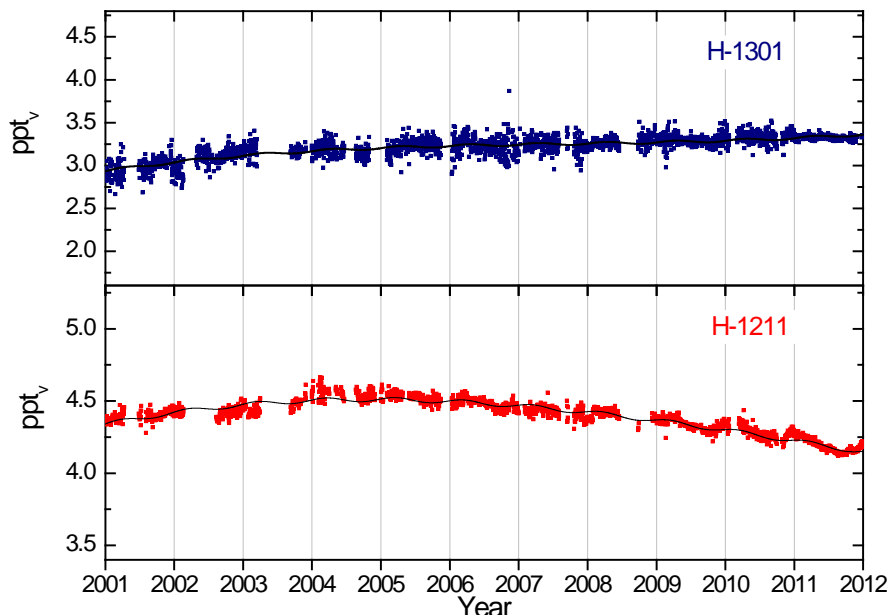


Figure 26: Daily average concentrations of the monitored halons: H-1301 (blue in the upper panel) and H-1211<sup>5</sup> (Red in the lower panel) for the period 2001-2011 at the Zeppelin observatory. The solid lines are modelled background mixing ratio.

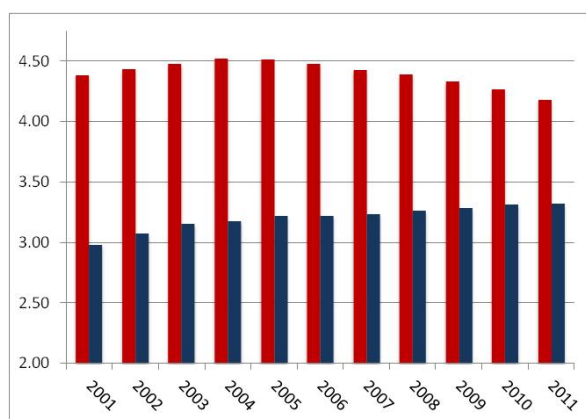


Figure 27: Development of the annual means the observed Halons at the Zeppelin Observatory for the period 2001-2011. Red: Halon-1301, Blue: H-1211.

for H-1301 the increase was around  $\sim 1.2$  ppt (WMO, 2011). Our observations of H-1301 in the Arctic region showed approximately no change from 2007-2008, but a decrease for H-1211 since 2004, also in 2007-2008.

The development of the annual means are shown in the Figure to the left, and the mixing ratios are quite stable over the measured period explained by low emissions and relatively long lifetimes (11 years for H-1211 and 65 years for H-1301.) According to the last Ozone Assessment (WMO, 2011) the total stratospheric Bromine concentration is no longer increasing and Bromine from halons stopped increasing during the period 2005-2008. H-1211 decreased for the first time in this period, while H-1301 continued to increase, but at a slower rate than previously. The global atmospheric decrease in H-1211 was  $\sim 0.04$  ppt in average in 2007-2008 and

#### 4.2.5 Observations of other chlorinated hydrocarbons in the period 2001-2011

This section includes observations of the components: trichloromethane (also called methyl chloroform,  $\text{CH}_3\text{CCl}_3$ ), dichloromethane ( $\text{CH}_2\text{Cl}_2$ ), chloroform ( $\text{CHCl}_3$ ), trichloroethylen ( $\text{CHClCCl}_2$ ), perchloroethylene ( $\text{CCl}_2\text{CCl}_2$ ). The main sources of all these substances are solvents. Note that Chloroform also has natural sources and the largest single source being in offshore sea water. The daily averaged concentrations are shown in Figure 28.

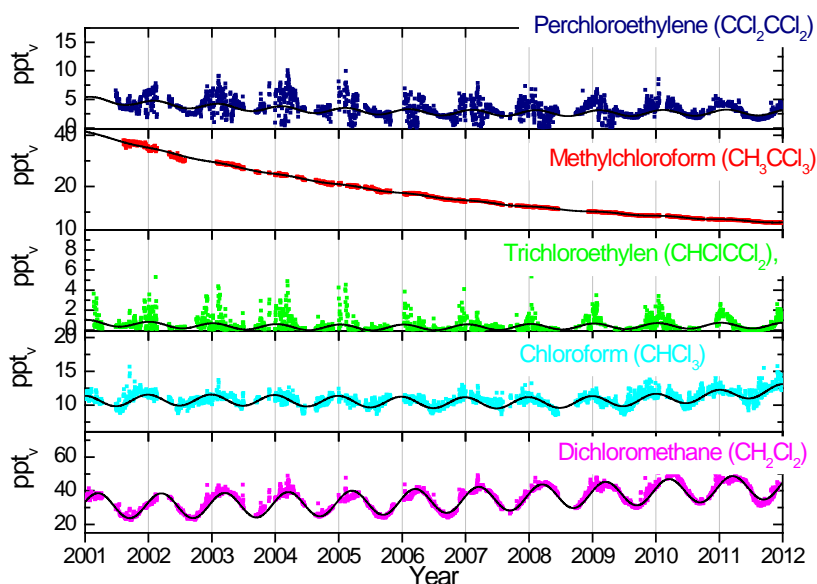


Figure 28: Daily average concentrations chlorinated hydrocarbons: From the upper panel: perchloroethylene (dark blue) methylchloroform (red), trichloroethylen (green), chloroform (light blue) and dichloromethane (pink) for the period 2001-2011 at the Zeppelin observatory. The solid lines are the modelled background mixing ratio.

Methylchloroform ( $\text{CH}_3\text{CCl}_3$ ) has continued to decrease and accounted only for 1% of the total tropospheric Chlorine in 2008, a reduction from a mean contribution of 10% in the 1980s (WMO, 2011). Globally averaged surface mixing ratios were around 10.5 ppt in 2008 (WMO, 2011) versus 22 ppt in 2004 (WMO, 2007). Our measurements at Zeppelin show that the component has further decreased to low levels, 6.5 ppt, a reduction of 83% since 2001.



Figure 29: Annual means of the chlorinated hydrocarbons. From upper panel: perchloroethylene (grey), trichloromethane (red), trichloroethylene (green), chloroform (blue) and dichloromethane (violet) for the period 2001-2011.

It is worth noting the recent increase in trichloroethylene (green), chloroform (blue). A considerable increase in chloroform is evident at Zeppelin the last years (14% since 2006), and also at other sites (e.g. Mauna Loa at Hawaii and Barrow in Alaska). This is not expected and the reason for this is not yet clear. Large seasonal variations are observed for this component as the lifetime is only 1 year (see Figure 28).

The concentration of trichloroethylene is very low, and uncertainties and missing data might explain at least part of the variations.

#### 4.2.6 Perfluorinated compounds

The only perfluorinated compound measured at Zeppelin is sulphurhexachloride, SF<sub>6</sub>. This is an extremely strong greenhouse gas emitted to the atmosphere mainly from the production of magnesium and electronics industry. The atmospheric lifetime of this compound is as much as 3200 years, and the global warming potential is 22200, which means that the emission of 1 kg of this gas has a warming potential which is 22200 times stronger than 1 kg emitted CO<sub>2</sub>.

The other perfluorinated compounds are also very powerful greenhouse gases thus NILU has extended the monitoring with Carbon tetrafluoride (CF<sub>4</sub>) and hexafluoroethane (C<sub>2</sub>F<sub>6</sub>) from 2010, as we have new and improved instrumentation installed at Zeppelin. However, these compounds are not a part of the national monitoring programme.

The current instrumentation is not the best suited for measurements of SF<sub>6</sub> thus there are larger uncertainties for this compound's mixing ratios than for most of the other compounds reported.<sup>13</sup> The daily averaged concentration of SF<sub>6</sub> is presented in Figure 30. The compound is increasing with a rate of 0.26 ppt/year, and has increased by more than 50% since the start of our measurements in 2001. Note that the variations through the year are not due to seasonal variations, but rather to instrumental adjustments, and also the improvement with the new instrumentation in 2010.

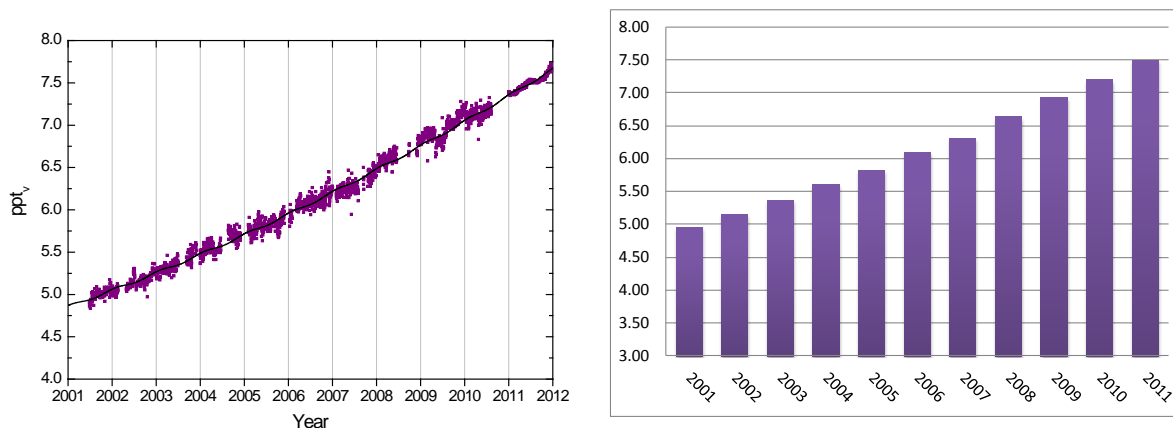


Figure 30: Daily average concentrations of SF<sub>6</sub> for the period 2001-2011<sup>13</sup> to the left, and the development of the annual mean concentrations in the right panel.

## 5. Observations of CO<sub>2</sub> and CH<sub>4</sub> at the Birkenes Observatory in Aust-Agder

In 2009 NILU upgraded and extended the observational activity at the Birkenes Observatory in Aust-Agder. Until 2009 the only Norwegian site measuring LLGHG greenhouse gases was Zeppelin, but from mid May 2009 there are also continues measurements of CO<sub>2</sub> and CH<sub>4</sub> at Birkenes. The results from the start and to 2011 are presented below.

The upper panel shows the daily (black line) and hourly (grey line) variations in CO<sub>2</sub>. It is clear that the variations are largest during the summer months. In this period there is a clear diurnal variation with high values during the night and lower values during daytime. This is mainly due to the plant respiration, but also the meteorological situation during summer contributes to larger variations in the compound. In the lower panel is the CH<sub>4</sub> measurements shown. The diurnal variation for this compound is smaller, but the variations are still largest during summer and early autumn. In addition to the diurnal variations, there are also episodes with higher levels of both components due to transport of pollution from various regions. In general there are high levels when the meteorological situation results in transport from Central Europe.

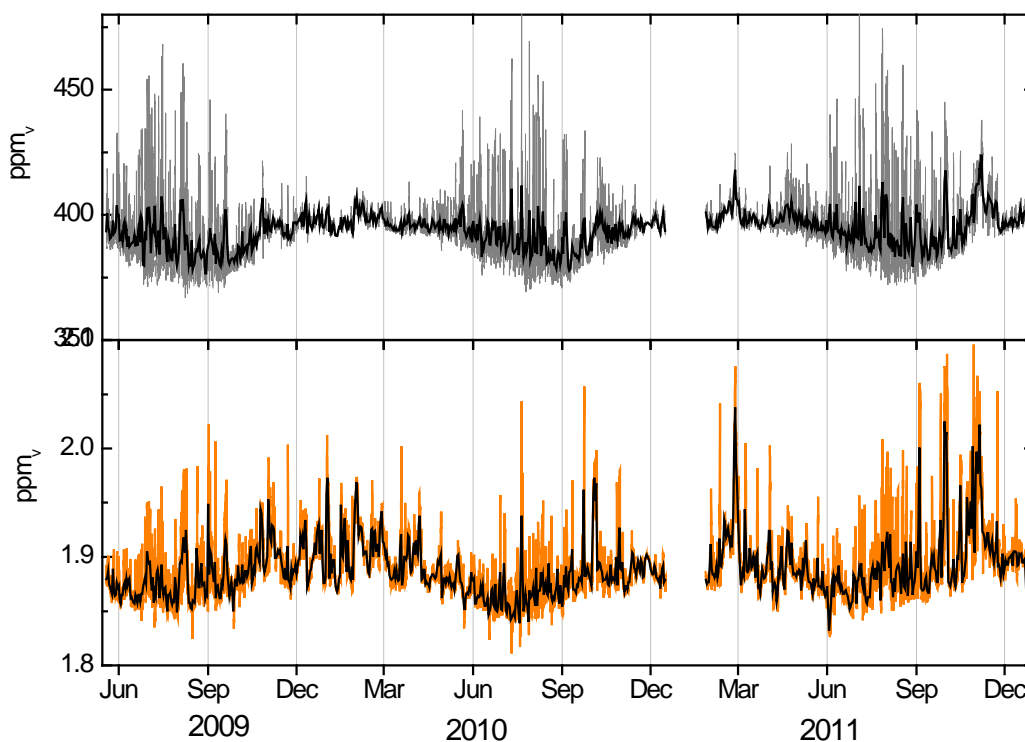
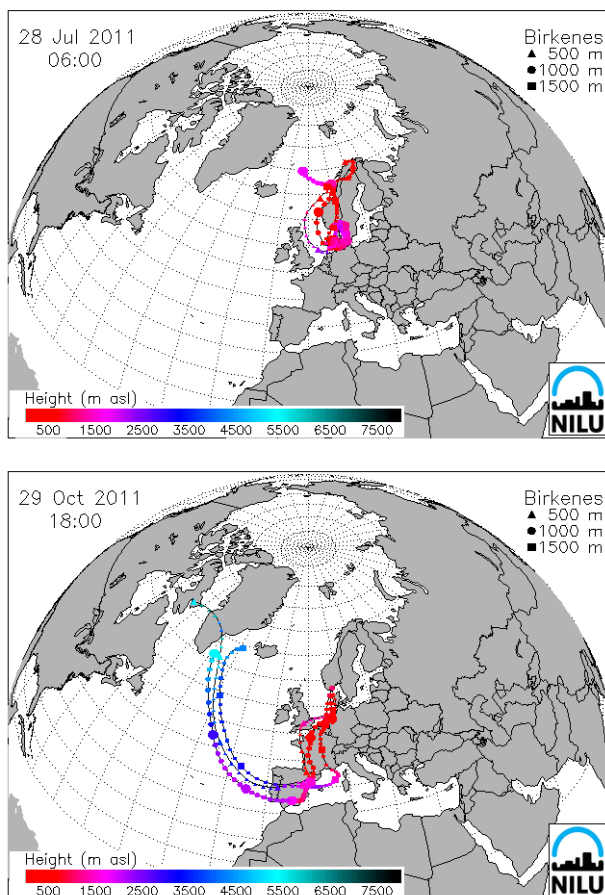


Figure 31: Greenhouse gas measurements at Birkenes Observatory from 19. May 2009 to 31. December 2011. Upper panel: CO<sub>2</sub> measurements, grey line: hourly mean, black line: daily mean. Lower panel: CH<sub>4</sub> from Birkenes, orange line: hourly mean, black line: daily mean.



The highest CO<sub>2</sub> measurements are during summer and particularly warm periods. Maximum value for CO<sub>2</sub> was 474 ppm during night and morning 28 July.

**Error! Reference source not found.** upper panel shows the typical for air mass transport to Birkenes that period. The maximum value of CH<sub>4</sub> is on 29<sup>nd</sup> October 2011, as high as 2.096 ppm. This episode is explained by long range transport of air from Atlantic Ocean and crossing Spain, central. Europe shifting to UK. During episodes with long range transport, both components are elevated, but particularly CH<sub>4</sub> in this episode.

Figure 32: Air mass transport to Birkenes at selected days.

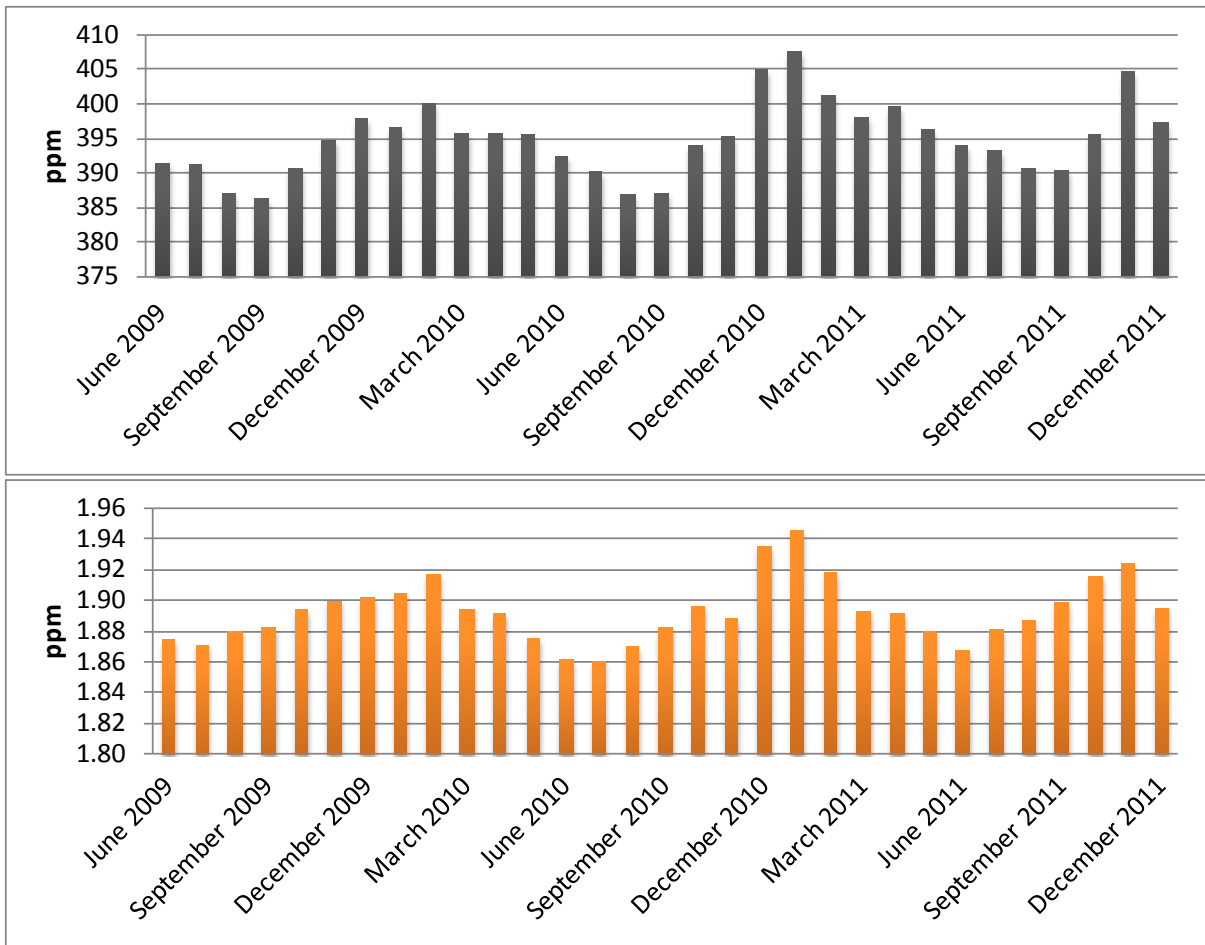


Figure 33: Monthly mean variations for CO<sub>2</sub> (upper panel) and CH<sub>4</sub> (lower panel) at Birkenes Observatory

Figure 33 show the monthly mean variations for both CO<sub>2</sub> and CH<sub>4</sub> at Birkenes. There is a clear minimum in the summer months and a maximum in the fall/winter as expected, and winter 2010/2011 is the period with highest values.

## 6. Analysis of CO from satellite observations to support ground based measurements at Birkenes

CO is a component of particular importance as tracer for biomass burning and knowledge of this compound is important for the understanding of sources and levels of both to aerosols (see chapter 7) and gases like CH<sub>4</sub> and CO<sub>2</sub>. Ground based monitoring of this compound is lacking in Norway, and only available at Svalbard far from fire sources. Based on a project financed by The Norwegian Space Centre (NRS) (Norsk Romsenter, <http://www.romsenter.no/>) we are now in a position where we can support the national monitoring of greenhouse gases and aerosols by exploring and utilize satellite observations of CO. The project, *SatMonAir*, started in January 2012 and ended December 2012. A new project following up the work is starting January 2013, and NRS is highly acknowledged for their support. The results from this work are included in this report (also in section 7.5 at page 69).

The relevant CO products from satellites we have explored is listed in Figure 34.

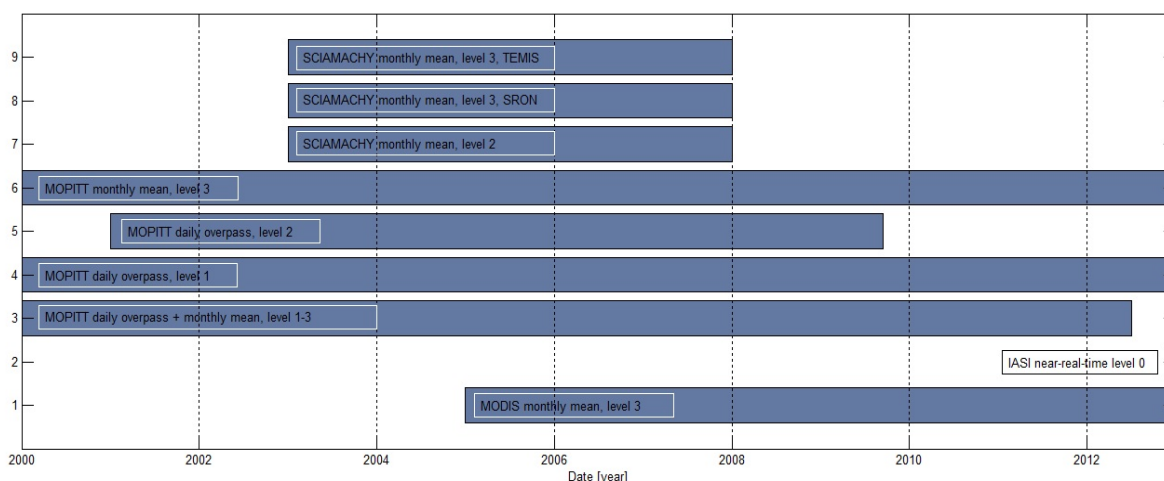
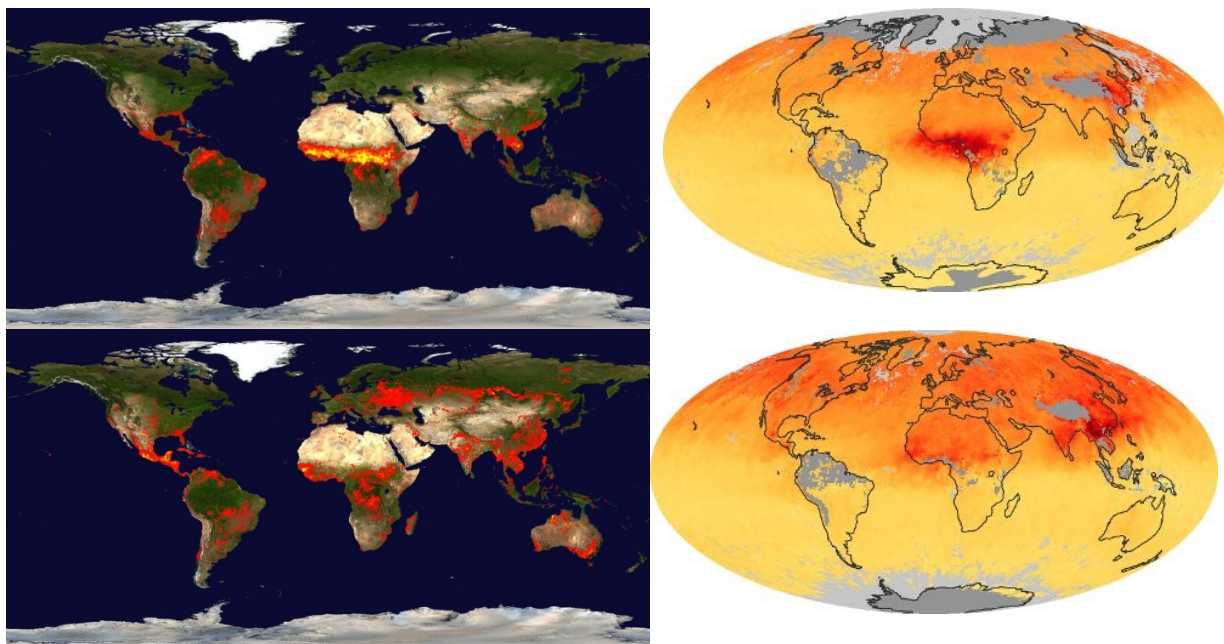


Figure 34: EO-based CO data of particular importance for national monitoring to KLIF.

The goal of this work is twofold; setting up an alert system to follow fires and possible influence on the observations in near real time, and secondly support the analysis of aerosols (particularly the absorbing aerosol) and CO<sub>2</sub> and CH<sub>4</sub>. Not all the above listed products are well suited for our purpose. The availability of data in time and space does in some cases not cover the region or the years of interest, and while investigating the available products in detail, we also discovered that the routines for searching, online plotting and download of data might not be straight forward.

A simple web page serves provides links to the relevant trace gas products, set up for internal use at <http://zardoz.nilu.no/~anm/satmonair/> and <http://zardoz.nilu.no/~anm/satmonair/plots/fires.html>. The web pages does not only contain a list of EO products used, but also URLs to online fire products provided by FIRMS (Fire Information for Resource Management System) <http://earthdata.nasa.gov/data/near-real-time-data/firms>. We have been using the products from FIRMS to investigate the number of fires in the Eastern Europe and Russian areas in the spring, as these are relevant regions for long-range transport of aerosols to Norway and Scandinavia.

Examples of global fire maps are shown in Figure 35. This will be further dealt with in the follow-up project in 2013.



*Figure 35 : Left panel: The geographical locations of all hot spots detected by MODIS on 11.-20 January 2011 (upper panel) and 21.-30 May 2011 (lower panel). Right panel: Monthly average CO for January 2011 (upper panel) and May 2011 (lower panel) from MOPITT.*

The figure show that in the northern hemisphere winter there are very few fires in the Eastern Europe and Russian Areas, and the CO the right, whilst spring shown in the lower panel, is an active season for fires in the Eastern Europe and Russian Areas.

We have further investigated high aerosol episodes in the Arctic and Scandinavian areas in the years 2004-2011 with special emphasis on 2011. In 2011 there were very few episodes at both Birkenes and Zeppelin influenced by direct emissions from fires, partly due to the meteorology mainly with prevailing winds from west in the spring season. This work will continue and be further developed in 2012 and 2013.

## 7. Aerosols and climate: Observations from Zeppelin and Birkenes Observatories

Atmospheric aerosol influences climate by scattering incoming visible solar radiation back into space before it can reach the ground, be absorbed there and warm the earth surface. This so called direct aerosol climate forcing is mostly cooling, but can be moderated if the aerosol itself absorbs solar radiation, e.g. if it consists partly of light absorbing carbon or light absorbing minerals. Atmospheric aerosol particles also affect the reflectivity and lifetime of clouds, which is termed the indirect aerosol climate effect. Also here, the effect can be cooling as well as warming for climate, but in most cases, the cloud reflectivity and lifetime are increased, leading again to a cooling effect.

In the ongoing debate on mitigation strategies for anthropogenic climate change, the effects of regulating short-lived climate forcers (SLCF), such as methane, ozone, and aerosol particles (including black carbon<sup>14</sup>(BC)), are often contrasted with the effects of regulating long-lived climate forcers such as carbon dioxide and nitrous oxide. It is argued that a reduction of anthropogenic emissions of SLCFs (there are warming as well as cooling SLCFs) could be more realistic to achieve than a reduction of anthropogenic carbon dioxide emissions, while at the same time keeping the international climate change mitigation efforts alive by yielding an easier progress (Zaelke & Ramanathan, 2012). This view is challenged by pointing out that regulating warming SLCFs, yielding quick but not sustainable results in mitigation of anthropogenic climate change, could reduce the pressure on reducing long-lived carbon dioxide emissions, leading to an ultimately larger build-up of atmospheric CO<sub>2</sub> concentrations and an overall larger increase in global mean temperatures (Myhre et al., 2011).

When contrasting the effects of regulating emissions of carbon dioxide versus SLCFs such as aerosol particles, care needs to be exercised not to generalise since the conclusion depends critically on the exact question considered:

### I. Long –term mitigation of anthropogenic climate change

As Myhre et al. (2011) point out, correctly, mitigation of anthropogenic climate warming that is long-term sustainable can only be achieved by reducing emissions of long-lived climate forcing agents such as carbon dioxide and nitrous oxide. Whether emission reductions of warming SLCFs are beneficial in a strategic sense to achieve this aim is probably more difficult to predict than climate.

### II. Improving accuracy of climate predictions as prerequisite for targeted climate change adaptation strategies

The 4<sup>th</sup> IPCC assessment report (IPCC, 2007) predicts increases of global mean temperature by the year 2100 relative to the year 2000 in a range between 1.8 K and 4 K, where the range is caused by uncertainties in emission scenarios. On top of this uncertainty comes a 50% uncertainty caused by discrepancy between the participating climate models. This internal model uncertainty is caused almost exclusively by

---

<sup>14</sup> The term "black carbon" (BC) is used here following a terminology paper drafted by the WMO Global Atmosphere Watch Scientific Advisory Group for aerosol. Black carbon is defined by 5 simultaneous properties: 1) high fraction of sp<sup>2</sup>-bonded carbon; 2) aggregate of carbon spherules; 3) thermally refractory up to 4000 K; 4) hydrophobic; 5) strong broadband absorption of visible light. There exists no measurement principle that is sensitive to all these properties at once, therefore no instrument that is sensitive to BC and only to BC. Only BC properties can be measured unambiguously, such as the absorption coefficient (using the broadband light absorptivity) or the elemental carbon (EC) concentration (using thermal refractiveness and carbonic composition).

uncertainty in direct aerosol effect (Kiehl, 2007). Reducing this internal model uncertainty is a prerequisite for more reliable climate predictions. This requires model improvements using on long-term observations of atmospheric aerosol properties, independently of the role of atmospheric aerosols in mitigating anthropogenic climate change.

### **III. Synergy between climate and health effects in regulating emissions of aerosol particles and aerosol precursors**

Certain types of anthropogenic atmospheric aerosol, in this context referred to as particulate matter (PM), are known to cause adverse effects on human health. According to conservative estimates, about 800000 lives and 6.4 million life years are lost globally and annually due to PM air pollution, not counting increases in morbidity (Cohen et al., 2005). Regulating anthropogenic aerosol emissions may therefore be beneficial independently of its role as SLCF.

## **7.1 Observations of climate relevant aerosol properties: recent developments in Norway and internationally**

NILU contributed to two scientific papers assessing long-term trends (i.e. 10 years or more) in atmospheric aerosol properties in 2012, one on optical aerosol properties, i.e. aerosol scattering and absorption coefficient (Collaud Coen et al., 2012), and one on trends in the total aerosol particle number concentration (Asmi et al., 2012). For the optical aerosol properties, no or inconclusive trends were found for the European sites, while the North American sites showed significant decreasing trends, with the exception of few high altitude and desert sites. Decreasing trends were observed for Arctic aerosol absorption, also showed in Hirdman et al (2010) while no other trends appeared in the polar optical aerosol properties. For the aerosol particle total number concentration, decreasing trends were observed all over the globe, especially pronounced in the winter months. Likely causes for this trend are decreasing anthropogenic emissions of primary particles and precursor gases such as sulphur dioxide.

NILU operates 3 observatories measuring advanced aerosol properties relevant for direct and indirect aerosol climate forcing: 1) Zeppelin Observatory / Ny Ålesund 2) Birkenes Atmospheric Observatory, Aust-Agder, Southern Norway; 3) Troll Atmospheric Observatory, Antarctica. The choice of locations reflects the priorities in Norwegian climate research: 1) atmospheric change at polar latitudes, since Norway itself includes polar territory and polar latitudes are more sensitive to climate change than other regions on the globe; 2) atmospheric change in regions with large influence of long-range transported air masses, supporting the EMEP programme. The Birkenes and Zeppelin Observatory is thoroughly described in section 3 and Appendix I, a brief overview of the program of the third site Troll, is included here due to the importance of these variables.

An overview of all aerosol parameters currently measured at the 3 observatories can be found in Table 3. Parameters where observations are funded by KLIF and which are covered in this report are written in green type (some are also covered by other KLIF programmes (*Klif/Background monitoring of ozone and particles* and "*Klif/Background monitoring of acidifying compounds*" ).

Table 3: Aerosol observations at the Zeppelin, Birkenes and Troll Observatory following the GAW recommendations. Parameters written in green are funded by KLIF and included in this report.

	Zeppelin/Ny-Ålesund	Birkenes	Troll
<b>Particle Number Size Distribution</b>	fine mode ( $0.01 \mu\text{m} < D_p < 0.8 \mu\text{m}$ ) in collaboration with Stockholm University	fine and coarse mode ( $0.01 \mu\text{m} < D_p < 10 \mu\text{m}$ )	fine mode ( $0.03 \mu\text{m} < D_p < 0.8 \mu\text{m}$ )
<b>Aerosol Scattering Coefficient</b>	spectral at 450, 550, 700 nm, in collaboration with Stockholm University	spectral at 450, 550, 700 nm	spectral at 450, 550, 700 nm
<b>Aerosol Absorption Coefficient</b>	single wavelength at 525 nm, in collaboration with Stockholm University	single wavelength at 525 nm, to be upgraded to 3 wavelengths in 2012	single wavelength at 525 nm
<b>Aerosol Optical Depth</b>	spectral at 368, 412, 500, 862 nm in collaboration with WORCC. Ny-Ålesund, in collaboration with WORCC; 11 wavelengths between 367.1 and 1039.7 nm, Zeppelin, in collaboration with AWI	spectral at 340, 380, 440, 500, 675, 870, 1020, 1640 nm, in collaboration with Univ. Valladolid	spectral at 368, 412, 500, 862 nm
<b>Aerosol Chemical Composition</b>	main components (ion chromatography), heavy metals (inductively-coupled-plasma mass-spectrometry)	main components (ion chromatography), heavy metals (inductively-coupled-plasma mass-spectrometry)	main components (ion chromatography), discontinued from 2011 due to local contamination.
<b>Particle Mass Concentration</b>	---	PM <sub>2.5</sub> , PM <sub>10</sub>	PM <sub>10</sub> , discontinued from 2011 due to local contamination
<b>Cloud Condensation Nuclei</b>	size integrated number concentration at variable supersaturation in collaboration with Korean Polar Research Institute	number concentration at variable supersaturation, installed in 2012	---

**Troll Atmospheric Observatory:** The observation programme of aerosol microphysical and optical properties continues in full despite considerable local contamination due to the close location of the observatory to the main station buildings (see the figure). The observations at Troll are nevertheless valuable due to the completeness of the programme, the whole year operation of the station, and the fact that the aerosol observations in question have high time resolution and can be filtered for local contamination semi-automatically. The data can be used for a number of scientific objectives including long-range transport of biomass burning aerosol (Fiebig et al., 2009) and studying the natural global aerosol background cycle in distinction to the anthropogenic contribution (Fiebig et al., in prep.). The data would be even more valuable without the local contamination issue, e.g. for studying the influence of naturally formed new particles on cloud properties, i.e. studying the indirect aerosol climate effect close to its undisturbed state. Currently, new particle formation is used as indicator for local contamination by emissions from the main station ventilation (from kitchen exhaust) and sewage system (from ammonia). The current location of the Troll atmospheric observatory, about 200 m from the main building, was chosen by the main station operator in disregard of agreements in the project planning phase and against explicit scientific advice because of expected local contamination issues.

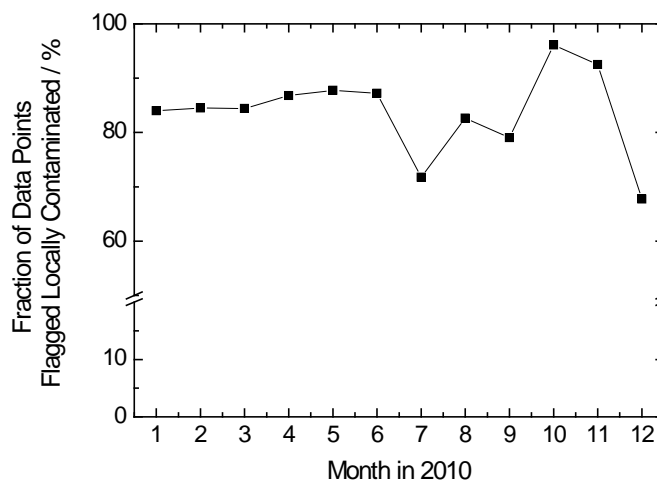


*Figure 36: Fraction of potentially locally contaminated hourly average data points as a function of month at Troll Atmospheric observatory. The following indicators are used for determining local contamination: 1) wind from contaminated sector, i.e. direction of the main station buildings; 2) wind speed below 1 m/s, i.e. stagnant conditions allowing for diffusion from the main station; 3) single scattering albedo below 0.8, indicating absorbing aerosol from passing vehicles using combustion engines; 4) presence of new particle formation indicating organic carbon exhaust from station ventilation or ammonia emissions from sewage system.*

## 7.2 Optical aerosol properties measured at Birkenes: estimating the local, instantaneous direct aerosol radiative forcing

Figure 37 shows a time series of the daily averaged optical properties for the dry-state PM<sub>10</sub> aerosol measured at Birkenes, the whole period January 2010-2011. Following the measurement protocol, the particle fraction with aerodynamic diameters smaller than 10  $\mu\text{m}$  is selected. The particles are brought close to the dry-state, which is defined as a relative humidity smaller than 40%, considered sufficient for hygroscopic particle growth to be negligible. This protocol follows the recommendations of the EMEP and WMO GAW aerosol network, and is identical with the recommendations of the relevant European projects (EUSAAR and ACTRIS see section 3.1). The rationale behind these recommendations is that any measurement protocol will alter the aerosol thermodynamic state from the ambient state before measurement by bringing the sample into the station building. By conditioning the

sample in the described way and following the same quality assurance procedures, the observations are nevertheless comparable across stations within the network.

The top panel of Figure 37 shows the time series of the aerosol scattering coefficient  $\sigma_{sp}$  at three wavelengths across the visible spectrum. It is measured by an instrument called integrating nephelometer. Together with the aerosol absorption coefficient  $\sigma_{ap}$ , depicted in the second panel of Figure 37, these parameters give the information necessary to quantify the local, ground-level direct aerosol effect. The absorption coefficient is measured by a filter absorption photometer that operates at 525 nm wavelength<sup>15</sup>. Whereas  $\sigma_{sp}$  and  $\sigma_{ap}$  shown in the 2 top panels of Figure 37 depend on the particle concentration, the parameters shown in the bottom 2 panels don't, and rather represent average properties the aerosol. The scattering Ångström coefficient  $\hat{a}_{sp}$  plotted in the third panel parameterises the wavelength dependence of  $\sigma_{sp}$ . The single scattering albedo  $\omega_0$  in the fourth panel quantifies the fraction of incident light interacting with the particles by scattering, vs the absorption. The lower  $\omega_0$ , the more absorbing are the particles. All panels also include the 8 week running median centred around the data point, plotted as heavy line, to facilitate detection of possible seasonal variations.

Values for  $\sigma_{sp}$  of  $8 \text{ Mm}^{-1}$  are typical for remote locations, but may increase to average values of  $40 \text{ Mm}^{-1}$  and peaks of  $100 \text{ Mm}^{-1}$  in continental background (Delene & Ogren, 2002). The  $\sigma_{sp}$  values measured at Birkenes are fairly typical for a remote location, with peaks more representative of a continental background air, pointing out the significance of long-range transport from the continent to Birkenes. It is also apparent that the variability isn't governed by a seasonal cycle, rather by the transport pattern of the air masses arriving at Birkenes, which change with the weather situation on a timescale of days. The same conclusion applies to the variability of  $\sigma_{ap}$ . For  $\sigma_{ap}$  there are reference values between  $0.1 \text{ Mm}^{-1}$  at remote locations and  $8 \text{ Mm}^{-1}$  in continental background air. Also here, the values measured at Birkenes fit in nicely. The Ångström coefficient  $\hat{a}_{sp}$  is largely determined by the concentration ratio of particles in the fine size range ( $D_p < 1 \mu\text{m}$ ) and coarse size range ( $D_p > 1 \mu\text{m}$ ). Values range from close to 2 for remote locations dominated by fine mode aerosol to closer to 0 for marine air masses with significant amount of coarse mode aerosol, and may even become negative for desert dust aerosol where fine mode aerosol amounts are negligible relative to the coarse mode concentrations. For Birkenes,  $\hat{a}_{sp}$  varies between 1 and 2, nicely fitting into the reference values, and also not exhibiting any temporal pattern. For the single scattering albedo  $\omega_0$ , the picture looks somewhat more interesting.

---

<sup>15</sup> For comparison with the nephelometer, the data has been transferred to a wavelength of 550 nm assuming an absorption Ångström coefficient  $\hat{a}_{ap}$  of -1, adding 2% systematic uncertainty to the data.

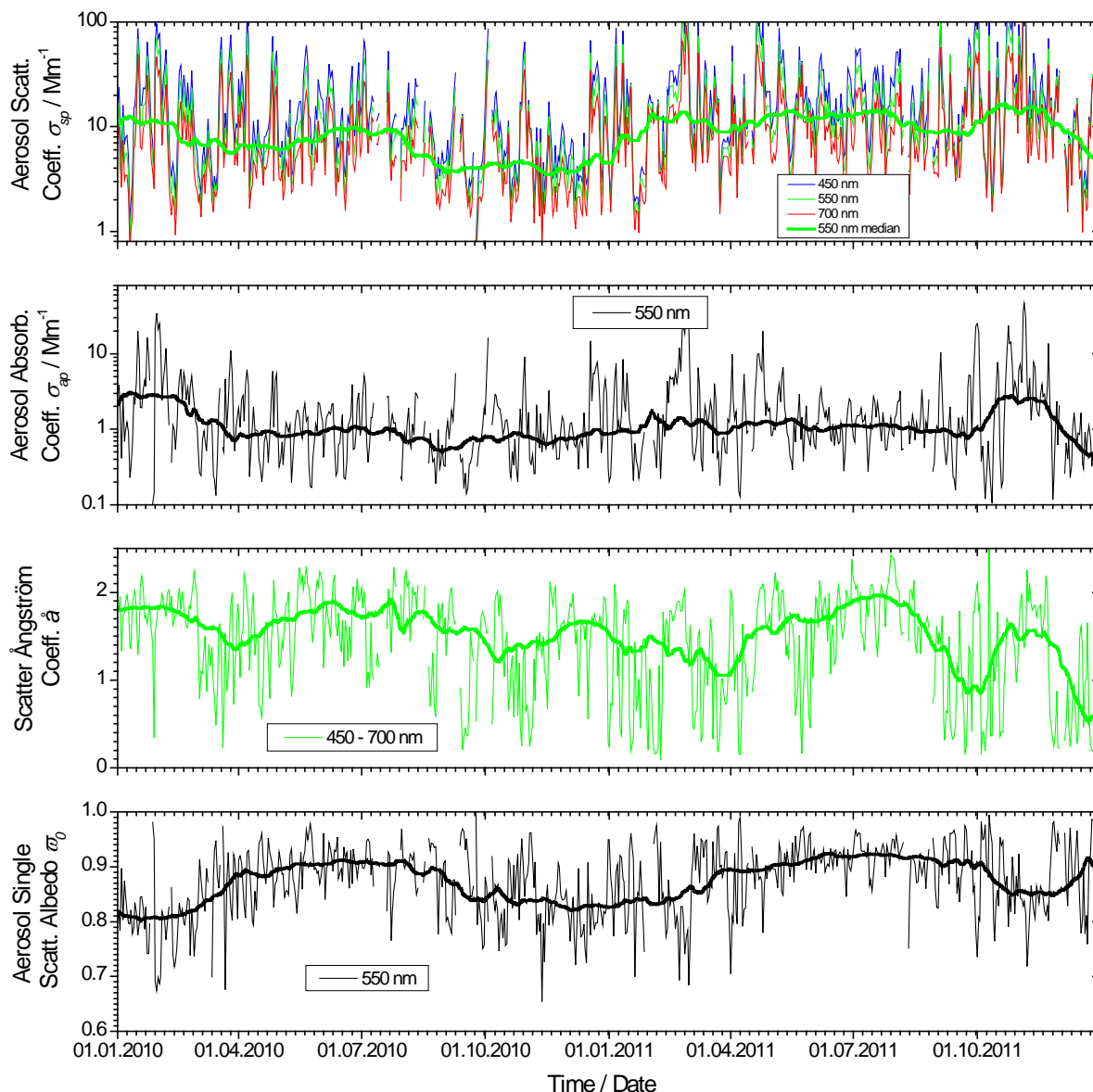


Figure 37: Aerosol optical properties daily means measured in 2010 and 2011 at Birkenes. Top panel: aerosol scattering coefficient  $\sigma_{sp}$  at 450, 550, and 700 nm wavelength. Second panel: aerosol absorption coefficient  $\sigma_{ap}$  at 550 nm wavelength. The third and fourth panels: the scattering Ångström coefficient  $\hat{a}_{sp}$  and the single scattering albedo  $\omega_0$  as derived properties, respectively.

For a purely scattering aerosol,  $\omega_0$  is 1, and decreases with increasing fraction of light absorbing components in the aerosol particle phase. The literature values range from close to 1 for polar locations, values around 0.92 for continental background locations to values even lower than 0.8 closer to source regions of absorbing aerosol components, e.g, sources of fossil fuel or biomass combustion. At Birkenes,  $\omega_0$  exhibits a dedicated seasonal cycle. Values around 0.92 are reached only during the summer months, whereas values around 0.81 are typical during winter, indicating the influence of a source of combustion aerosol in winter. In previous year's report, biomass burning aerosol from regional domestic heating has been indicated as likely source of this phenomenon. This link will be investigated further in the next section.

To estimate direct aerosol effect  $\Delta F_{ae}$ , a full scale radiative transfer model is required. However, by making a number of assumptions, it is possible to estimate the radiative forcing efficiency  $\Delta F_{ae}/\delta$  of the direct aerosol effect, i.e the radiative forcing normalised by the aerosol optical depth. Using the approach of Haywood & Shine (1995, eq. 3) as quoted in Sheridan & Ogren (1999),  $\Delta F_{ae}/\delta$  can be calculated from the aerosol optical parameters measured at Birkenes. The approach may not allow to calculate the true aerosol direct effect, but allows to study the dependence of  $\Delta F_{ae}/\delta$  on changes in the aerosol properties by using the following assumptions:

- a constant fractional day length of 0.5
- an constant atmospheric transmissivity of 0.76 above the aerosol layer assumed to be located in the boundary layer.
- a constant fractional cloud cover of 0.6
- a constant surface albedo of 0.15 (forest), alternatively one of 0.85 when considering a snowcovered surface.
- an integration of  $\Delta F_{ae}$  across the solar spectrum by using the aerosol optical property values at 550 nm wavelength where the spectral intensity of the solar radiation reaching the earth surface is highest.
- neglecting the fact that all ground-based instruments measure the aerosol optical properties for the dry-state aerosol (relative humidity < 40%), whereas the AOD is measured for ambient conditions of relative humidity.

Since the aerosol optical depth is also measured at Birkenes,  $\Delta F_{ae}$  may be calculated from  $\Delta F_{ae}/\delta$  when the aerosol optical depth  $\delta$  is available, which happens more often in summer since this measurement requires a direct and cloud-free view of the sun.

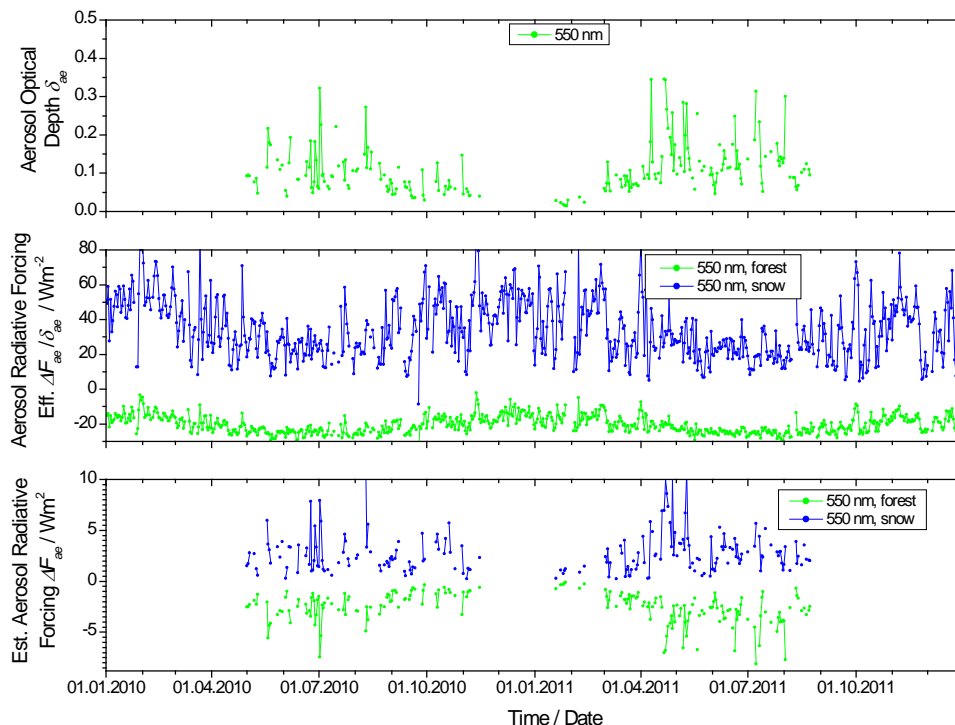


Figure 38: 2010 and 2011 time series aerosol optical depth (AOD) at 550 nm wavelength above Birkenes (upper panel), as well as the radiative forcing efficiency  $\Delta F_{ae}/\delta$  (middle panel) and the estimated local, instantaneous, solar aerosol radiative forcing  $\Delta F_{ae}$ , the latter two for surface albedo for forest and snow, respectively.

Figure 38 summarises the results of the aerosol optical depth  $\delta_{550\text{ nm}}$  (top panel), the radiative forcing efficiency  $\Delta F_{ae}/\delta$  (middle panel), and the estimated direct, local, instantaneous radiative forcing  $\Delta F_{ae}$  (bottom panel), all at 550 nm wavelength. The latter two for the standard surface albedo of forest and covered landscape. It is obvious that the likelihood of  $\delta_{550\text{ nm}}$  data being collected is largest during the summer months, with more frequent cloud-free view to the sun. However, a slight trend to lower  $\delta_{550\text{ nm}}$  values, around 0.04, in winter as compared to higher values, around 0.15, in summer is discernible. For the radiative forcing efficiency  $\Delta F_{ae}/\delta$ , a clear annual cycle is obvious in the time series, with more negative (cooling tendency) values in summer and more positive (warming tendency) in winter. This finding is a direct result of the annual cycle of the single scattering albedo  $\omega_0$  observed at Birkenes, with lower values in winter than in summer. The time series of the estimated direct, local, instantaneous radiative forcing  $\Delta F_{ae}$  shows that the atmospheric aerosol at Birkenes may even have a warming effect in winter already over a surface without snow cover, but certainly when the ground is snow covered.

### 7.3 Physical aerosol properties measured at Birkenes in 2011

Even though a particle size distribution isn't uniquely connected to a specific air mass type, it is normally fairly characteristic, and can serve as valuable indication of air mass origin, which at Birkenes shifts with the synoptic weather situation. In describing particle number size distributions, it is often referred to log-normal modes the size distribution consists of, which are commonly referred to as "Aitken-mode" for the one peaking at  $10\text{ nm} < D_p < 100\text{ nm}$ , and accumulation-mode for the one peaking between  $100\text{ nm} < D_p < 500\text{ nm}$ . Reconfirming findings of previous years' reports, the most common types of air masses occurring at Birkenes and their particle size distribution include (omitting special cases of long-range transport):

- **Clean Arctic background aerosol**, characterised by a distinct accumulation mode peaking at 150 nm particle diameter, with peak particle concentrations of  $200\text{ cm}^{-3}$ .
- **Continental aerosol**, characterised by an accumulation mode peaking between 150 – 240 nm particle diameter, depending on how long the aerosol had time to self-process, and peak particle concentrations between  $1000 - 1500\text{ cm}^{-3}$ , in addition to the presence of an Aitken-mode.
- **Arctic haze**, characterised by the absence of an Aitken-mode, and an accumulation mode peaking at 200 nm particle diameter, with peak particle concentrations of  $1500\text{ cm}^{-3}$ .

At Birkenes, these aerosol types can appear combined with an additional mode in the Aitken size range ( $10\text{ nm} < D_p < 100\text{ nm}$ ). These have an atmospheric lifetime of a couple of hours to a day (Jaenicke, 1980) before they either grow larger by mass uptake from the gas-phase, or coagulate with particles in the accumulation mode size range ( $100\text{ nm} < D_p < 500\text{ nm}$ ). Particles in the Aitken-size range are therefore relatively young, and have to be of local or regional origin, where a locally generated Aitken-mode peaks around 30 nm particle diameter, a regionally generated around 70 nm particle diameter. As mentioned previously, at least two possible sources for such particles are known for continental background locations like Birkenes:

- **Biogenic aerosol**, generated from condensing oxidised precursor gases, e.g. terpenes, emitted by vegetation. Events of heavy biogenic aerosol formation are characterised by the formation of new particles. These events show by the appearance of a new mode in the particle size distribution that first quickly grows from particle diameters below 10 nm, then with decelerating velocity to particle diameters of about 60 nm.
- **Wood combustion aerosol**, generated usually by domestic heating with wood burning stoves.

However, wood combustion aerosol is distinguished by another characteristic. It contains significant amounts of light absorbing carbon, and therefore has a single scattering albedo of around or below 0.85.

The physical aerosol properties covered here include the particle number size distribution in the particle diameter range  $30 \text{ nm} < D_p < 550 \text{ nm}$  measured by a Differential Mobility Size Spectrometer (DMPS). The data collected in 2011 by the DMPS is displayed in Figure 39 as colour contour plot. In this type of plot, the x-axis holds the time of the observation, whereas the y-axis holds the particle diameter  $D_p$  on a logarithmic scale. This is common practice since  $D_p$  usually spans several orders of magnitude. The colour scale holds the particle concentration, normalised to the logarithmic size interval,  $dN / d \log D_p$ , also on a logarithmic (colour) scale. (A large data gaps obvious in Figure 39 caused by a failing pump in the DMPS system and coincident delivery problems of the supplier for a spare.)

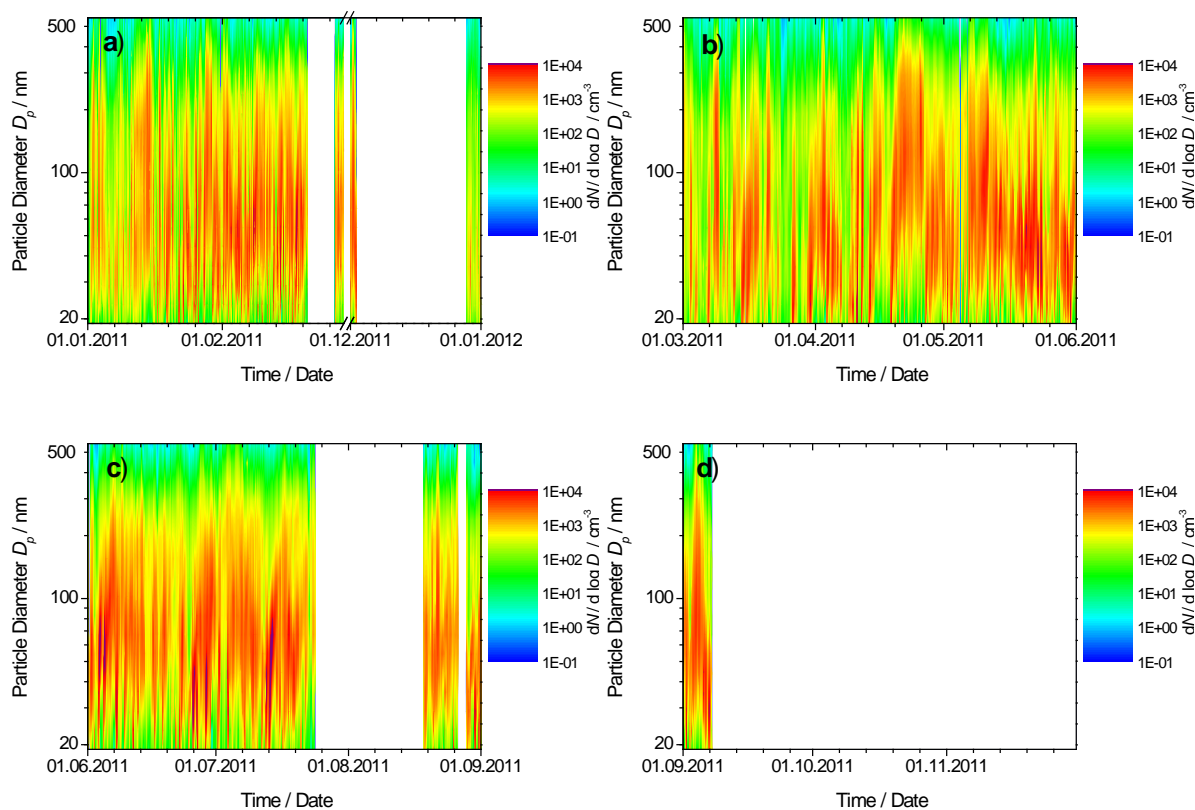


Figure 39: 2011 time series of particle number size distribution at Birkenes, panel a) winter, panel b) spring, panel c) summer, panel d) autumn.

In order to quantify the occurrence of these two aerosol types of regional origin on top of the advected aerosol types and find more objective criteria for their occurrence, a statistical analysis was performed using the datasets of 2010 and 2011 for a more representative sample.

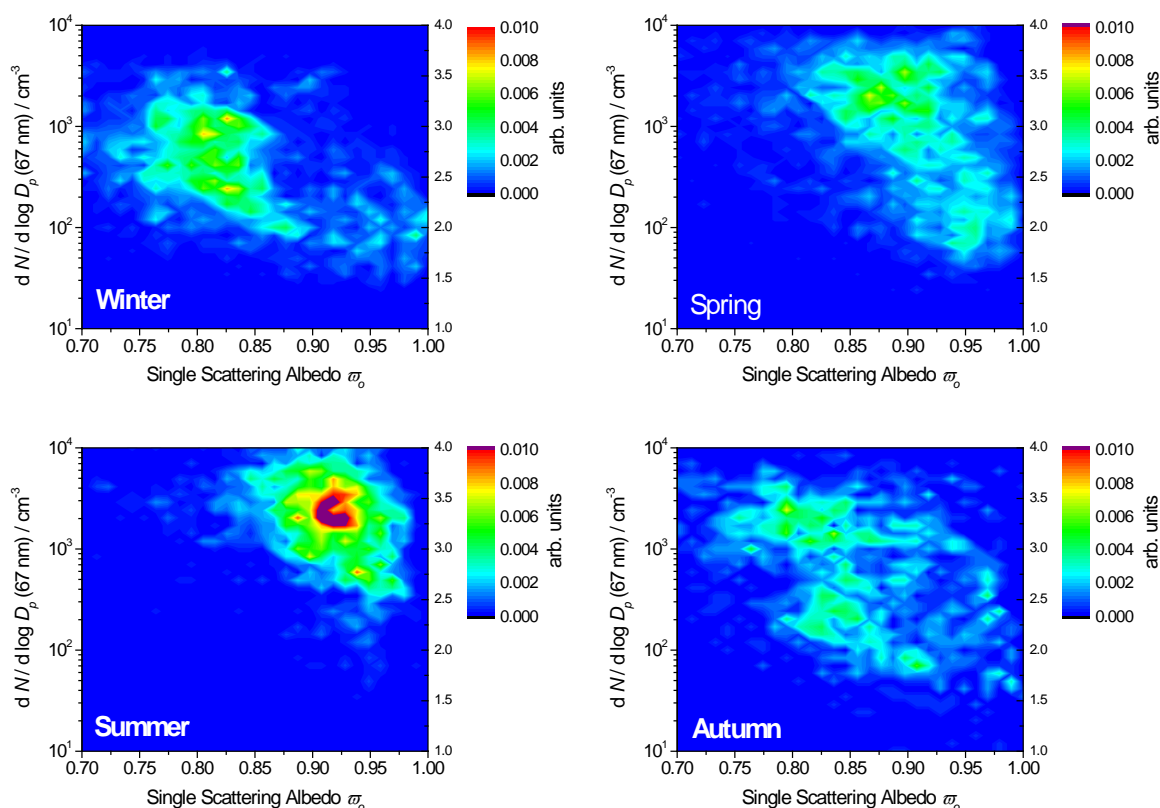


Figure 40: 2011 particle number size distribution at Birkenes together with single scattering albedo panel a) winter, panel b) spring, panel c) summer, panel d) autumn.

In this analysis, these characteristics are used to learn something about the reasons for the annual cycle of the aerosol single scattering albedo  $\omega_0$ , which was discussed in the previous section. To this end, the frequency of occurrence of particle formation events (characterised by the distinctly growing nucleation mode) and of wood combustion aerosol (characterised by a distinct Aitken-mode in the particle size distribution and a value of  $\omega_0$  below 0.85) have been determined as a function of season. If the annual cycle of  $\omega_0$  is associated with local or regional emissions of wood combustions aerosol, its frequency of occurrence should exhibit the same annual cycle.

Figure 41 visualises the thus determined frequency of occurrence of particle formation events and local or regional combustion events as bar graph. It is obvious that in summer, the Aitken mode in the aerosol at Birkenes, most likely consists of newly formed particles, likely of biogenic origin. In winter however, no such events occurred in 2010. For biomass combustion aerosol events, the situation is exactly opposite. Here, the likelihood of the Aitken-mode due to biomass combustion is maximised in winter, and minimised in summer. For both types of events, spring and autumn are transition periods.

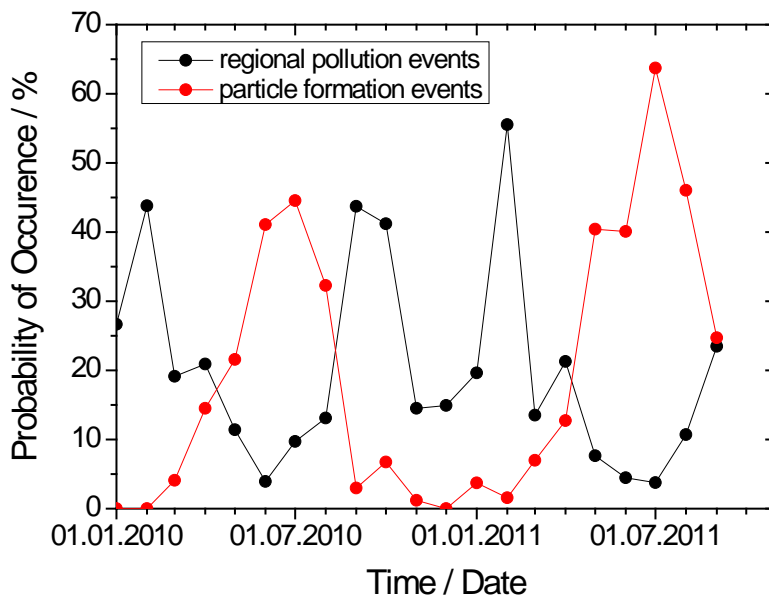


Figure 41: Frequency of occurrence of influence by local or regional combustion, as well as occurrence of new particle formation in Birkenes in 2010 as determined by combined analysis of particle number size distribution and single scattering albedo.

With all caution due to the limited statistical significance of a one-year data series, it can be stated that the annual cycle of  $\tau_0$  observed at Birkenes is very likely due to local and regional emissions of domestic biomass burning. Further studies on archived filter samples from Birkenes that use levoglucosan as tracer for biomass burning are currently being conducted to confirm this finding. It can thus be stated further that emissions of domestic biomass burning very likely have a significant effect on the direct aerosol effect in the Agder region in making it less cooling, in cases of snow covered surface maybe even positive, i.e. warming, in contrast to the global average.

#### 7.4 Observations of the total aerosol load above Zeppelin and Birkenes Observatories

The aerosol optical depth (AOD) is a quantitative measure of the extinction of solar radiation by aerosol scattering and absorption between the point of observation and the top of the atmosphere. It is determined by the total concentration of particulates in the atmosphere. The wavelength dependence of AOD, described by the Ångström exponent (AE) is a qualitative indicator of the particle size and contains information about the aerosol type. The larger the Ångström exponent, the smaller the size of the particles measured.

During the last years the number of stations measuring AOD has increased significantly. Figure 42 shows the networks of sun-photometer operated in Scandinavia (from Toledano et al., 2012). Photos of the standard instruments used in Ny-Ålesund and Birkenes and their characteristics are described in Appendix I.

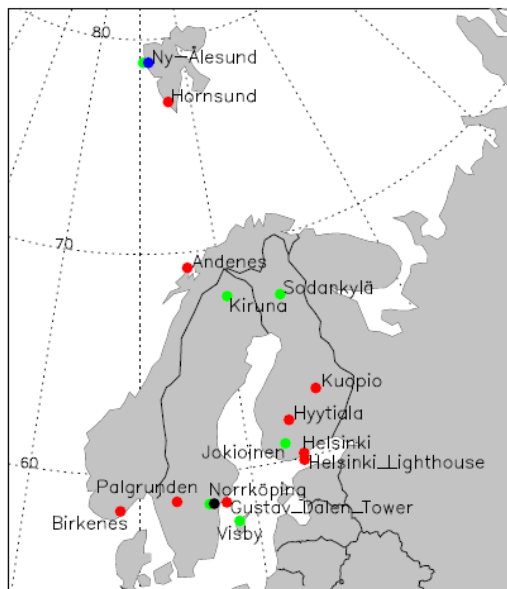


Figure 42: Location of sun photometer sites in the European Arctic sector and Scandinavia. Colour symbols denote networks: AERONET sites (red), GAW-PFR (green), Polar-AOD (blue) [this Figure is equal to Figure 1 from Toledano et al, 2012).

In 2002, PMOD/WRC in collaboration with NILU, started AOD observations in Ny-Ålesund, as part of the global network of AOD observations on behalf of the WMO GAW program. A Precision Filter Radiometer (PFR, Wehrli, 2000 and 2005) is utilized to measure extinction in four narrow spectral bands, by the WMO recommended wavelengths: at 368 nm, 415 nm, 500 nm and 862 nm. Direct sun measurements are performed with the instrument located on the roof of the Sverdrup. Samples are recorded with one minute time resolution. Data quality control includes instrumental control like detector temperature and solar pointing control as well as objective cloud screening. SCIAMACHY TOMSOMI ozone columns and meteorological data from Ny-Ålesund were used in the retrieval. Ångström coefficients are derived for each set of measurements using all four PFR channels. Calibration is performed annually at PMOD/WRC. NRT data are displayed at [www.pmodwrc.ch/worcc](http://www.pmodwrc.ch/worcc) and can also be downloaded from the WDCA site (<https://ebas.nilu.no>).

Since spring 2009 a CIMEL type CE-318 sun-photometer (#513) is in operation at the Birkenes observatory. The instrument is an automatic sun and sky radiometer, with spectral interference filters centered at selected wavelengths: 340, 380, 440, 500, 675, 870, 1020, and 1640 nm, which is a standard instrument of the Aerosol Robotic Network AERONET network (Holben et al., 1998; NASA, 2011). Measurements are made in collaboration with the University of Valladolid (Spain), who also perform the annual calibration (RIMA-AERONET sub-network). The data processing is centrally performed by AERONET. NRT and analyzed data are displayed at AERONET website (see [aeronet.gsfc.nasa.gov](http://aeronet.gsfc.nasa.gov)).

The associated AOD uncertainty is 0.0-0.02 (larger for shorter wavelengths). The Ångström exponent (AE), indicating size predominance is obtained from AOD at different wavelengths. The wavelength region used for calculation AE from PFR measurements is 368-862 nm. AERONET uses the range between 440 and 870 nm.

#### 7.4.1 Measurements of the total aerosol load above Ny-Ålesund

NILU's measurements of the aerosol optical depth in Ny-Ålesund started in May 2002. Due to low aerosol load in Polar region, accuracy requirements for AOD measurements are more stringent than those usually encountered in established sun photometer networks. Polar AOD, including Ny-Ålesund measurements, are shown in Tomasi et al. (2007). Results from sun-photometer inter-comparison campaigns, which were held during spring 2006 at Ny-Ålesund (Svalbard) and autumn 2008 at Izaña (Tenerife) within the framework of the IPY POLAR-AOD project, were recently published by Mazzola et al. (2012).

In Ny-Ålesund the polar night lasts from 26<sup>th</sup> October to 16<sup>th</sup> February, limiting the observational seasons the months between March and September. In 2011 measurements

started May, 23<sup>rd</sup> to October, 12<sup>th</sup>. Clear sky-AOD is available from the period May, 24<sup>th</sup> to September, 20<sup>th</sup>. The late start in 2011 was caused by DHL, who lost the instrument during transport between Davos, where it was calibrated by PMOD/WRC, and Ny-Ålesund. Luckily it was found, but only in May 2011 it reached its destination.

The monthly mean and sunlight-season average values of AOD at 500 nm and Ångström coefficients measured between 2002 and 2011 are summarized in Table 4 and visualized in Figure 43. Monthly mean data are calculated from hourly averaged values with more than 10% of valid observations included. The results show a clear inter-annual variability. Individual episodes have a large impact on observed monthly averages. Huge emissions from boreal forest fires in North America are likely to explain the elevated AOD levels end of July 2004 (Stohl et al. 2006). Agricultural fires in Eastern Europe resulted in elevated pollution levels in Arctic in spring 2006 (Stohl et al., 2007; Myhre et al., 2007). The increase in AOD in August and September 2008 was caused by the plume from the Kasatochi Volcano (52.17°N, 175.51°W), erupting on 7 to 8 August 2008, reaching Ny-Ålesund (see e.g. Hoffman et al., 2010; Kristiansen et al., 2010).

Seasonal variations for AOD and Ångström coefficient are shown in Figure 44. For comparison, previously published results, including the measurements from Hornsund (77.0°N, 15.6°E), which is an AERONET site on Svalbard, are shown. The measurements reveal the expected pattern, high aerosol load with larger AOD (about 0.12 at 500 nm wavelength) during the Arctic haze period in spring, and low summer values (about 0.06). According to the analysis of aerosol transport into the Arctic, Stohl et al. (2006) demonstrated that the region north of 70°N is isolated from mid-latitude sources in summer, whereas in winter and spring the sources with larger potential impact are located in Eurasia (rather than North America or East Asia). During summer the aerosol removal processes are likely more active in Svalbard.

The monthly averaged density distribution of AOD and AE is given in the right panel of Figure 44. The Ångström exponent in Svalbard does not show such a clear seasonal pattern as the AOD. Apparently there is a minimum in May at the end of the haze season, and then the AE increases slightly during the summer. In any case the multi-annual monthly means were above 1.0, thus indicating dominance of fine particle. If one sets a limit of AE at 1.05 to separate fine from large particles, in March 65% were fine particles. This number goes up to 70% in April, 72 % in May, 85% in June, July and September, and 86% in August.

Table 4: Monthly mean and sunlight-season average values of AOD at 500 nm (upper panel) and Ångström coefficient (lower panel) measured in Ny-Ålesund between 2002 and 2011. The values given are mean and standard deviation.

Month	March	April	May	June	July	August	September
AOD							
2002		0.06 ± 0.01	0.08 ± 0.03	0.06 ± 0.02	0.07 ± 0.12	0.07 ± 0.08	0.06 ± 0.05
2003	0.15 ± 0.12	0.11 ± 0.05	0.15 ± 0.06	0.10 ± 0.03	0.04 ± 0.01	0.05 ± 0.02	0.06 ± 0.03
2004	0.06 ± 0.00	0.12 ± 0.08	0.13 ± 0.09	0.06 ± 0.01	0.10 ± 0.07	0.05 ± 0.02	0.04 ± 0.02
2005	0.08 ± 0.03	0.12 ± 0.07	0.10 ± 0.03	0.05 ± 0.02	0.05 ± 0.02	0.04 ± 0.03	0.03 ± 0.01
2006	0.12 ± 0.03	0.16 ± 0.07		0.04 ± 0.00	0.05 ± 0.02	0.05 ± 0.04	0.04 ± 0.03
2007		0.10 ± 0.05	0.10 ± 0.12	0.07 ± 0.03	0.05 ± 0.01	0.05 ± 0.02	0.04 ± 0.03
2008	0.13 ± 0.05	0.14 ± 0.06	0.14 ± 0.04	0.06 ± 0.02	0.06 ± 0.02	0.09 ± 0.03	0.16 ± 0.03
2009			0.11 ± 0.03	0.08 ± 0.02	0.11 ± 0.04	0.10 ± 0.02	0.09 ± 0.01
2010	0.11 ± 0.03	0.08 ± 0.03	0.08 ± 0.01	0.06 ± 0.01	0.05 ± 0.01	0.05 ± 0.01	
2011			0.08 ± 0.02	0.08 ± 0.01	0.05 ± 0.01	0.06 ± 0.02	0.05 ± 0.01
AE							
2002		0.9 ± 0.1	1.4 ± 0.1	1.2 ± 0.3	1.2 ± 0.2	1.3 ± 0.4	1.2 ± 0.5
2003	0.9 ± 0.5	1.3 ± 0.3	1.3 ± 0.2	1.5 ± 0.1	1.5 ± 0.3	1.4 ± 0.5	1.4 ± 0.3
2004	1.3 ± 0.1	1.2 ± 0.3	1.4 ± 0.5	1.7 ± 0.2	1.6 ± 0.4	1.5 ± 0.3	1.3 ± 0.3
2005	1.1 ± 0.3	1.4 ± 0.4	1.0 ± 0.2	1.6 ± 0.3	1.7 ± 0.2	1.4 ± 0.7	1.5 ± 0.4
2006	0.9 ± 0.1	0.9 ± 0.3		1.7 ± 0.2	1.4 ± 0.3	1.3 ± 0.6	1.4 ± 0.3
2007		1.4 ± 0.4	1.4 ± 0.6	1.7 ± 0.2	1.6 ± 0.2	1.7 ± 0.3	1.5 ± 0.4
2008	1.4 ± 0.2	1.3 ± 0.2	1.4 ± 0.2	1.4 ± 0.4	1.2 ± 0.2	1.3 ± 0.3	1.4 ± 0.3
2009			1.3 ± 0.4	1.4 ± 0.2	1.3 ± 0.3	1.2 ± 0.1	1.1 ± 0.1
2010	1.0 ± 0.03	1.4 ± 0.02	1.3 ± 0.02	1.3 ± 0.03	1.4 ± 0.02	1.0 ± 0.01	
2011			1.7 ± 0.03	1.8 ± 0.1	1.5 ± 0.1	1.4 ± 0.3	1.6 ± 0.2

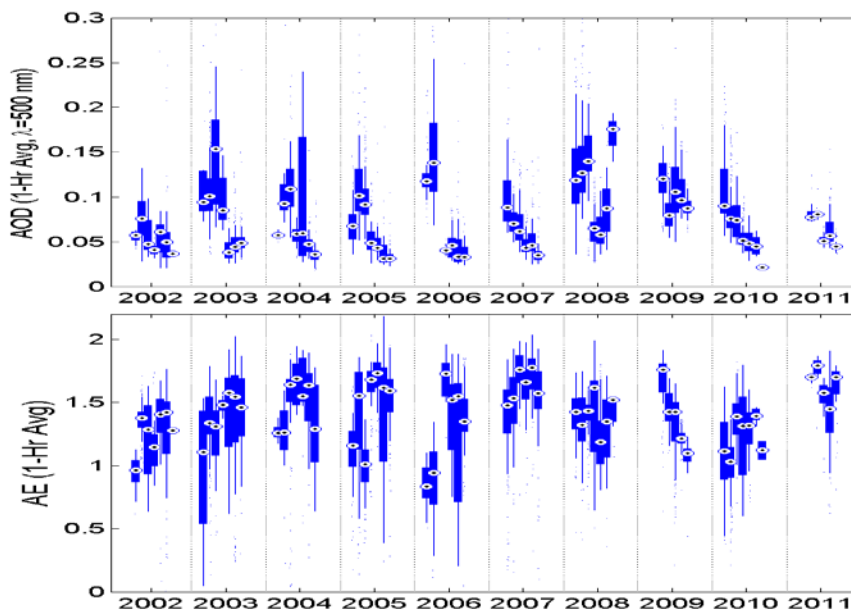


Figure 43: Monthly average aerosol optical depth (AOD at 500 nm) (upper panel) and Ångström exponent (lower panel) measured in Ny-Ålesund during the sunlight time periods in 2002 - 2011. On each box, the central mark is the median, the edges of the box are the 25th and 75th percentiles, the whiskers extend to the most extreme data points not considered outliers, and outliers (in terms of monthly averages, although not considered outlier in terms of pollutions events with high aerosol loads) are shown as very small dots.

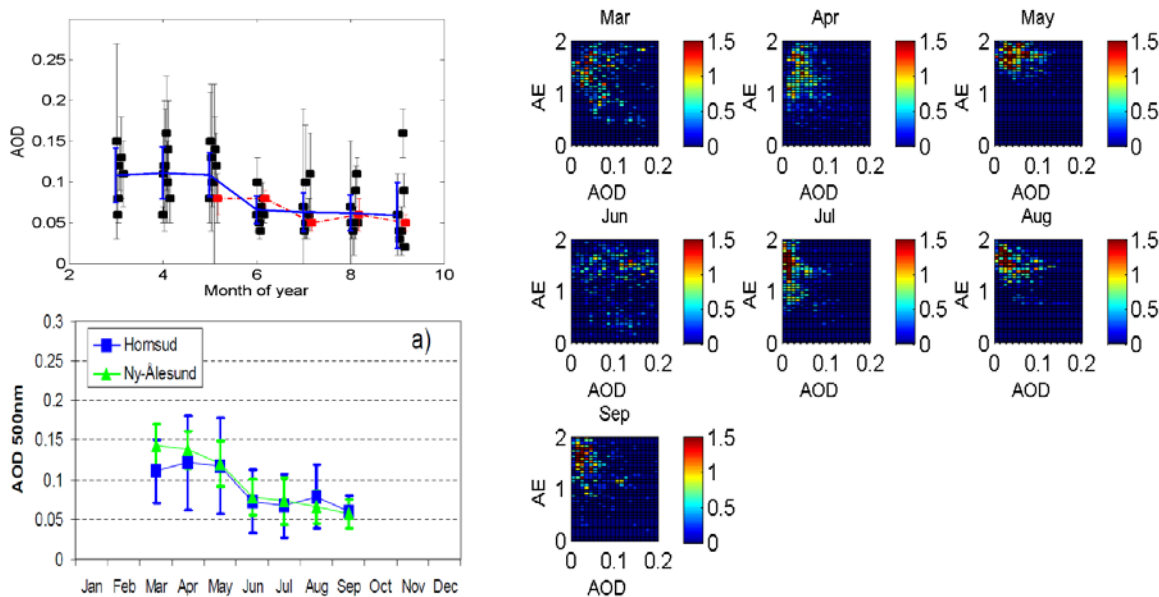


Figure 44: Multi-annual monthly means of (a) aerosol optical depth (500 nm) for Ny-Ålesund 2002-2011 (upper lift panel. For comparison) the published observations from Ny-Ålesund (2002-2010); Hornsund (2004-2010) are given (lower left panel). Error bars give standard deviation [this Figure is equal to Figure 2 from Toledano et al., 2012]. The monthly averaged density distribution of AOD and AE is given in the right panel.

### 7.4.2 Measurements of the total aerosol load above the Birkenes observatory

Aerosol optical depth measurements started at the Birkenes observatory in spring 2009, utilizing an automatic sun and sky radiometer (CIMEL type CE-318). The retrieval method is that of the AERONET version 2 direct sun algorithm (for details:

<http://aeronet.gsfc.nasa.gov>). Quality assured (Level 2) data are available for the first three years of operation, 2009-2011. In 2011 measurements were made between January and August. After that, the instrument was shipped to Spain for calibration.

Monthly mean averages of AOD at 500 nm and the Ångström exponent (440-870 nm), together with their associated standard deviations (sigma) and the number of days (N) for 2009 to 2011 are given in Table 5.

*Table 5: Monthly mean and sunlight-season average values of AOD at 500 nm and Ångström coefficient AE measured at the Birkenes observatory in the time period between 2009 and 2011. The values given are mean, standard deviation and number of days with observations (#).*

Year	2009		2010		2011	
Month	AOD/#	AE	AOD/#	AE	AOD/#	AE
January					0.02 ± 0.01 /	0.96 ± 0.15
February					0.03 ± 0.01 / 02	1.04 ± 0.07
March					0.07 ± 0.02 / 20	0.98 ± 0.33
April	0.29 ± 0.00 / 01	1.52 ± 0.00			0.21 ± 0.19 / 23	1.17 ± 0.46
May	0.09 ± 0.05 / 22	1.16 ± 0.31	0.10 ± 0.04 / 13	1.34 ± 0.28	0.13 ± 0.07 / 18	1.30 ± 0.25
June	0.09 ± 0.05 / 25	1.42 ± 0.27	0.09 ± 0.04 / 16	1.38 ± 0.26	0.10 ± 0.04 / 20	1.46 ± 0.19
July	0.18 ± 0.06 / 11	1.43 ± 0.44	0.10 ± 0.07 / 18	1.44 ± 0.22	0.13 ± 0.06 / 15	1.58 ± 0.27
August	0.17 ± 0.07 / 13	1.14 ± 0.20	0.10 ± 0.05 / 15	1.49 ± 0.24	0.09 ± 0.05 / 13	1.59 ± 0.14
September	0.10 ± 0.04 / 15	0.96 ± 0.24	0.05 ± 0.02 / 16	1.30 ± 0.26		
October	0.08 ± 0.03 / 12	1.05 ± 0.18	0.07 ± 0.03 / 10	1.30 ± 0.26		
November			0.04 ± 0.01 / 06	1.30 ± 0.23		

The monthly averaged data (see Figure 45) show a maximum aerosol load (high AOD) during summer period, July and August, which is consistent with what is seen in the rest of Southern Scandinavia. So far, the data set is not long enough to confirm the occurrence of the second AOD maxima around April. The larger Ångström exponent between June and August indicate a predominance of finer particulates in Southern Norway during summer. The Ångström exponent decreased towards winter-time, indicating larger particles. The annual cycle can be linked to long-range transport patterns from e.g. the European continent.

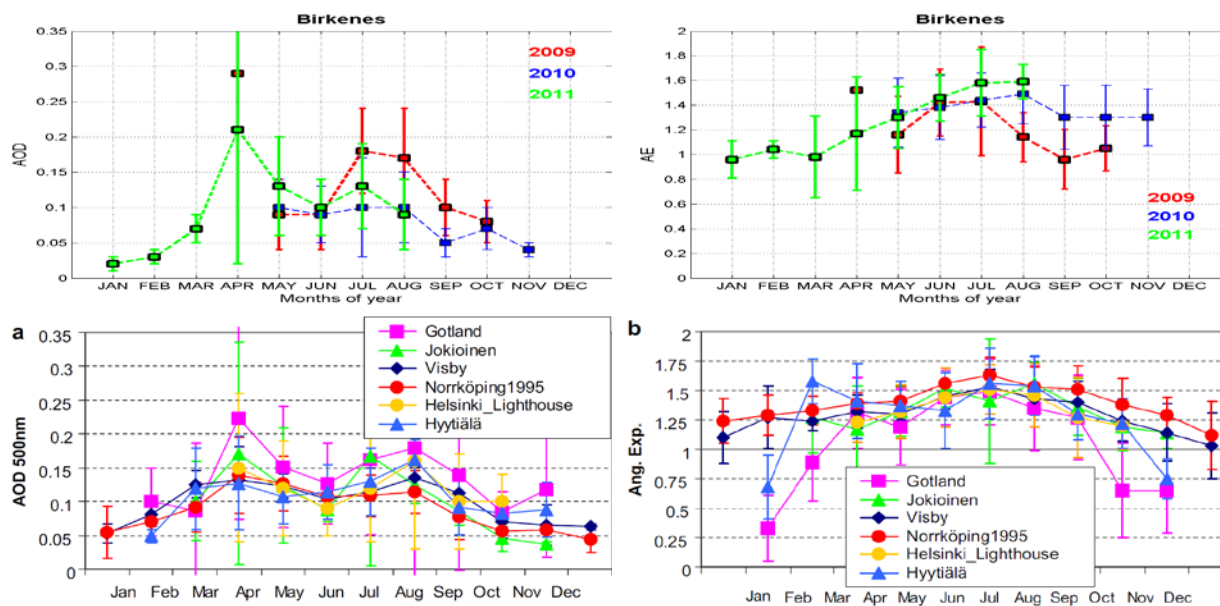


Figure 45: Monthly mean values ( $\pm$  standard deviation) of Aerosol Optical Depth between 2009 and 2011 (left, middle panel) and Ångström coefficient AE for the same time period (right, middle panel). The number of observations each month used to calculate the mean value is given in the upper left panel. For comparison, in the lower panel the seasonal variation of AOD and AE for selected Scandinavian sites is given [the Figures in the lower panel are equal to the upper and lower panel of Figure 4 in Toledano et al., 2012].

Monthly means of aerosol particle size distribution and the fine mode fractions  $V_f/V_t$  are shown in Figure 46. Note that for some months only a few days contribute to the averaged profile (indicated in brackets). The volume particle size distribution  $dV(r)/d\ln r$  ( $\mu\text{m}^3/\mu\text{m}^2$ ) is an AERONET inversion product (see [http://aeronet.gsfc.nasa.gov/new\\_web/Documents/Inversion\\_products\\_V2.pdf](http://aeronet.gsfc.nasa.gov/new_web/Documents/Inversion_products_V2.pdf) [NASA (2011)]). It is retrieved in 22 logarithmically equidistant bins in the range of sizes  $0.05\mu\text{m} \leq r \leq 15\mu\text{m}$ . The highest fine mode fraction is observed during the summer months (around 80%). The averaged fine mode fraction is 64%. A comparison to results published by Toledano is given in Table 6. The total aerosol load seems somewhat lower than in Gotland and Helsinki, the fine mode fraction is comparable with Helsinki.

During the coming years, the dataset will be complemented, which will enable us to draw more general conclusions about the seasonality and origin of the total column aerosol in Southern Norway.

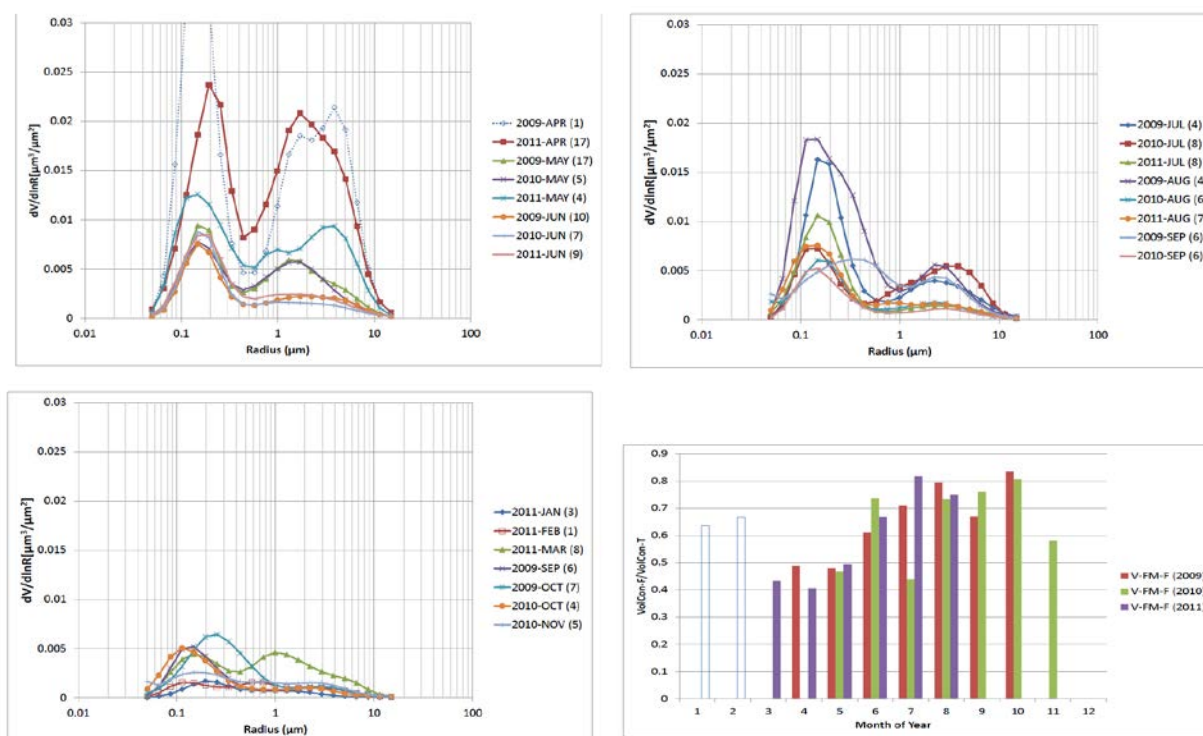


Figure 46: Monthly means of aerosol particle size distribution (upper and lower left panel). Note that for some months only a few days contribute to the averaged profile (indicated in brackets). The lower right panel shows the fine mode fraction  $V_f/V_t$ .

Table 6: Aerosol optical depth (500 nm), Ångström exponent, and fine mode fraction ( $V_f/V_t$ ) for Birkenes and two other sites in S-Scandinavia (from Toledano et al., 2012).

Site		AOD (500nm)	AE	$V_f/V_t$
Birkenes	58.4°N, 8.3°E	0.11	1.29	0.64
Gotland	57.9°N, 19.0°E	0.14	1.05	0.50
Helsinki_Lighthouse	59.9°N, 24.9°E	0.12	1.35	0.64

## 7.5 Utilization of satellite data as a complement to aerosol observations above Scandinavia and the European Arctic

Despite relative high uncertainties of satellite aerosol products in the Arctic, the use of earth-observation (EO) data in polar region is steadily increasing. Beside total column measurements, the global 3-D distribution of tropospheric aerosols can be nowadays characterized from satellite data, like the CALIOP lidar (see Winker et al., 2012). As another example for utilization of EO data in the Arctic, we can mention the work of Sodemann et al. (2011), describing episodes of cross-polar transport in the Arctic troposphere during July 2008 as seen from models, satellite, and aircraft observations. The authors use CO from the IASI passive infrared sensor onboard the MetOp-A satellite and aerosol backscatter and depolarization from the CALIPSO satellite; Kristiansen et al. (2010) use SO<sub>2</sub> columns from GOME-2, OMI, and AIRS, and total attenuated backscatter at 532 nm and 1064 nm (level 1B

data) from CALIOP, to study the transport of the Kasatochi (52.2°N, 175.5°W) eruption sulfur dioxide cloud on 7 to 8 August 2008, leading to an increase of total aerosol column above Ny-Ålesund in August and September 2008.

Before embedding earth observation data into National monitoring activities, their quality and added value has to be assessed, as the retrievals are generally not tuned to polar and high latitude regions. A poster presentation by Glantz et. al. (2012) showed that by introducing MODIS005 retrievals of aerosol optical density (AOD) over the area around Svalbard substantially better time coverage (~75%), compared to ground-based sun-photometer data (~30%) is obtained for the Subarctic marine region. MODIS005 AOD was found to be within 30% of the ground-based estimates and, for values lower than 0.2, on the whole within the expected uncertainty range of MODIS retrievals over ocean surfaces.

As an example, in Figure 47, we show a comparison of daily averaged aerosol optical depth (AOD) data within  $\pm 2$  degrees from Ny-Ålesund and Palgrunden (a South-Swedish AERONET site), from the Advanced Along-Track Scanning Radiometer AATSR, which have been developed in the framework of ESA's AEROSOL-CCI project: AATSR SU 4.0 (developed at Swansea University), AATSR ADV v1.42 (developed at the Finnish Meteorological Institute), and AATSR ORAC v. 2.02 (developed at University of Oxford). A full year data set – 2008 – is available, for details see: [www.esa-aerosol-cci.org](http://www.esa-aerosol-cci.org).

A rough assessment of the suitability of the individual retrievals for the Norwegian National monitoring would conclude that the AATSR ORAC v. 2.02 would be the most promising choice. The cut-off for AATSR SU 4.0 is around 70°N and no data are available for the region around Svalbard. The general seasonal pattern seen in Ny-Ålesund seems nicely reproduced by AATSR ADV v1.42, but the retrieved AOD values seem underestimated. A correlation of 0.52 (Ny-Ålesund) and 0.66 (Palgrunden) is obtained by using data from AATSR ORAC v. 2.02.

In Figure 48a/b we show the monthly averaged data from AATSR ORAC v. 2.02 (left panel) and the AOD observations from the ground-based AERONET network (plus Ny-Ålesund), as reported in Toledano et al. (2012). Due to lack of sun, no data are available for the month of January and December 2008. It is obvious that the satellite data are adding the spatial information not covered by ground-based observations from Ny-Ålesund and Birkenes (started in 2009), which are the two sites at present funded via Klif's monitoring program. Nevertheless, further analysis is needed to assess the added value of these observations, e.g. can they be used for correctly described inter-annual variability and trends. A multi-annual data set will be provided through ESA's AEROSOL-CCI project in 2013. If available in time, trend studies utilizing this long-term average will be results included in the 2013 annual monitoring report.

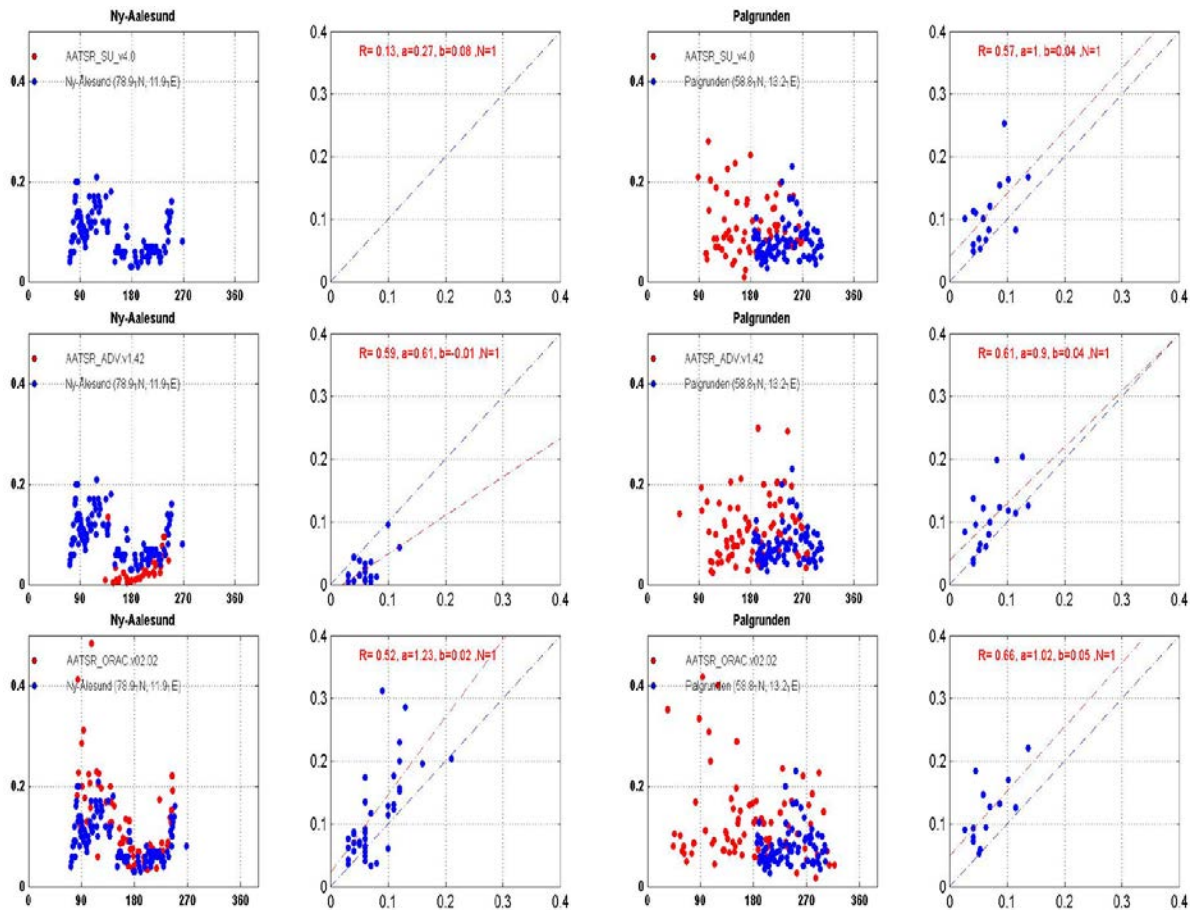


Figure 47: Time-series and comparison of daily average aerosol optical depth measured from satellite around Ny-Ålesund and Palgrunden during the sunlight time periods in 2008. The satellite data are averaged within  $\pm 2$  degrees around the stations. Shown are retrievals from AATSR, which have been developed in the framework of ESA's AEROSOL-CCI project: AATSR SU 4.0 from Swansea University (upper panel), AATSR ADV v1.42 from the Finnish Meteorological Institute (middle panel), and AATSR ORAC v. 2.02 from University of Oxford (lower panel).

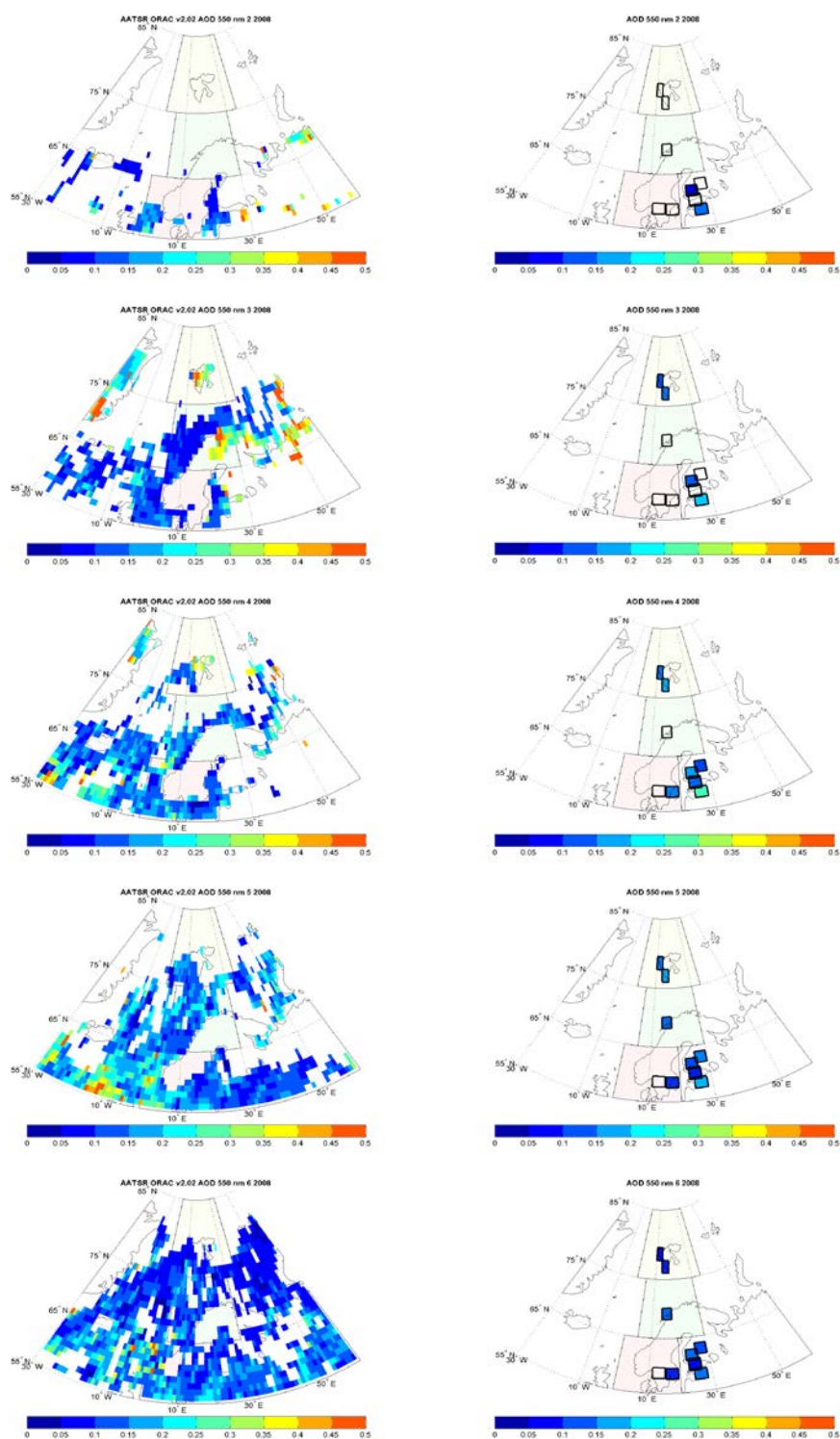


Figure 48 a: Monthly mean aerosol optical depth measured from the AATSR satellite, AATSR ORAC v. 2.02 from University of Oxford, and ground-based AOD network (see Toledano et al., 2012). Shown are the month February – June 2008.

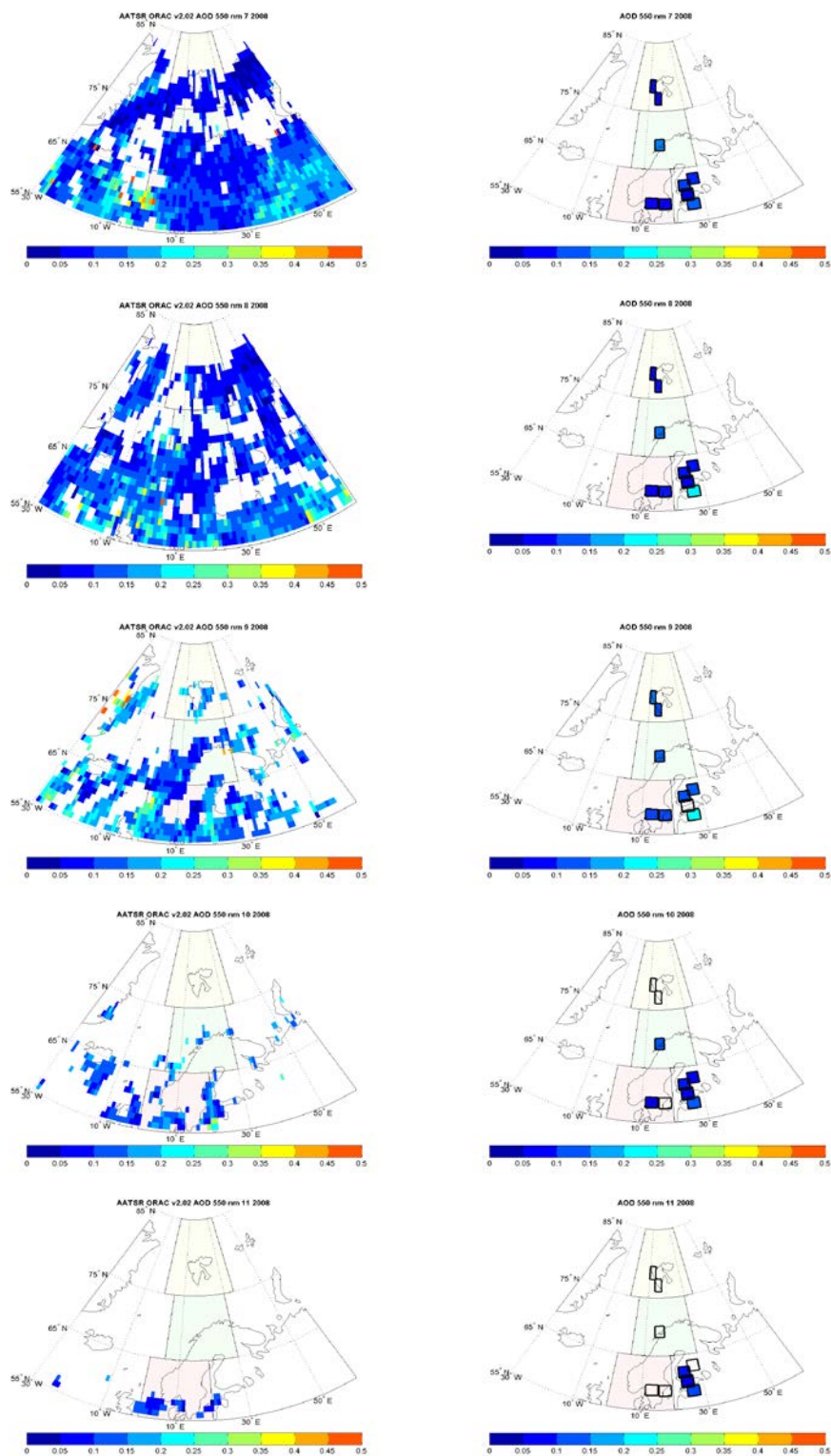
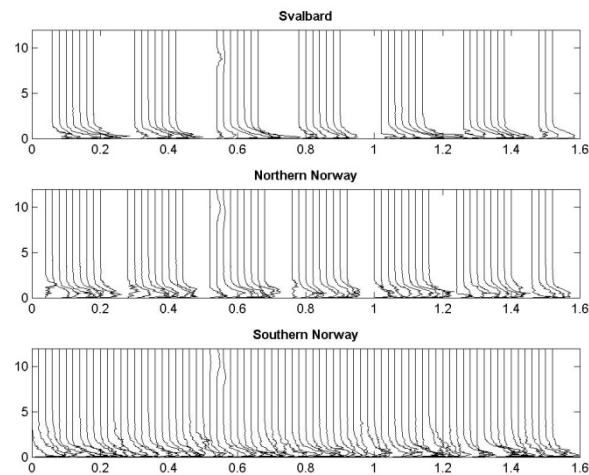


Figure 48 b: Monthly mean aerosol optical depth measured from the AATSR satellite, AATSR ORAC v. 2.02 from University of Oxford, and ground-based AOD network (see Toledano et al., 2012). Shown are the months July – November 2008.

As a final example, in Figure 49 monthly mean aerosol extinction profiles from the CALIOP lidar are shown. Night-time monthly averaged Level 3 data are plotted. Combined data (cloud free + above cloud) with horizontal resolution of  $5^\circ \times 2^\circ$  (longitude x latitude) and a vertical resolution of 60 m are given (CAL\_LID\_L3\_APro\_AllSky-Beta-V1-00). For details see [http://eosweb.larc.nasa.gov/PRODOCS/calipso/table\\_calipso.html](http://eosweb.larc.nasa.gov/PRODOCS/calipso/table_calipso.html) for more details). The data are averaged within the 3 areas, indicated in Figure 2, representative for Svalbard, Northern and Southern Norway. *The profiles shown cover the time period from June 2006 to November 2012.* Clearly, the contribution of the volcanic aerosol to the total aerosol load in autumn 2008 can be seen. In addition a lower boundary for the aerosol layer is seen above Svalbard. Furthermore, a seasonal cycle in the lower troposphere, related to Arctic haze, is seen. In-depths analysis is still outstanding, and will be presented in the 2013 report.



*Figure 49: Monthly mean night-time aerosol extinction profile, averaged within 3 areas (upper panel: latitude  $[75^\circ\text{N} - 85^\circ\text{N}]$ , longitude  $[-0^\circ\text{E} - 35^\circ\text{E}]$ ; middle panel: latitude  $[65^\circ\text{N} - 75^\circ\text{N}]$ , longitude  $[5^\circ\text{E} - 30^\circ\text{E}]$  and lower pane: latitude  $[55^\circ\text{N} - 65^\circ\text{N}]$ , longitude  $[0^\circ\text{E} - 20^\circ\text{E}]$ ). Profiles from the June 2006 until November 2012 are shown.*

## 8. Transport of air to the Zeppelin Observatory

We have performed an analysis and assessment of the source regions of the air masses arriving at Zeppelin in the period 2001-2011. Analyses of the air mass origin are important for the understanding of the observed levels of the gases and aerosols. We have analysed the origin of the air arriving at Zeppelin in 2011 and compared to previous years. Air mass trajectories are calculated using the FLEXTRA trajectory model (<http://www.nilu.no/trajectories/>) and using meteorological data provided from European Centre for Medium Range Weather Forecasts (ECMWF). 7 days backward trajectories from ECMWF have been used to investigate the major transport pathways to Svalbard and Zeppelin.<sup>16</sup> The origin of the air arriving at Zeppelin is categorised in following 6 sectors:

1. **Arctic region:** Clean Arctic air: Air mass trajectories with all trajectory points north of 65°N
2. **Atlantic sector:** Clean marine air: Air mass trajectories with all trajectory points between 10°W and 70°W and from south of 65°N.
3. **North American sector:** Polluted air: If at least 50% of the trajectory points are between 70°W and 180°W, and from south of 65°N.
4. **European sector:** Polluted air: If at least 50% of the trajectory points were between 10°W and 30°E, and from south of 65°N.
5. **Russian sector:** Polluted air: If air mass trajectories with all points between 30°E and 180°E and from south of 65°N.
6. **Undefined sector:** 20% the trajectories do not come from a distinct sector.

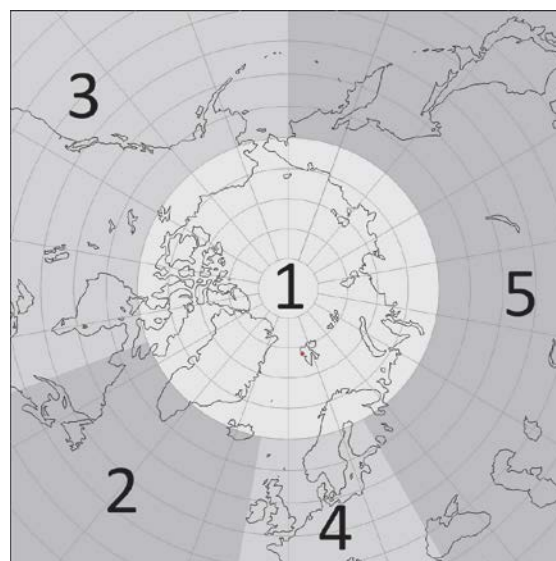


Figure 50: The sectors used to classify the air arriving at the Zeppelin Observatory. 1 is Arctic sector, 2 is Atlantic sector, 3 is North American sector, 4 is European sector and 5 is Russian sector.

Air from the Arctic and Atlantic sector are assumed to contain minimal influence of pollution, as there are almost no industrial sources in these areas, and one can say that the air is 'clean' (although there are increasing industrial activity in the northern part of Russia). Background values of the greenhouse gases components are defined from those 'clean air' areas with 6 out of 8 trajectories (sampling day +/- 12 hours) within the sector, as described above.

Figure 51 shows the share of polluted and clean air arriving at the Zeppelin observatory for the years 2001-2011. The most striking result of this analysis is that in particularly 2007 and

<sup>16</sup> The spatial resolution is T106, which correspond to a latitude/longitude resolution of 1x1 degrees, the temporal resolution is 6 hours, and 91 levels (60 levels before February 2006) are available in the vertical direction. The data sets used are so-called analysis, which is a combination of observations and numerical calculations. This includes measurements from satellites, radio sondes, buoys, weather stations, etc. which are assimilated into a meteorological model that produce an estimate of the state of the atmosphere at a given time.

2008 the fraction of air arriving at Zeppelin categorized as clean marine and Arctic air was clearly higher than the previous years. As described in section 4.1 the CH<sub>4</sub> concentration has increased since 2005. This can point in the direction of a possible Arctic source or accumulation of methane in the Arctic, particularly during late summer and autumn. Also the year 2003 with high methane concentration had a large fraction of clean air arriving at Zeppelin. 2009 is a somewhat different. In 2009 there were many episodes with polluted air transported to Zeppelin but no episodes as extreme as the record one observed in spring 2006 (Stohl et al., 2007; Myhre et al 2007). In contrast to the last years the site experienced higher influence of polluted air masses from central Europe and from the Russian sector in 2009. Clean arctic marine air dominated only on 59% of the days which is considerable lower than previous years. At the same time the category with mixed air from various sectors has increased slightly, thus the results are connected with uncertainty. 2010 and 2011 show similar results to several previous years with typical fraction of clean air, and air from the Russian and European sector, but a larger fraction of mixed air in 2011.

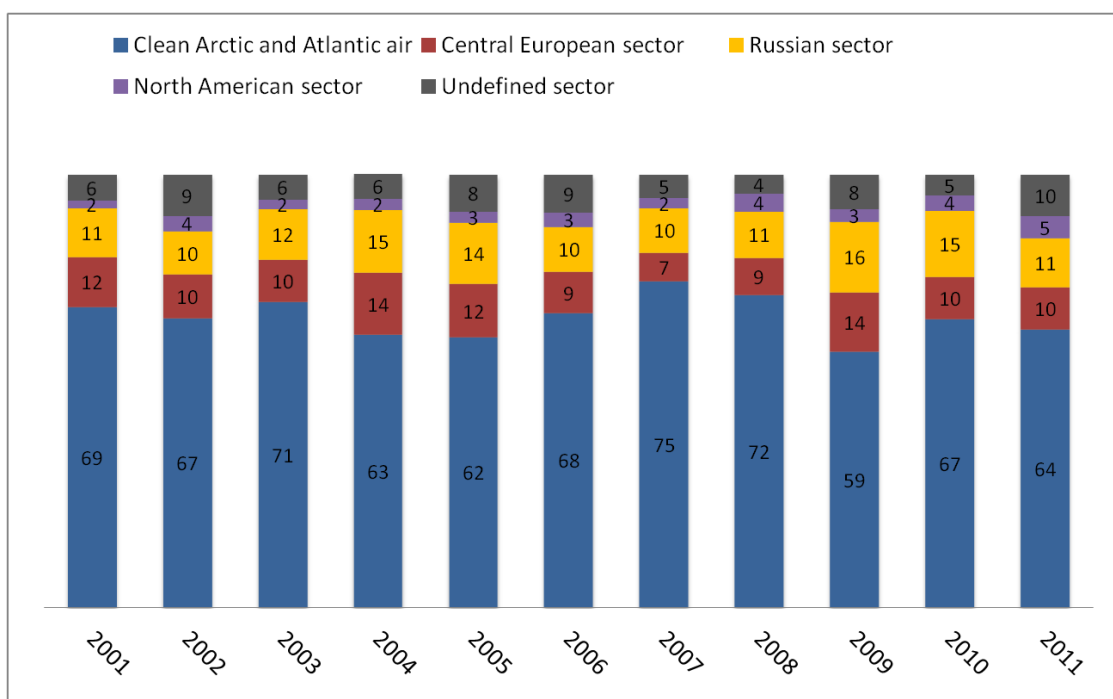


Figure 51: The percentage of polluted and clean air arriving at Zeppelin in the period 2001-2011 from the various sectors.

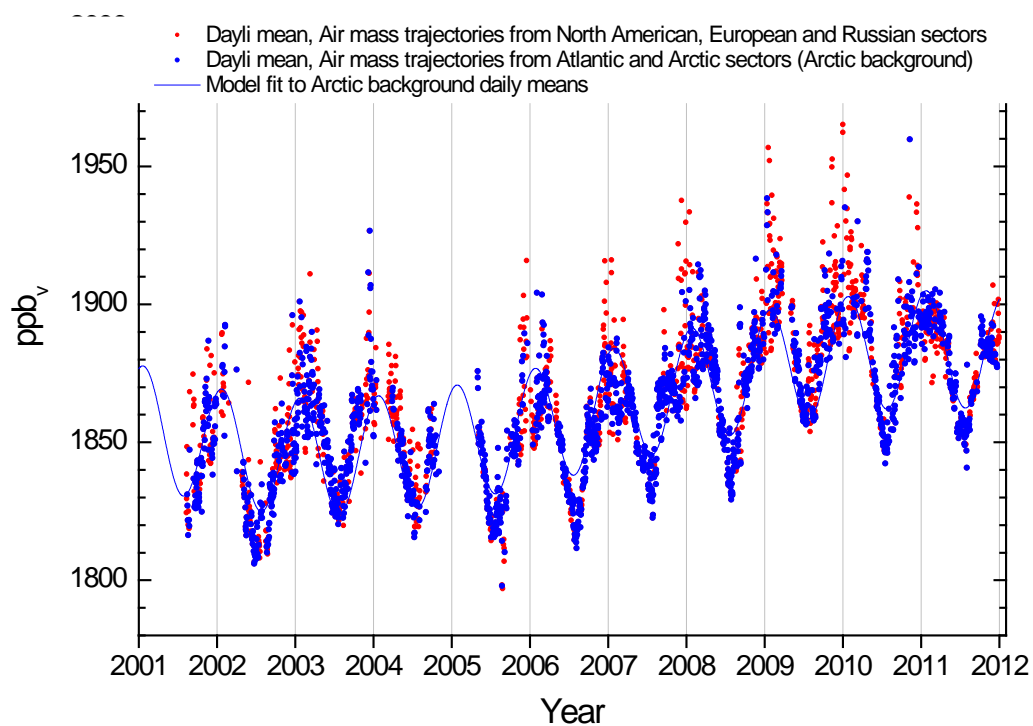


Figure 52: The daily mean methane observations when clean air is arriving (blue dots), compared to daily mean influenced by air from the polluted sections (reds dots).

## 9. References

- Aas, W., Solberg, S., Manø, S., Yttri, K.E. (2012) Monitoring of long-range transboundary air pollution. Annual report 2011. [In Norwegian]. Kjeller, NILU (Statlig program for forurensningsovervåking. Rapport 1126/2012. TA-2940/2012) (NILU OR 19/2012).
- Andreae, M.O., Jones, C.D., Cox, P.M. (2005) Strong present-day aerosol cooling implies a hot future. *Nature*, 435, 1187-1190.
- Asmi, A., Collaud Coen, M., Ogren, J.A., Andrews, E., Sheridan, P., Jefferson, A., Weingartner, E., Baltensperger, U., Bukowiecki, N., Lihavainen, H., Kivekäs, N., Asmi, E., Aalto, P.P., Kulmala, M., Wiedensohler, A., Birmili, W., Hamed, A., O'Dowd, C., Jennings, S.G., Weller, R., Flentje, H., Fjaeraa, A.M., Fiebig, M., Lund Myhre, C., Hallar, A.G., Laj, P. (2012) Aerosol decadal trends – Part 2: In-situ aerosol particle number concentrations at GAW and ACTRIS stations. *Atmos. Chem. Phys. Discuss.*, 12, 20849-20899.
- Bergamaschi, P., Frankenberg, C., Meirink, J.F., Krol, M., Dentener, F., Wagner, T., Platt, U., Kaplan, J. O., Körner, S., Heimann, M., Dlugokencky, E.J., Goede, A. (2007) Satellite cartography of atmospheric methane from SCIAMACHY onboard ENVISAT 2. Evaluation based on inverse model simulations. *J. Geophys. Res.*, 112, D02304, doi:10.1029/2006JD007268.
- Bousquet, P., Ringeval, B., Pison, I., Dlugokencky, E. J., Brunke, E.-G., Carouge, C., Chevallier, F., Fortems-Cheiney, A., Frankenberg, C., Hauglustaine, D. A., Krummel, P. B., Langenfelds, R. L., Ramonet, M., Schmidt, M., Steele, L. P., Szopa, S., Yver, C., Viovy, N., Ciais, P. (2011) Source attribution of the changes in atmospheric methane for 2006–2008. *Atmos. Chem. Phys.*, 11, 3689-3700, doi:10.5194/acp-11-3689-2011.
- Cohen, A.J., Anderson, H.R., Ostro, B., Pandey, K.D., Krzyzanowski, M., Künzli, N., Gutschmidt, K., Pope, A., Romieu, I., Samet, J.M., Smith, K. (2005) The global burden of disease due to outdoor air pollution. *J. Toxicol. Environ. Health A*, 68, 1301-1307.
- Collaud Coen, M., Andrews, E., Asmi, A., Baltensperger, U., Bukowiecki, N., Day, D., Fiebig, M., Fjaeraa, A.M., Flentje, H., Hyvärinen, A., Jefferson, A., Jennings, S.G., Kouvarakis, G., Lihavainen, H., Lund Myhre, C., Malm, W.C., Mihapopoulos, N., Molnar, J.V., O'Dowd, C., Ogren, J.A., Schichtel, B.A., Sheridan, P., Virkkula, A., Weingartner, E., Weller, R., Laj, P. (2012) Aerosol decadal trends – Part 1: In-situ optical measurements at GAW and IMPROVE stations. *Atmos. Chem. Phys. Discuss.*, 12, 20785-20848.
- Delene, D.J., Ogren, J.A. (2002) Variability of aerosol optical properties at four North American surface monitoring sites. *J. Atmos. Sci.*, 59, 1135-1150.
- Dubovik, O., Holben, B. N., Eck, T. F., Smirnov, A., Kaufman, Y. J., King, M. D., Tanre, D., Slutsker, I. (2002) Variability of absorption and optical properties of key aerosol types observed in worldwide locations. *J. Atmos. Sci.*, 59, 590-608.
- Dubovik, O., Smirnov, A., Holben, B.N., King, M.D., Kaufman, Y.J., Eck, T.F., Slutsker, I. (2000) Accuracy assessments of aerosol optical properties retrieved from Aerosol Robotic Network (AERONET) Sun and sky radiance measurements. *J. Geophys. Res.*, 105, 9791-9806.
- Dusek, U., Frank, G.P., Hildebrandt, L., Curtius, J., Schneider, J., Walter, S., Chand, D., Drewnick, F., Hings, S., Jung, D., Borrmann, S., Andreae, M.O. (2006) Size matters more than chemistry for cloud-nucleating ability of aerosol particles. *Science*, 312, 1375-1378.
- Fisher, R.E., Sriskantharajah, S., Lowry, D., Lanoisellé, M., Fowler, C.M.R., James, R.H., Hermansen, O., Lund Myhre, C. Stohl, A., Greinert, J., Nisbet-Jones, P.B.R., Mienert, J., Nisbet, E.G. (2011) Arctic methane sources: Isotopic evidence for atmospheric inputs. *Geophys. Res. Lett.*, 38, L21803, doi:10.1029/2011GL049319.
- Forster, P., Ramaswamy, V., Artaxo, P., Berntsen, T., Betts, R., Fahey, D.W., Haywood, J., Lean, J., Lowe, D.C., Myhre, G., Nganga, J., Prinn, R., Raga, G., Schulz, M., Van Dorland, R. (2007)

- Changes in atmospheric constituents and in radiative forcing. In: *Climate Change 2007: The physical science basis. Contribution of Working Group I to the fourth assessment report of the Intergovernmental Panel on Climate Change*. Ed. by Solomon, S., D. Qin, M. Manning, Z. Chen, M. Marquis, K.B. Averyt, M. Tignor, H.L. Miller. Cambridge, Cambridge University Press.
- Glantz, P., Tesche, M., Struthers, H., Stebel, K. (2012) Satellite and ground-based observations of aerosol optical properties in the Arctic for the period 2003-2011. Poster presented at the CRAICC meeting, Oslo, 26<sup>th</sup> – 28<sup>th</sup> August, 2012.
- Haywood, J.M., Shine, K.P. (1995) The effect of anthropogenic sulfate and soot aerosol on the clear sky planetary radiation budget. *Geophys. Res. Lett.*, 22, 603-606.
- Heintzenberg, J. (1980) Particle size distribution and optical properties of arctic haze. *Tellus*, 32, 251-260.
- Herber, A., Thomason, L.W., Gernandt, H., Leiterer, U., Nagel, D., Schulz, K., Kaptur, J., Albrecht, T., Notholt, J. (2002) Continuous day and night aerosol optical depth observations in the Arctic between 1991 and 1999. *J. Geophys. Res.*, 107, 4097, doi:10.1029/2001JD000536.
- Hoffmann, A., Ritter, C., Stock, M., Maturilli, M., Eckhardt, S., Herber, A., Neuber, R. (2010) Lidar measurements of the Kasatochi aerosol plume in August and September 2008 in Ny-Alesund, Spitsbergen, *J. Geophys. Res.*, 115, D00L12, doi:10.1029/2009JD013039.
- Holben, B., Eck, T., Slutsker, I., Tanré, D., Buis, J., Setzer, A., Vermote, E., Reagan, J., Kaufman, Y. (1998) AERONET- a federated instrument network and data archive for aerosol characterization. *Remote Sens. Environ.*, 66, 1-16.
- Hirdman, D., Burkhart, J.F., Sodemann, H., Eckhardt, S., Jefferson, A., Quinn, P.K., Sharma, S., Ström, J., Stohl, A. (2010) Long-term trends of black carbon and sulphate aerosol in the Arctic: changes in atmospheric transport and source region emissions. *Atmos. Phys. Chem.*, 10, 9351-9368.
- IPCC (2007) Summary for Policymakers. In: *Climate Change 2007: The Physical Science Basis. Contribution of Working Group I to the Fourth Assessment Report of the Intergovernmental Panel on Climate Change*. Ed.d by Solomon, S., D. Qin, M. Manning, Z. Chen, M. Marquis, K.B. Averyt, M. Tignor, H.L. Miller. Cambridge, Cambridge University Press.
- Isaksen, I.S.A., Hov, Ø. (1987) Calculation of trends in the tropospheric concentration of O<sub>3</sub>, OH, CO, CH<sub>4</sub> and NO<sub>x</sub>. *Tellus*, 39B, 271-285.
- Isaksen, I.S.A., Gauss, M., Myhre, G., Walter Anthony, K.M., Ruppel, C. (2010) Strong atmospheric chemistry feedback to climate warming from Arctic methane emissions. *Global Biogeochem. Cycles*, 25, GB2002, doi:10.1029/2010GB003845.
- Jaenicke, R. (1980) Natural aerosols. *Ann. New York Acad. Sci.*, 338, 317-329.
- Kiehl, J.T. (2007) Twentieth century climate model response and climate sensitivity. *Geophys. Res. Lett.*, 34, L22710, doi:10.1029/2007GL31383.
- Kreidenweis, S.M., Petters, M.D., Chuang, P.Y. (2009) Cloud particle precursors. In: *Clouds in the perturbed climate system : Their relationship to energy, balance, atmospheric dynamics, and precipitation*. Ed. by: Heintzenberg, J., Charlson, R.J. Cambridge, MA, MIT Press (Strüngmann Forum Reports). pp. 291-318.
- Kristiansen, N. I., Stohl, A., Prata, A.J., Richter, A., Eckhardt, S., Seibert, P., Hoffmann, A., Ritter, C., Bitar, L., Duck, T.J., Stebel, K. (2010) Remote sensing and inverse transport modeling of the Kasatochi eruption sulfur dioxide cloud. *J. Geophys. Res.*, 115, D00L16, doi:10.1029/2009JD013286.
- Kulmala, M., Vehkamäki, H., Petäjä, T., DalMasó, M., Lauri, A., Kerminen, V.-M., Birmili, W., McMurry, P.H. (2004) Formation and growth rates of ultrafine atmospheric particles: a review of observations. *J. Aerosol Sci.*, 35, 143-176.

- Law, K., Stohl, A. (2007) Arctic air pollution: Origins and impacts. *Science*, 315, 1537-1540.
- Mazzola, M., Stone, R.S., Herber, A., Tomasi, C., Lupi, A., Vitale, V., Lanconelli, C., Toledano, C., Cachorro, V.E., O'Neill, N.T., Shiobara, M., Aaltonen, V., Stebel, K., Zielinski, T., Petelski, T., Ortiz de Galisteo, J.P., Torres, B., Berjon, A., Goloub, P., Li, Z., Blarel, L., Abboud, I., Cuevas, E., Stock, M., Schulz, K.-H., Virkkula, A. (2011) Evaluation of sun photometer capabilities for retrievals of aerosol optical depth at high latitudes: The POLAR-AOD intercomparison campaigns. *Atmos. Environ.*, 52, 4-17, doi:10.1016/j.atmosenv.2011.07.042.
- McFiggans, G., Artaxo, P., Baltensperger, U., Coe, H., Facchini, M. C., Feingold, G., Fuzzi, S., Gysel, M., Laaksonen, A., Lohmann, U., Mentel, T. F., Murphy, D. M., O'Dowd, C. D., Snider, J. R., Weingartner, E. (2006) The effect of physical and chemical aerosol properties on warm cloud droplet activation. *Atmos. Chem. Phys.*, 6, 2593-2649, doi:10.5194/acp-6-2593-2006.
- Myhre, C.L., Hermansen, O., Fjæraa, A.M., Lunder, C., Schmidbauer, N., Stebel, K., Prata, F. (2010) Greenhouse monitoring at the Zeppelin station - annual report 2008. Kjeller, NILU (Statlig program for forurensningsovervåking. Rapport 1071/2010) (TA 2633/2010) (NILU OR 24/2010).
- Myhre, C.L., Toledano, C., Myhre, G., Stebel, K., Yttri, K.E., Aaltonen, V., Johnsrud, M., Frioud, M., Cachorro, V., de Frutos, A., Lihavainen, H., Campbell, J.R., Chaikovskiy, A.P., Shiobara, M., Welton, E.J., Tørseth, K. (2007) Regional aerosol optical properties and radiative impact of the extreme smoke event in the European Arctic in spring 2006. *Atmos. Chem. Phys.*, 7, 5899-5915.
- Myhre, G., Fuglestad, J.S., Berntsen, T.K., Lund, M.T. (2011) Mitigation of short-lived heating components may lead to unwanted long-term consequences. *Atmos. Environ.*, 45, 6103-6106.
- NASA Goddard Space Flight Center (2011) AERONET Aerosol Robotic Network. **URL:** <http://aeronet.gsfc.nasa.gov/> [2011-06-09]
- O'Neill, N., Eck, T., Smirnov, A., Holben, B. (2008) Spectral Deconvolution Algorithm (SDA), Technical memo, version 4.1. AERONET, NASA. **URL:** [http://aeronet.gsfc.nasa.gov/new\\_web/PDF/tauf\\_tauc\\_technical\\_memo.pdf](http://aeronet.gsfc.nasa.gov/new_web/PDF/tauf_tauc_technical_memo.pdf)
- O'Neill, N.T., Eck, T.F., Smirnov, A., Holben, B.N., Thulasiraman, S. (2003) Spectral discrimination of coarse and fine mode optical depth. *J. Geophys. Res.*, 108, 4559, doi:10.1029/2002JD002975.
- Prather, M., Ehhalt, D., Dentener, F., Derwent, R.G., Dlugokencky, E., Holland, E., Isaksen, I.S.A., Katima, J., Kirchhoff, V., Matson, P., Midgley, P.M., Wang, M. (2001) Atmospheric chemistry and greenhouse gases. In: *Climate Change 2001: The Scientific Basis, Contribution of Working Group I to the Third Assessment Report of the Intergovernmental Panel on Climate Change*. Ed. by: Houghton, J.T. et al. Cambridge, Cambridge University Press. pp. 239-287.
- Raes, F., Van Dingenen, R., Vignati, E., Wilson, J., Putaud, J.-P., Seinfeld, J. H., Adams, P. (2000) Formation and cycling of aerosols in the global troposphere. *Atmos. Environ.*, 34, 4215-4240.
- Repo, M.E., Susiluoto, S., Lind, S.E., Jokinen, S., Elsakov, V., Biasi, C., Virtanen, T., Pertti, J., Martikainen, P.J. (2009) Large N<sub>2</sub>O emissions from cryoturbated peat soil in tundra. *Nature Geosci.*, 2, 189-192.
- Rigby, M., Prinn, R.G., Fraser, P.J., Simmonds, P.G., Langenfelds, R.L., Huang, J., Cunnold, D.M., Steele, L.P., Krümmel, P.B., Weiss, R.F., O'Doherty, S., Salameh, P.K., Wang, H.J., Harth, C.M., Mühle, J., Porter, L.W. (2008) Renewed growth of atmospheric methane. *Geophys. Res. Lett.*, 35, L22805, doi:10.1029/2008GL036037.
- Rodríguez, E., Toledano, C., Cachorro, V.E., Ortiz, P., Stebel, K., Berjón, A., Blindheim, S., Gausa, M., de Frutos, A.M. (2012) Aerosol characterization at the sub-Arctic site Andenes (69°N, 16°E), by the analysis of columnar optical properties. *Quart. J. Roy. Meteorol. Soc.*, 138, 471-482, doi:10.1002/qj.921.
- Schuur, E., Abbot, B. (2011) High risk of permafrost thaw. *Nature*, 480, 32-33,

- Seinfeld, J., Pandis, S. (1998) Atmospheric chemistry and physics: From air pollution to climate change. New York, John Wiley & Sons.
- Sheridan, P. J., Ogren, J.A. (1999) Observations of the vertical and regional variability of aerosol optical properties over central and eastern North America. *J. Geophys. Res.*, *104*, 16793-16805.
- Shindell, D., Faluvegi, G. (2009) Climate response to regional radiative forcing during the twentieth century. *Nature Geosci.*, *2*, 294-300.
- Simmonds, P.G., Manning, A.J., Cunnold, D.M., Fraser, P.J., McCulloch, A., O'Doherty, S., Krummel, P.B., Wang, R.H.J., Porter, L.W., Derwent, R.G., Grealley, B., Salameh, P., Miller, B.R., Prinn, R.G., Weiss, R.F. (2006) Observations of dichloromethane, trichloroethene and tetrachloroethene from the AGAGE stations at Cape Grim, Tasmania, and Mace Head, Ireland. *J. Geophys. Res.*, *111*, D18304, doi:10.1029/2006JD007082.
- Sodemann, H., Pommier, M., Arnold, S. R., Monks, S. A., Stebel, K., Burkhardt, J. F., Hair, J. W., Diskin, G. S., Clerbaux, C., Coheur, P.-F., Hurtmans, D., Schlager, H., Blechschmidt, A.-M., Kristjánsson, J. E., Stohl, A. (2011) Episodes of cross-polar transport in the Arctic troposphere during July 2008 as seen from models, satellite, and aircraft observations, *Atmos. Chem. Phys.*, *11*, 3631-3651, doi:10.5194/acp-11-3631-2011.
- Stohl, A., Seibert, P. (1998) Accuracy of trajectories as determined from the conservation of meteorological tracers. *Quart. J. Roy. Meteorol. Soc.*, *124*, 1465-1484.
- Stohl, A., Andrews, E., Burkhardt, J.F., Forster, C., Herber, A., Hoch, S.W., Kowal, D., Lunder, C., Mefford, T., Ogren, J.A., Sharma, S., Spichtinger, N., Stebel, K., Stone, R., Strom, J., Tørseth, K., Wehrli, C., Yttri, K.E. (2006) Pan-Arctic enhancements of light absorbing aerosol concentrations due to North American boreal forest fires during summer 2004. *J. Geophys. Res.*, *111*, D22214, doi:10.1029/2006JD007216.
- Stohl, A., Berg, T., Burkhardt, J.F., Fjæraa, A.M., Forster, C., Herber, A., Hov, Ø., Lunder, C., McMillan, W.W., Oltmans, S., Shiobara, M., Simpson, D., Solberg, S., Stebel, K., Ström, J., Tørseth, K., Treffeisen, R., Virkkunen, K., Yttri, K.E. (2007) Arctic smoke – record high air pollution levels in the European Arctic due to agricultural fires in Eastern Europe in spring 2006. *Atmos. Chem. Phys.*, *7*, 511-534.
- Stohl, A., Forster, C., Frank, A., Seibert, P., Wotawa, G. (2005) Technical note: The lagrangian particle dispersion model flexpart version 6.2. *Atmos. Chem. Phys.*, *5*, 2461-2474.
- Stohl, A., Hittenberger, M., Wotawa, G. (1998) Validation of the lagrangian particle dispersion model FLEXPART against large scale tracer experiment data. *Atmos. Environ.*, *32*, 4245–4264.
- Stohl, A., Wotawa, G., Seibert, P., Kromp-Kolb, H. (1995) Interpolation errors in wind fields as a function of spatial and temporal resolution and their impact on different types of kinematic trajectories. *J. Appl. Meteor.*, *34*, 2149-2165.
- Toledano, C., Cachorro, V., Gausa, M., Stebel, K., Aaltonen, V., Berjón, A., Ortiz de Galisteo, J.P., de Frutos, A.M., Bennouna, Y., Blindheim, S., Myhre, C.L., Zibordi, G., Wehrli, C., Kratzer, S., Hakansson, B., Carlund, T., de Leeuw, G., Herber, A., Torres, B. (2011) Overview of sun photometer measurements of aerosol properties in Scandinavia and Svalbard. *Atmos. Environ.*, *52*, 18-28, doi:10.1016/j.atmosenv.2011.10.022.
- Tomasi, C., Vitale, V., Lupi, A., Di Carmine, C., Campanelli, M., Herber, A., Treffeisen, R., Stone, R.S., Andrews, E., Sharma, S., Radionov, V., von Hoyningen-Huene, W., Stebel, K., Hansen, G.H., Myhre, C.L., Wehrli, C., Aaltonen, V., Lihavainen, H., Virkkula, A., Hillamo, R., Ström, J., Toledano, C., Cachorro, V.E., Ortiz, P., de Frutos, A.M., Blindheim, S., Frioud, M., Gausa, M., Zielinski, T., Petelski, T., Yamanouchi, T. (2007) Aerosols in polar regions: A historical overview based on optical depth and in situ observations. *J. Geophys. Res.*, *112*, D16205, doi:10.1029/2007JD008432.

- Walter, K.M., Edwards, M.E., Grosse, G., Zimov, S.A., Chapin III, F.S. (2007) Thermokarst lakes as a source of atmospheric CH<sub>4</sub> during the last deglaciation. *Science*, 318, 633–636.
- Wehrli, C. (2000) Calibrations of filter radiometers for determination of atmospheric optical depth. *Metrologia*, 37, 419-422.
- Wehrli, C. (2005) GAWPFR: A network of aerosol optical depth observations with precision filter radiometers. In: *WMO/GAW Experts workshop on a global surface based network for long term observations of column aerosol optical properties*. Geneva, World Meteorological Organization (GAW Report No. 162, WMO TD No. 1287).
- Winker, D.M., J. L. Tackett, B. J. Getzewich, Z. Liu, M. A. Vaughan, and R. R. Rogers (2012) The global 3-D distribution of tropospheric aerosols as characterized by CALIOP, *Atmos. Chem. Phys. Discuss.*, 12, 24847-24893.
- WMO (2012) Greenhouse Gas Bulletin. The state of greenhouse gases in the atmosphere using global observations through 2011. Geneva (Bulletin No. 8, 19 November 2012). **URL:** [http://www.wmo.int/pages/prog/arep/gaw/ghg/documents/GHG\\_Bulletin\\_No.8\\_en.pdf](http://www.wmo.int/pages/prog/arep/gaw/ghg/documents/GHG_Bulletin_No.8_en.pdf)
- WMO (2011) Scientific assessment of ozone depletion: 2010. Geneva, World Meteorological Organization (Global ozone research and monitoring project, Report No. 52).
- WMO (2009) Greenhouse Gas Bulletin. The state of greenhouse gases in the atmosphere using global observations through 2008. Geneva (Bulletin No. 5, 23 November 2009). **URL:** [http://www.wmo.int/pages/prog/arep/gaw/ghg/documents/ghg-bulletin2008\\_en.pdf](http://www.wmo.int/pages/prog/arep/gaw/ghg/documents/ghg-bulletin2008_en.pdf)
- Zaelke, D.J., Ramanathan, V. (2012) Going beyond carbon dioxide. *The New York Times*, Dec 6, 2012. **URL:** [https://www.nytimes.com/2012/12/07/opinion/going-beyond-carbon-dioxide.html?\\_r=1&](https://www.nytimes.com/2012/12/07/opinion/going-beyond-carbon-dioxide.html?_r=1&)

## ***Appendix I: Description of instruments, methods and trend analysis***

In this appendix are the instrumental methods used for the measurements of the various greenhouse gases presented. Additionally we explain the theoretical methods used in the calculation of the trends. In the end of the section we show how the annual mean values presented in Table 2 are calculated.

### **Details about greenhouse gas measurements and recent improvement and extensions**

#### *Halogenated compounds*

NILU performs measurements of halogenated greenhouse gases as well as methane and carbon monoxide using automated gas chromatographs with high sampling frequencies at Zeppelin. A mass spectrometric detector is used to determine more than 20 halogenated compounds, automatically sampled 12 times per day. Methane and CO are sampled 3 times per hour. This high sampling frequency gives valuable data for the examination of episodes caused by long-range transport of pollutants as well as a good basis for the study of trends and global atmospheric change. Close cooperation with AGAGE-partners on the halocarbon instrument and audits on the methane and CO-instruments (performed by EMPA on the behalf of GAW/WMO) results in data of high quality.

At the Birkenes Observatory a very different approach is used. At this site Picarro Cavity Ring-Down Spectroscopy (CRDS) is employed. This is a state of the art infrared spectrometer for field measurements with very high time resolution and precision. The Picarro CRDS are utilizing a near-infrared laser to measure spectral signatures of the molecule. Gas is introduced in an optical measurement cavity with an effective path length of up to 20 km making it possible to measure very low concentrations. The CRDS technology allows monitoring of CO<sub>2</sub> and CH<sub>4</sub> in moist air. During post-processing concentrations are re-calculated for dry air. This is required to remove the variability of moisture in the atmosphere, and to make the monitoring results comparable with traditional FTIR monitoring methods.

Table 7: Instrumental details for greenhouse gas measurements at Zeppelin and Birkenes.

Component		Instrument and method	Time res.	Calibration procedures	Comment
<b>Methane (Birkenes)</b>	CH <sub>4</sub>	Picarro CRDS G1301 CO <sub>2</sub> /CH <sub>4</sub> /H <sub>2</sub> O	5 s	Waiting for calibration gases from NOAA. Currently only initial calibration from Picarro.	Measurements started 19. May 2009
<b>Methane (Zeppelin)</b>	CH <sub>4</sub>	GC-FID-	15 min	Hourly, working std. calibrated vs. GAW std.	Data coverage 2010: 70% (97% for daily values). Low coverage due to a problem with the ventilation system in the station building causing contamination of samples during last part of the year.
<b>Nitrous oxide (Zeppelin)</b>	N <sub>2</sub> O	GC--ECD	15 min	Hourly, working std. calibrated vs. GAW std.	Data coverage 2010: 77%. Measurements started 02.04.2010.
<b>Carbon monoxide</b>	CO	GC-MgO/UV	20 min	Every 20 min, working std. calibrated vs. GAW std.	Data coverage 2011: 75%
<b>Carbon dioxide (Zeppelin)</b>	CO <sub>2</sub>		1 h		CO <sub>2</sub> measurements performed by ITM Stockholm University (SU)
<b>Carbon dioxide (Birkenes)</b>	CO <sub>2</sub>	Picarro CRDS G1301 CO <sub>2</sub> /CH <sub>4</sub> /H <sub>2</sub> O	5 s	Waiting for calibration gases from NOAA. Currently only initial calibration from Picarro.	Measurements started 19. May 2009.
<b>CFC-11</b> <b>CFC-12</b> <b>CFC-113</b> <b>CFC-115</b> <b>HFC-125</b> <b>HFC-134a</b> <b>HFC-152a</b> <b>HFC-365mfc</b> <b>HCFC-22</b> <b>HCFC-141b</b> <b>HCFC-142b</b> <b>H-1301</b> <b>H-1211</b>	CFCl <sub>3</sub> CF <sub>2</sub> Cl <sub>2</sub> CF <sub>2</sub> ClCFCl <sub>2</sub> CF <sub>3</sub> CF <sub>2</sub> Cl CHF <sub>2</sub> CF <sub>3</sub> CH <sub>2</sub> FCF <sub>3</sub> CH <sub>3</sub> CHF <sub>2</sub> CF <sub>3</sub> CH <sub>2</sub> CHF <sub>2</sub> CH <sub>3</sub> CHF <sub>2</sub> Cl CH <sub>3</sub> CFCl <sub>2</sub> CH <sub>3</sub> CF <sub>2</sub> Cl CF <sub>3</sub> Br CF <sub>2</sub> ClBr	ADS-GCMS	4 h	Every 4 hours, working std. calibrated vs. AGAGE std.	Data coverage 2011: no data reported from this instrument after 31.12.2010 The measurements of the CFCs have higher uncertainty and are not within the required precision of AGAGE. See next section for details.

Table 7, cont.

Component		Instrument and method	Time res.	Calibration procedures	Comment
<b>Methyl Chloride</b>	CH <sub>3</sub> Cl				
<b>Methyl Bromide</b>	CH <sub>3</sub> Br				
<b>Methylendichloride</b>	CH <sub>2</sub> Cl <sub>2</sub>				
<b>Chloroform</b>	CHCl <sub>3</sub>				
<b>Methylchloroform</b>	CH <sub>3</sub> CCl <sub>3</sub>				
<b>TriChloroethylene</b>	CHClCCl <sub>2</sub>				
<b>Perchloroethylene</b>	CCl <sub>2</sub> CCl <sub>2</sub>				
<b>Sulphurhexafluoride</b>	SF <sub>6</sub>				
<b>Tetrafluormethane</b>	CF <sub>4</sub>	Medusa-GCMS	2 h	Every 2	Data coverage 2011:
<b>PFC-116</b>	C <sub>2</sub> F <sub>6</sub>	No. 19		hours,	90%
<b>PFC-218</b>	C <sub>3</sub> F <sub>8</sub>			working std.	
<b>PFC-318</b>	c-C <sub>4</sub> F <sub>8</sub>			calibrated vs.	The precision is
<b>Sulphurhexafluoride</b>	SF <sub>6</sub>			AGAGE std	improved and more
<b>Sulfuryl fluoride</b>	SO <sub>2</sub> F <sub>2</sub>				components are
<b>HFC-23</b>	CHF <sub>3</sub>				measured compared
<b>HFC-32</b>	CH <sub>2</sub> F <sub>2</sub>				to the ADS-GCMS.
<b>HFC-125</b>	CHF <sub>2</sub> CF <sub>3</sub>				
<b>HFC-134a</b>	CH <sub>2</sub> FCF <sub>3</sub>				
<b>HFC-143a</b>	CH <sub>3</sub> CF <sub>3</sub>				
<b>HFC-152a</b>	CH <sub>3</sub> CHF <sub>2</sub>				
<b>HFC-227ea</b>	CF <sub>3</sub> CHFCF <sub>3</sub>				
<b>HFC-236fa</b>	CF <sub>3</sub> CH <sub>2</sub> CF <sub>3</sub>				
<b>HFC-245fa</b>	CF <sub>3</sub> CH <sub>2</sub> CHF <sub>2</sub>				
<b>HFC-365mfc</b>	CF <sub>3</sub> CH <sub>2</sub> CHF <sub>2</sub> CH <sub>3</sub>				
<b>HCFC-22</b>	CHF <sub>2</sub> Cl				
<b>HCFC-124</b>	CHClFCF <sub>3</sub>				
<b>HCFC-141b</b>	CH <sub>3</sub> CFCl <sub>2</sub>				
<b>HCFC-142b</b>	CH <sub>3</sub> CF <sub>2</sub> Cl				
<b>CFC-11</b>	CFCl <sub>3</sub>				
<b>CFC-12</b>	CF <sub>2</sub> Cl <sub>2</sub>				
<b>CFC-113</b>	CF <sub>2</sub> ClCFCl <sub>2</sub>				
<b>CFC-114</b>	CF <sub>2</sub> ClCF <sub>2</sub> Cl				
<b>CFC-115</b>	CF <sub>3</sub> CF <sub>2</sub> Cl				
<b>H-1211</b>	CF <sub>3</sub> Br				
<b>H-1301</b>	CF <sub>2</sub> ClBr				
<b>H-2402</b>	CF <sub>2</sub> BrCF <sub>2</sub> Br				
<b>Methyl Chloride</b>	CH <sub>3</sub> Cl				
<b>Methyl Bromide</b>	CH <sub>3</sub> Br				
<b>Methyl Iodide</b>	CH <sub>3</sub> I				
<b>Methylendichloride</b>	CH <sub>2</sub> Cl <sub>2</sub>				
<b>Chloroform</b>	CHCl <sub>3</sub>				
<b>Methylchloroform</b>	CH <sub>3</sub> CCl <sub>3</sub>				
<b>Dibromomethane</b>	CH <sub>2</sub> Br <sub>2</sub>				
<b>Bromoform</b>	CHBr <sub>3</sub>				
<b>TriChloroethylene</b>	TCE				
<b>Perchloroethylene</b>	PCE				
<b>Ethane</b>	C <sub>2</sub> H <sub>6</sub>				
<b>Benzene</b>	C <sub>6</sub> H <sub>6</sub>				
<b>Carbonyl Sulfide</b>	COS				
<b>Ozone</b>	O <sub>3</sub>		5 min		

*Data quality and uncertainties;* In 2001 – 2010 measurements of a wide range of hydrochlorofluorocarbons, hydrofluorocarbons (HCFC-141b, HCFC-142b, HFC-134a etc.), methyl halides (CH<sub>3</sub>Cl, CH<sub>3</sub>Br, CH<sub>3</sub>I) and the halons (e.g. H-1211, H-1301) was measured with good scientific quality by using ADS-GCMS. The system also measured other compounds like the chlorofluorocarbons, but the quality and the precision of these measurements was not at the same level. Table 8 shows a list over those species measured with the ADS-GCMS at Zeppelin Observatory. The species that are in blue are of acceptable scientific quality and in accordance with recommendations and criteria of the AGAGE network for measurements of halogenated greenhouse gases. Those listed in red have higher uncertainty and are not within the required precision of AGAGE. There are various reasons for this increased uncertainty; unsolved instrumental problems e.g. possible electron overload in detector (for the CFC's), influence from other species, detection limits (CH<sub>3</sub>I, CHClCCl<sub>2</sub>) and unsolved calibration problems (CHBr<sub>3</sub>).

*Table 8: ADS-GCMS measured species. Good scientific quality data in Blue; Data with reduced quality data in Red. The data are available through <http://ebas.nilu.no>. Please read and follow the stated data policy upon use.*

Compound	Typical precision (%)	Compound	Typical precision (%)
SF <sub>6</sub>	1.5	H1301	1.5
HFC134a	0.4	H1211	0.4
HFC152a	0.6	CH <sub>3</sub> Cl	0.6
HFC125	0.8	CH <sub>3</sub> Br	0.8
HFC365mfc	1.7	CH <sub>3</sub> I	5.1
HCFC22	0.2	CH <sub>2</sub> Cl <sub>2</sub>	0.4
HCFC141b	0.5	CHCl <sub>3</sub>	0.3
HCFC142b	0.5	CHBr <sub>3</sub>	15
HCFC124	2.3	CCl <sub>4</sub>	0.5
CFC11	0.3	CH <sub>3</sub> CCl <sub>3</sub>	0.6
CFC12	0.3	CHClCCl <sub>2</sub>	1.2
CFC113	0.2	CCl <sub>2</sub> CCl <sub>2</sub>	0.7
CFC115	0.8		

*New Medusa-GCMS instrument installed at Zeppelin and improved air inlet system*

To have the suitable and necessary scientific quality of the GHG measurements and fulfill the requirements of AGAGE, NILU installed a new Medusa-GCMS at the Zeppelin Observatory Autumn 2010. The instrument is developed to provide more accurate measurements of halocarbon gases and also extending the range of compounds monitored.

The new Medusa-GCMS instruments not only extend the number of species measured by original ADS-GCMS instruments to 40 species, but also improve the quality and precision of measurements of most of the species, especially the CFC's. But even though the improvements, there are still a few issues related to the measurements of the CFC's and a few others of the 40 species that are unresolved. Therefore, the AGAGE network has decided to report their CFC data measured with their old GC-MD system from the AGAGE stations that both have a GC-MD and a Medusa-GCMS.

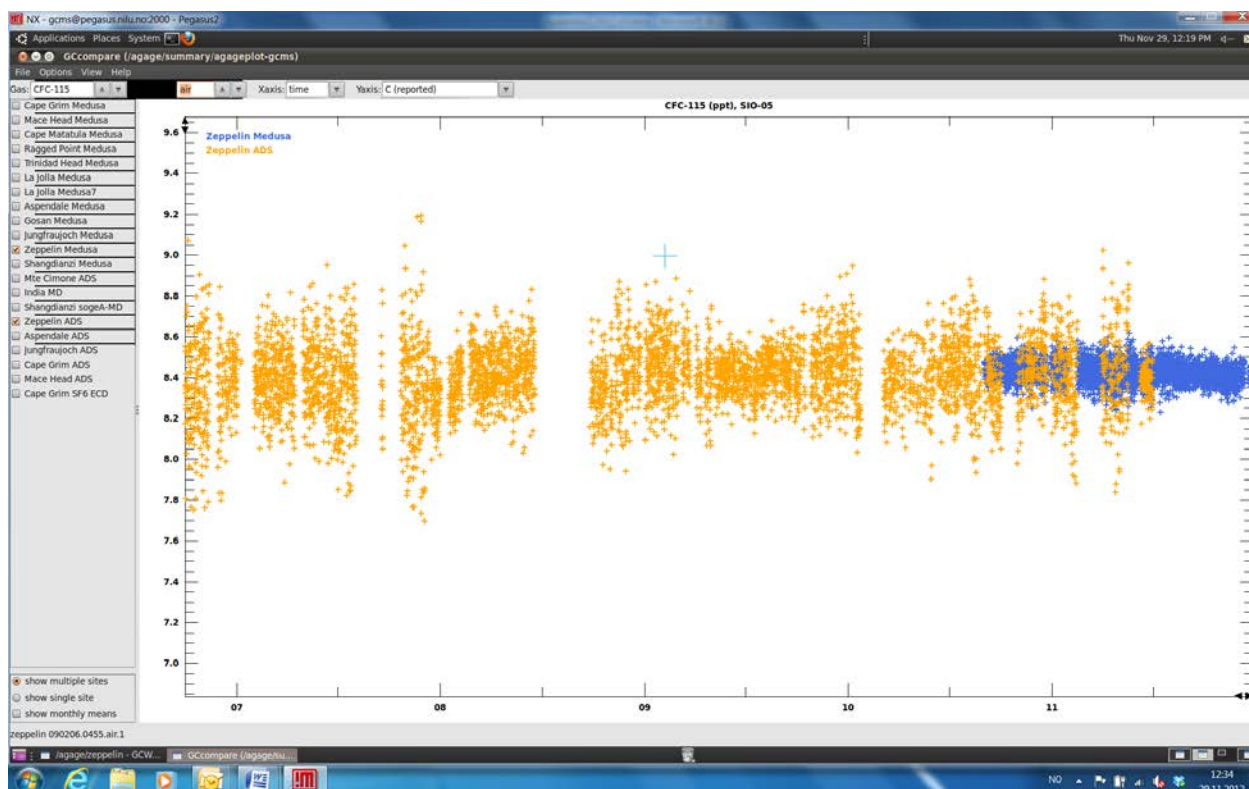


Figure 53: Measurements of CFC-115 at Zeppelin Observatory. The measurement precision improves when using results from the Medusa-GCMS (in blue) compared to the ADS-GCMS (in yellow).

Table 9 gives an overview over the species measured with the Medusa-GCMS and GC-MD systems at the AGAGE stations and the typical precision with the different instruments. After the installation of the Medusa-GCMS instrument and implementation of the same calibration scale and QA/QC routines as the rest of the AGAGE station, the Zeppelin Observatory is considered as an AGAGE station and the measurements performed meet the same criteria as shown in Table 9.

Table 9: AGAGE measured species. *Medusa in Blue; GC-MD green; Both: Red.*

Compound	Typical precision (%)	Compound	Typical precision (%)
CF <sub>4</sub>	0.15	H1301	1.5
C <sub>2</sub> F <sub>6</sub>	0.9	H1211	0.5
C <sub>3</sub> F <sub>8</sub>	3	H2402	2
SF <sub>6</sub>	0.4	CH <sub>3</sub> Cl	0.2
SO <sub>2</sub> F <sub>2</sub>	1.6	CH <sub>3</sub> Br	0.5
HFC23	0.7	CH <sub>3</sub> I	2
HFC32	5	CH <sub>2</sub> Cl <sub>2</sub>	0.8
HFC134a	0.4	CHCl <sub>3</sub>	0.6
HFC152a	1.2	CHBr <sub>3</sub>	0.6
HFC125	1	CCl <sub>4</sub>	1
HFC143a	1.2	CH <sub>3</sub> CCl <sub>3</sub>	0.7
HFC365mfc	10	CHClCCl <sub>2</sub>	2.5
HCFC22	0.3	CCl <sub>2</sub> CCl <sub>2</sub>	0.5
HCFC141b	0.4	C <sub>2</sub> H <sub>2</sub>	0.5
HCFC142b	0.6	C <sub>2</sub> H <sub>4</sub>	2
HCFC124	2	C <sub>2</sub> H <sub>6</sub>	0.3
CFC11	0.15	C <sub>6</sub> H <sub>6</sub>	0.3
CFC12	0.05	C <sub>7</sub> H <sub>8</sub>	0.6
CFC13	2	GC-MD only*	
CFC113	0.2	CH <sub>4</sub>	0.05
CFC114	0.3	N <sub>2</sub> O	0.05
CFC115	0.8	CO	0.2
		H <sub>2</sub>	0.6

\*CO and H<sub>2</sub> are measured by GC-MD at Mace Head and Cape Grim only  
(ppt = parts per trillion, ppb = parts per billion)

To improve the quality of the ADS-GCMS measurements at Zeppelin Observatory 2001-2010, the two instruments (Medusa and ADS-GCMS) were run in parallel for 6 months. Results from the comparison between the two were used to improve the quality of the species measured with the ADS-GCMS.

### *Methane and nitrous oxide*

#### *New instrument for monitoring of methane and nitrous oxide*

A new gas chromatograph (GC) for measurements of CH<sub>4</sub> and N<sub>2</sub>O was installed at the Zeppelin station late 2009. After a period of tuning and verification, methane measurements with the new instrument were started early 2010. Measurements of N<sub>2</sub>O were started early April 2010. The new gas chromatograph is a dual channel system equipped with a Flame Ionization Detector for CH<sub>4</sub> -measurements and an Electron Capture Detector for N<sub>2</sub>O-measurements. The new system enables better control of the calibration process and increased frequency for calibration against reference standards. Precision on methane measurements calculated from working standards over a 24 hour period of normal measurements is improved from ~0.2% to ~0.1%. The old and the new instrument show good agreement when run in parallel.

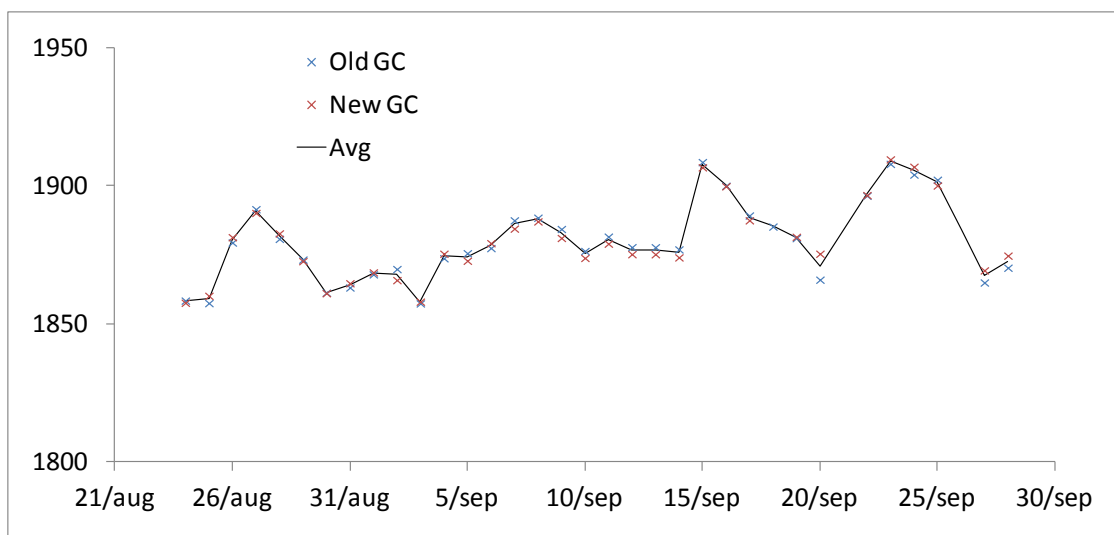


Figure 54: Comparison of old and new measurements of methane at Zeppelin.



Figure 55: The new Gas Chromatograph for Methane and Nitrous Oxide measurements (left) side by side with the old system for Methane measurements.

#### Revision of the methane data series in 2012

The methane data series from Zeppelin has been revised as part of the EU project INGOS, WP2 - Correction and harmonisation of historic concentration measurements (<http://www.ingos-infrastructure.eu/>) during 2012. All original measurement signals have been processed with new improved software to recalculate every single measurement over the last 12 years. This new software facilitates systems for QA/QC and detection of measurement errors. The data series has got a cleanup and the precision of existing measurements has improved.

Over the last 12 years period a selected number of working standards have been stored and was last year analysed against new reference standards using new improved instrumentation.

All other working standards are linked to these through comparative measurements. Hence, all calibrations over the 12 year period have been recalculated and the whole time series adjusted accordingly.

There were two instruments, the GC-FID and a new Picarro (Cavity Ring-Down Spectrometer) run in parallel in 2012. The Picarro also participated in a GAW audit during autumn 2012 with good results (report not finalized yet). Comparisons of the data from the two instruments are shown below.

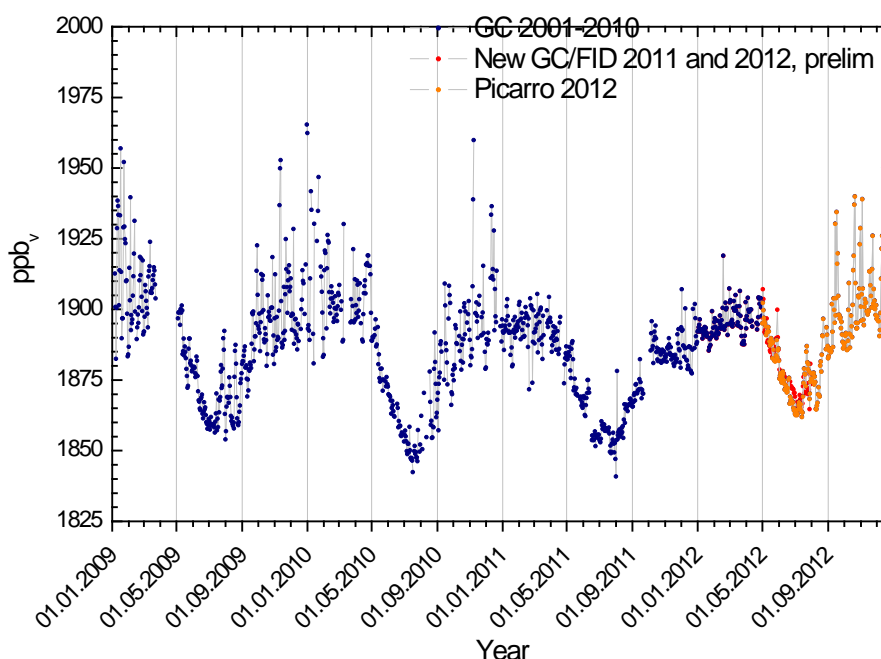


Figure 56: Daily mean of methane measured with the old GC (2001-2010), new GC-FID in 2011 -> and a new Picarro (Cavity Ring-Down Spectrometer) run in parallel in 2012.

#### *CO<sub>2</sub> measurements performed by ITM Stockholm University (SU)*

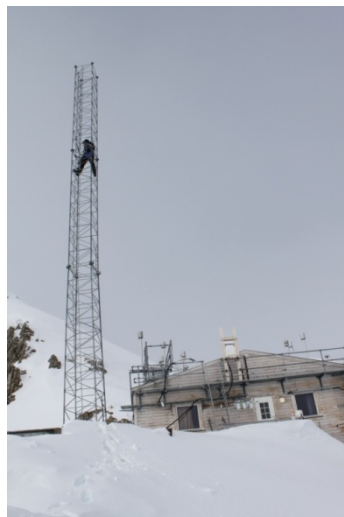
At the Zeppelin station carbon dioxide (CO<sub>2</sub>) and atmospheric particles are measured by Stockholm University (Institute of Applied Environmental Research, ITM).

SU maintains a continuous infrared CO<sub>2</sub> instrument, which has been monitoring since 1989. The continuous data are enhanced by the weekly flask sampling programme in co-operation with NOAA CMDL. Analysis of the flask samples provides CH<sub>4</sub>, CO, H<sub>2</sub>, N<sub>2</sub>O and SF<sub>6</sub> data for the Zeppelin station.

#### **Air inlet at Zeppelin**

There has also been improved air inlet for the GHG measurements at Zeppelin to reduce possible influence from the station and visitors at the stations. The inlet is now moved away from the station and taken from a tower nearby for the following components:

- N<sub>2</sub>O/CH<sub>4</sub>
- CO
- Halogenated compounds
- NOAA flasks sampling program



NILU engineer Are Bäcklund about to install a new air inlet for the Medusa instrument.  
Photo: Ove Hermansen, NILU

### Details about aerosol optical depth measurements

The amount of particles in the air is monitored by use of a Precision-Filter-Radiometer (PFR) sun photometer (NILU) in Ny-Ålesund and a Cimel instrument at Birkenes, see details below.



#### AERONET - Cimel C-318

- Sun (9 channels) and sky radiances
- Wavelength range: 340-1640 nm
- 15 min sampling
- No temperature stabilized
- AOD uncertainty: 0.01-0.02



#### PFR-GAW - Precision Filter Radiometer

- Direct sun measurements (4 channels)
- Wavelength range: 368-862 nm
- Continuous sampling (1 min)
- Temperature stabilized
- AOD uncertainty: 0.01

Figure 57: Photos and typical features of the standard instrument of the AERONET (left panel) and GAW PFR network instruments (right panel) (adapted from Toledano et al., 2010).

Aerosol optical depth measurements started at the new Birkenes observatory in spring 2009, utilizing an automatic sun and sky radiometer (CIMEL type CE-318), with spectral interference filters centered at selected wavelengths: 340, 380, 440, 500, 675, 870, 1020, and 1640 nm. The measurement frequency is approximately 15 minutes (depends on the air-mass and time). Calibration was performed in Izaña in the period 13 May to 24 of July 2008 (RIMA-AERONET sub-network). Between 11 December 2009 and 26 January 2010 and between 16 September and

November 2011, at Autilla del Pino (Palencia, Spain), the operational calibration platform managed by GOA for RIMA-AERONET sun photometers. The data analysis is centralized and performed by AERONET. All data reported are quality assured data (AERONET level 2.0).

The PFR measurements in Ny-Ålesund are part of the global network of aerosol optical depth (AOD) observations, which started in 1999 on behalf of the WMO GAW program. The instrument is located on the roof of the Sverdrup station, Ny-Ålesund, close to the EMEP station on the Zeppelin Mountain (78.9°N, 11.9°E, 474 m a.s.l.). The PFR has been in operation since May 2002. In Ny-Ålesund the polar night lasts from 26<sup>th</sup> October to 16<sup>th</sup> February, leading to short observational seasons. However during the summer it is possible to measure day and night if the weather conditions are satisfactory. The instrument measures direct solar radiation in four narrow spectral bands centered at 862, 501, 411, and 368 nm. Data quality control includes instrumental control like detector temperature and solar pointing control as well as objective cloud screening. Measurements are made at full minutes are averages of 10 samples for each channel made over a total duration of 1.25 seconds. SCIAMACHY TOMSOMI ozone columns and meteorological data from Ny-Ålesund were used in the AOD retrieval.

### **Outlook on observations of aerosol properties in Ny-Ålesund in and beyond 2012**

After a test period in 2011 NILU and the Alfred Wegener Institute (AWI) jointly operate an instrument to monitor AOD on top of the Zeppelin Mountain. This is an unique opportunity to separate the boundary layer contribution from the total column, and thereby get new insights into the contribution of local versus long range transport of aerosols. Initial results from 2012 will be reported in 2013, when routine will start.

### **On the observations of aerosol properties at Birkenes**

Up to 2009, the instrumentation for observing properties of atmospheric aerosol particles at Birkenes consisted of a Differential Mobility Particle Sizer (DMPS), a single-wavelength Particle Soot Absorption Photometer (PSAP), and a PM<sub>2.5</sub> and PM<sub>10</sub> filter samplers for collecting samples for chemical analysis. A DMPS measures the particles number size distribution, usually in the range of about 0.02 – 0.8 µm particle diameter. After putting the aerosol particle phase into a defined state of charge by exposing them to an ionised atmosphere in thermal equilibrium, the DMPS uses a cylindrical capacitor to select a narrow size fraction of the particle phase. The particle size in the selected size fraction is determined by the voltage applied to the capacitor. The particle number concentration in the selected size fraction is then counted by a Condensation Particle Counter (CPC). A mathematical inversion that considers charge probability, transfer function of the capacitor, and counting efficiency of the CPC is then used to calculate the particle number size distribution. A PSAP measures the aerosol absorption coefficient by measuring the decrease in optical transmissivity of a filter while the filter is loaded with the aerosol sample. The transmissivity time series is subsequently translated into a absorption coefficient time series by using Lambert-Beer's law, the same law also used in optical spectroscopy. The PM<sub>2.5</sub> and PM<sub>10</sub> filter samples of the aerosol particle phase are analysed by ion chromatography to reveal the chemical speciation.

From 2010, all instruments measuring aerosol properties in Birkenes listed in section 7.1 were in full operation. This now also includes a 3-wavelength integrating nephelometer and an Optical Particle Counter (OPC). The integrating nephelometer measures the aerosol scattering coefficient at three wavelengths across the visible spectrum by illuminating an aerosol-filled confined volume with a Lambertian light source, and collecting the light scattered by the particles in the volume. This observation is complementary to the measurements of the aerosol absorption coefficient by PSAP, can be used to increase the accuracy of the PSAP measurements. The OPC measures the particle number size distribution in the size range of

0.25 – 10 µm particle diameter, and is thus complementary to the DMPS measurements. Together, DMPS and OPC cover the full particle size range commonly considered by atmospheric aerosol observations. In the OPC, the particles in the sample pass through a laser beam. By correlating the amplitude of the peak of scattered light generated while passing the laser beam with particle size, the particle size distribution is measured.

Moreover, the measurement programme at Birkenes is extended in 2012 with a multi-wavelength absorption photometer and a cloud condensation nucleus counter (CCNC). The absorption photometer will measure the aerosol absorption coefficient at three wavelength across the visible spectrum, and will, after an intercomparison period, replace the old single wavelength instrument used so far. The information on spectral particle absorption will allow conclusion about the nature of the absorber, and its distribution with particle size. The CCNC will measure the number of particles available for acting as cloud condensation nuclei as a function of particle size and water vapour supersaturation. The instrument achieves this by exposing the sample to an “artificial cloud” of defined user-selectable supersaturation. This will ultimately allow statements not only on the direct, but also the indirect aerosol climate effect.

This full picture will not only allow a better source apportionment of the aerosol observed. The full set of optical properties will also facilitate an estimate of local, instantaneous direct aerosol radiative forcing, and a comparison with the radiative forcing of greenhouse gases at the site.

#### **Model studies: calculation of trends**

To calculate the annual trends the observations have been fitted as described in Simmonds et al. (2006) by an empirical equation of Legendre polynomials and harmonic functions with linear, quadratic, and annual and semi-annual harmonic terms:

$$f(t) = a + b \left( \frac{N}{12} \right) \cdot P_1 \left( \frac{t}{N} - 1 \right) + \frac{1}{3} \cdot d \left( \frac{N}{12} \right)^2 \cdot P_2 \left( \frac{t}{N} - 1 \right) + c_1 \cdot \cos(2\pi t) + s_1 \sin(2\pi t) + c_2 \cos(4\pi t) + s_2 \sin(4\pi t)$$

The observed  $f$  can be expressed as functions of time measures from the 2N-months interval of interest. The coefficient  $a$  defines the average mole fraction,  $b$  defines the trend in the mole fraction and  $d$  defines the acceleration in the trend. The  $c$  and  $s$  define the annual and inter-annual cycles in mole fraction.  $N$  is the mid-point of the period of investigation.  $P_i$  are the Legendre polynomials of order  $i$ .

#### **Determination of background data**

Based on the daily mean concentrations an algorithm is selected to find the values assumed as clean background air. If at least 75% of the trajectories within +/- 12 hours of the sampling day are arriving from a so-called clean sector, defined below, one can assume the air for that specific day to be non-polluted. The remaining 25% of the trajectories from European, Russian or North-American sector are removed before calculating the background.

## **Appendix II: Acknowledgments**

We thank the AERONET and RIMA staff for their support calibrating the Cimel instrument, located at the Birkenes observatory. We also acknowledge the European Union Seventh Framework Programme (FP7/2007-2013) under grant agreement Nr. 262254 [ACTRIS] for support for developing the measurements of trace gases and aerosol prorates at Birkenes and Zeppelin.

We thank the Dr. Susanne Kratzer, from Stockholm University, Sweden, and for establishing and maintaining the Palgrunden (58.8°N, 13.2°E) AERONET sites used in this investigation. The CALIOP L3 data were obtained from the NASA Langley Research Center Atmospheric Science Data Center. Access to the data is greatly appreciated.

We gratefully acknowledge the work of the station personnel from the Norwegian Polar Institute for taking care of the observations in Ny-Ålesund. The authors acknowledge the NOAA Air Resources Laboratory (ARL) for the provision of the HYSPLIT transport and dispersion model and/or READY website ([arl.noaa.gov/ready.php](http://arl.noaa.gov/ready.php)). Analyses and visualization used in this report were produced with the Giovanni online data system, developed and maintained by the NASA GES DISC. We also acknowledge the MODIS mission scientists and associated NASA personnel for the production of the data used here. SCIAMACHY TOSOMI ozone overpass data were obtained from the TEMIS website ([temis.nl/protocols/o3field/overpass\\_scia.html](http://temis.nl/protocols/o3field/overpass_scia.html)), Meteorological data for Ny-Ålesund were received via eKlima ([www.eklima.no](http://www.eklima.no)), the web portal from the Norwegian Meteorological Institute. We greatly acknowledge the personnel for obtaining the data and making them publically available.

Christoph Wehrli and Carlos Toledano are acknowledged due to their contributions with the aerosol observations, quality assurance and interpretations.

Christoph Wehrli  
WORCC, PMOD/WRC, Dorfstrasse 33, Davos Dorf  
CH-7260, Switzerland

Carlos Toledano  
Grupo de Óptica Atmosférica  
Universidad de Valladolid  
Prado de la Magdalena s/n  
47071 Valladolid, Spain

<b>Utførende institusjon</b> NILU – Norwegian Institute for Air Research NILU project no.: O-99093/O-105020 NILU report no.: OR 18/2013	<b>ISBN-nummer</b> ISBN 978-82-425-2580-2 (trykt) ISBN 978-82-425-2581-9 (elektronisk)
--	--

<b>Oppdragstakers prosjektansvarlig</b> Cathrine Lund Myhre	<b>Kontaktperson i Klif</b> Harold Leffertstra	<b>TA-nummer</b> TA-3035
		<b>SPFO-nummer</b> 1145/2013

	<b>År</b> 2013	<b>Sidetall</b> 94	<b>Klifs kontraktnummer</b> 4011022
--	-------------------	-----------------------	--

<b>Utgiver</b> NILU – Norsk institutt for luftforskning	<b>Prosjektet er finansiert av</b> Klima- og forurensningsdirektoratet (Klif) og NILU – Norsk institutt for luftforskning
--	--

<b>Forfatter(e)</b> C.L. Myhre, O. Hermansen, A.M. Fjæraa, C. Lunder, M. Fiebig, N. Schmidbauer, T. Krognæs, K. Stebel
---

<b>Tittel - norsk og engelsk</b> Overvåking av klimagasser og partikler på Svalbard og Birkenes: Årsrapport 2011 Monitoring of greenhouse gases and aerosols at Svalbard and Birkenes: Annual report 2011
---

<b>Sammendrag – summary</b>  Rapporten presenterer aktiviteter og måleresultater fra klimagassovervåkingen ved Zeppelin observatoriet på Svalbard for årene 2001-2011 og klimagassmålinger og klimarelevant partikkelmålinger fra Birkenes for 2009-2011.  Overvåkingsprogramet utføres av NILU – Norsk institutt for luftforskning og er finansiert av Statens forurensningstilsyn (SFT) (nå Klima- og forurensningsdirektoratet (Klif)) og NILU – Norsk institutt for luftforskning.  The report summaries the activities and results of the greenhouse gas monitoring at the Zeppelin and observatory situated on Svalbard in Arctic Norway during the period 2001-2011 and the greenhouse gas monitoring and aerosol observations from Birkenes for 2011.  The monitoring programme is performed by the NILU – Norwegian Institute for Air Research and funded by the Norwegian Pollution Control Authority (SFT) (now Climate and Pollution Agency) and NILU – Norwegian Institute for Air Research.
---

<b>4 emneord</b> Drivhusgasser, partikler, Arktis, halokarboner	<b>4 subject words</b> Greenhouse gases, aerosols, Arctic, halocarbons
--	---



**Klima- og forurensningsdirektoratet**

Postboks 8100 Dep,  
0032 Oslo

Besøksadresse: Strømsveien 96

Telefon: 22 57 34 00

Telefaks: 22 67 67 06

E-post: [postmottak@klif.no](mailto:postmottak@klif.no)

[www.klif.no](http://www.klif.no)

## Om Statlig program for forurensningsovervåking

Statlig program for forurensningsovervåking omfatter overvåking av forurensningsforholdene i luft og nedbør, skog, vassdrag, fjorder og havområder. Overvåkingsprogrammet dekker langsiktige undersøkelser av:

- overgjødsling
- forsuring (sur nedbør)
- ozon (ved bakken og i stratosfæren)
- klimagasser
- miljøgifter

Overvåkingsprogrammet skal gi informasjon om tilstanden og utviklingen av forurensningssituasjonen, og påvise eventuell uheldig utvikling på et tidlig tidspunkt. Programmet skal dekke myndighetenes informasjonsbehov om forurensningsforholdene, registrere virkningen av iverksatte tiltak for å redusere forurensningen, og danne grunnlag for vurdering av nye tiltak. Klima- og forurensningsdirektoratet er ansvarlig for gjennomføringen av overvåkingsprogrammet.

SPFO-1145/2013

TA-3035

ISBN 978-82-425-2580-2 (trykt)

ISBN 978-82-425-2581-9 (elektronisk)